Modeling ISM Dynamics and Star Formation

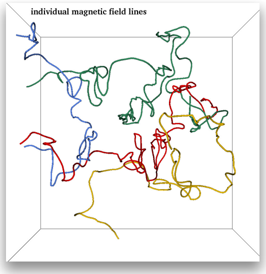


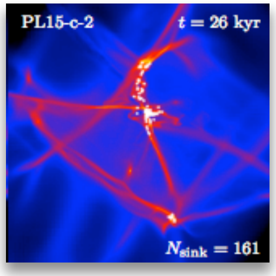

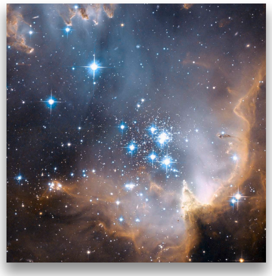
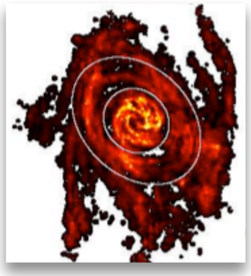
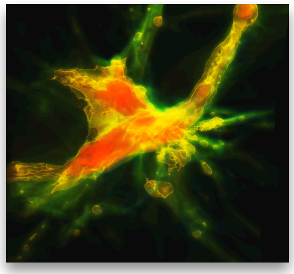

Ralf Klessen

Universität Heidelberg, Zentrum für Astronomie
Institut für Theoretische Astrophysik

Disclaimer

- I try to cover the field as broadly as possible, however, there will clearly be a bias towards my personal interests and many examples will be from my own work.

Literature

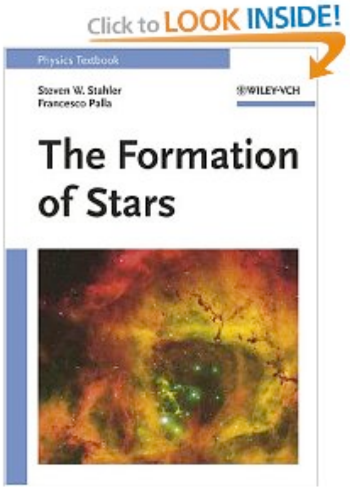
Click to LOOK INSIDE!
Physics Textbook
Steven W. Stahler
Francesco Palla
WILEY-VCH
The Formation of Stars

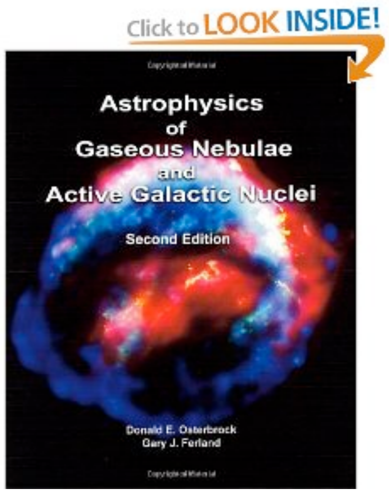
Click to LOOK INSIDE!
Astrophysics of Gaseous Nebulae and Active Galactic Nuclei
Second Edition
Donald E. Osterbrock
Gary J. Ferland

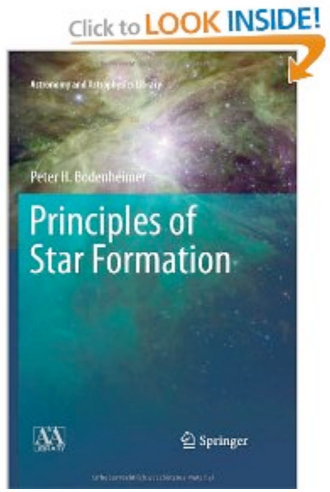
Click to LOOK INSIDE!
Peter H. Bodenheimer
Principles of Star Formation
Springer

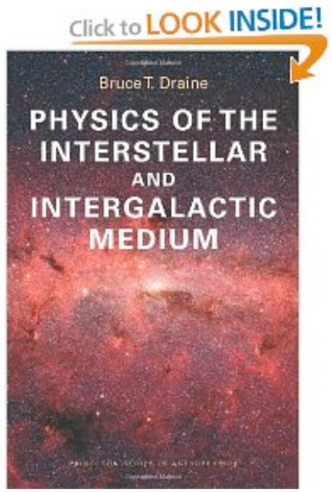
Click to LOOK INSIDE!
Bruce T. Draine
PHYSICS OF THE INTERSTELLAR AND INTERGALACTIC MEDIUM

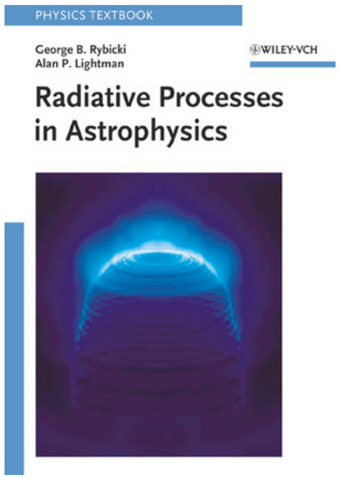
PHYSICS TEXTBOOK
George B. Rybicki
Alan P. Lightman
WILEY-VCH
Radiative Processes in Astrophysics

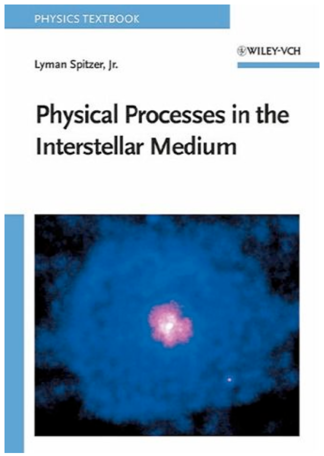
PHYSICS TEXTBOOK
Lyman Spitzer, Jr.
WILEY-VCH
Physical Processes in the Interstellar Medium

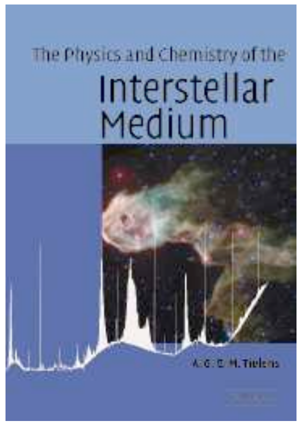
The Physics and Chemistry of the
Interstellar Medium
A. G. G. M. Tielens

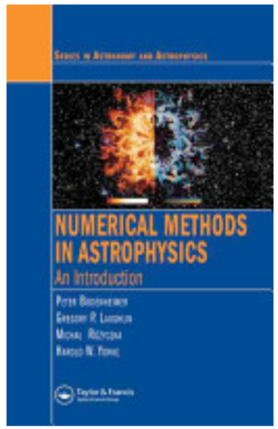
NUMERICAL METHODS IN ASTROPHYSICS
An Introduction

Books

- Spitzer, L., 1978/2004, Physical Processes in the Interstellar Medium (Wiley-VCH)
- Rybicki, G.B., & Lightman, A.P., 1979/2004, Radiative Processes in Astrophysics (Wiley-VCH)
- Stahler, S., & Palla, F., 2004, "The Formation of Stars" (Weinheim: Wiley-VCH)
- Tielens, A.G.G.M., 2005, The Physics and Chemistry of the Interstellar Medium (Cambridge University Press)
- Osterbrock, D., & Ferland, G., 2006, "Astrophysics of Gaseous Nebulae & Active Galactic Nuclei, 2^{nd} ed. (Sausalito: Univ. Science Books)
- Bodenheimer, P., et al., 2007, Numerical Methods in Astrophysics (Taylor & Francis)
- Draine, B. 2011, "Physics of the Interstellar and Intergalactic Medium" (Princeton Series in Astrophysics)
- Bodenheimer, P. 2012, "Principles of Star Formation" (Springer Verlag)

Literature

- Review Articles
  - Mac Low, M.-M., Klessen, R.S., 2004, "The control of star formation by supersonic turbulence", Rev. Mod. Phys., 76, 125
  - Elmegreen, B.G., Scalo, J., 2004, "Interstellar Turbulence 1", ARA&A, 42, 211
  - Scalo, J., Elmegreen, B.G., 2004, "Interstellar Turbulence 2", ARA&A, 42, 275
  - Bromm, V., Larson, R.B., 2004, "The first stars", ARA&A, 42, 79
  - Zinnecker, H., Yorke, McKee, C.F., Ostriker, E.C., 2008, "Toward Understanding Massive Star Formation", ARA&A, 45, 481 - 563
  - McKee, C.F., Ostriker, E.C., 2008, "Theory of Star Formation", ARA&A, 45, 565
  - Kennicutt, R.C., Evans, N.J., 2012, "Star Formation in the Milky Way and Nearby Galaxies", ARA&A, 50, 531

Further resources

- Internet resources
  - Cornelis Dullemond: *Radiative Transfer in Astrophysics*
    http://www.ita.uni-heidelberg.de/~dullemond/lectures/radtrans_2012/index.shtml
  - Cornelis Dullemond: *RADMC-3D: A new multi-purpose radiative transfer tool*
    http://www.ita.uni-heidelberg.de/~dullemond/software/radmc-3d/index.shtml
  - List of molecules in the ISM (wikipedia):
    http://en.wikipedia.org/wiki/List_of_molecules_in_interstellar_space
  - Leiden database of molecular lines (LAMBDA)
    http://home.strw.leidenuniv.nl/~moldata/

Part 2: Dynamics of the ISM

Ralf Klessen

Universität Heidelberg, Zentrum für Astronomie
Institut für Theoretische Astrophysik

inventory of Galactic disc component

- **stellar disc**
  - thin disc (80% of mass): stars of all ages 0-12Gyr
  - thick disc (5% of mass): older stars with lower metallicity
- **interstellar medium (ISM)**
  - gas (15% of mass): hot, warm, and cool component (atomic and molecular)
  - dust (<1% of gas mass): well mixed with the cool gas
  - cosmic rays: relativistic particles
  - magnetic fields: frozen to the gas (field lines are co-moving with the gas); energy density comparable to the kinetic energy of gas

multi-wavelength observations

different wavelengths provide different information.

→astronomer use the full electromagnetic spectrum

- radio: interstellar gas (line emission -> velocity information)
- sub-mm range: dust (thermal emission)
- infrared & optical: stars
- x-rays: stars (coronae), supernovae remnants (very hot gas)
- γ-rays: supernovae remnants (radioactive decay, e.g. ^{26}Al), compact objects, merging of neutron stars (γ-ray burst)

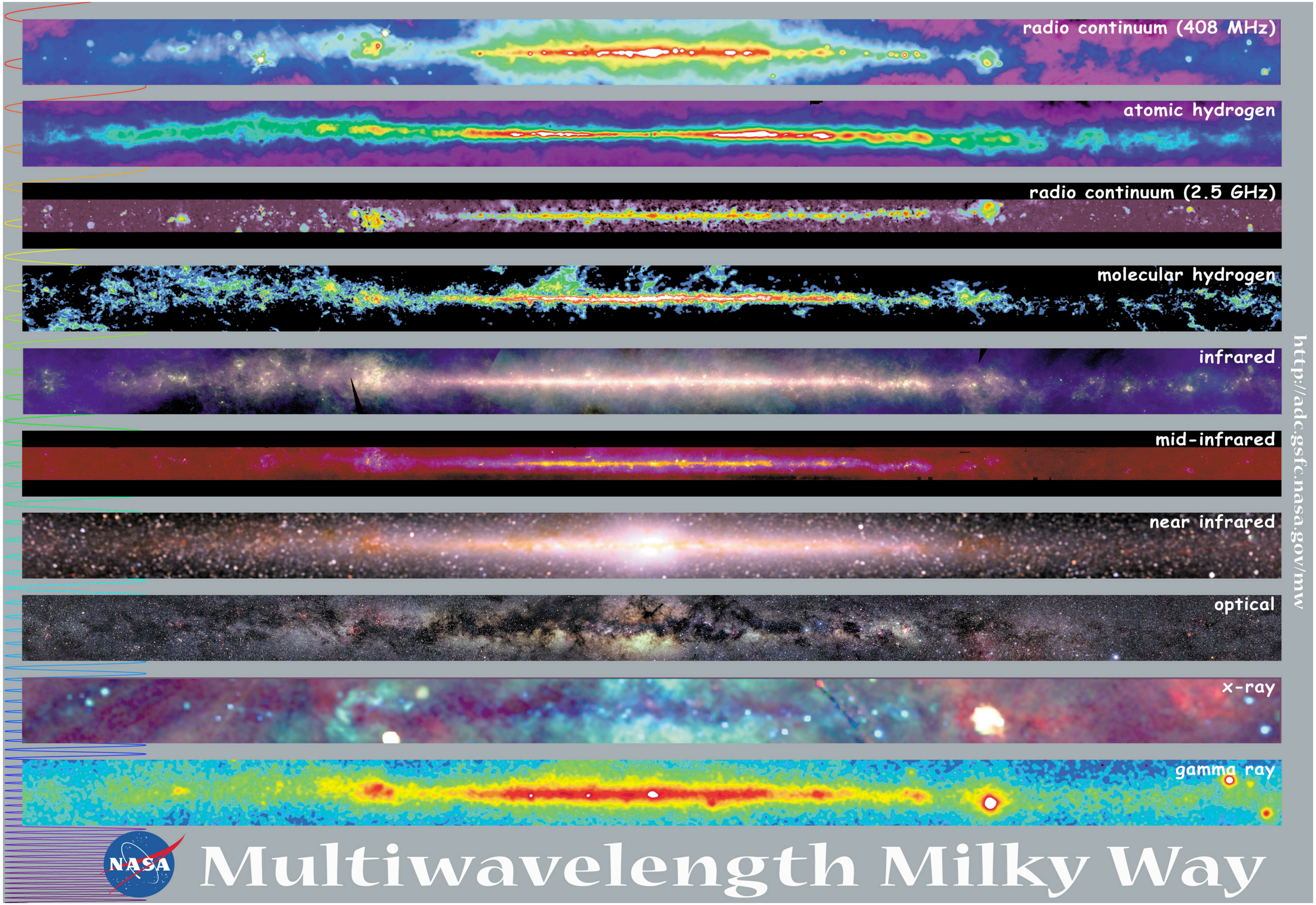
radio continuum (408 MHz)
atomic hydrogen
radio continuum (2.5 GHz)
molecular hydrogen
infrared
mid-infrared
near infrared
optical
x-ray
gamma ray
http://adc.gsfc.nasa.gov/mw
NASA
Multiwavelength Milky Way

interstellar radiation field

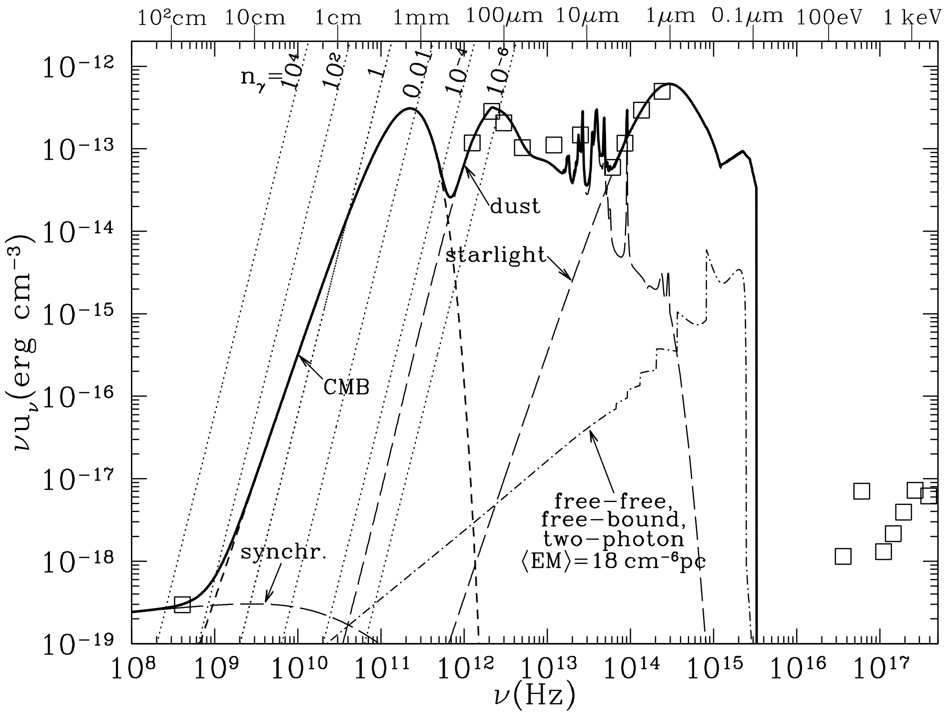

HI cloud in solar neighborhood

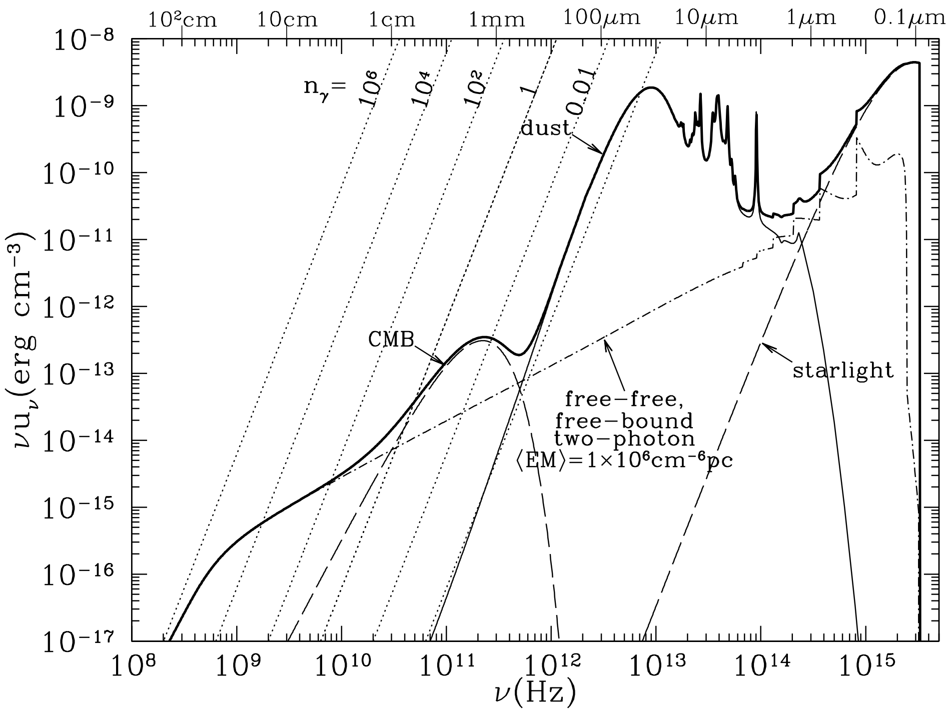

in vicinity of massive star

- cosmic microwave background at small frequencies (mm range)
- dust at μm wavelengths
- starlight at IR and optical frequencies (including UV and near x-rays)

Figures from Draine, B. Physics and Chemistry in the ISM (2011, Princeton)

interstellar radiation field

- at far-ultraviolet (FUV) wavelength the interstellar radiation field (ISRF) is dominated by early-type stars (O, B)
- the strength of the FUV field is often expressed in terms of the

Habing field = 1.2×10^{-4} erg cm^{-2} s^{-1} sr^{-1}

- Current estimates put the average FUV radiation field in the solar neighborhood to

G_0 = 1.7 Habing fields = 1.6×10^{-4} erg cm^{-2} s^{-1} sr^{-1}

- the stellar photons are absorbed mostly by dust and re-emitted at longer wavelength

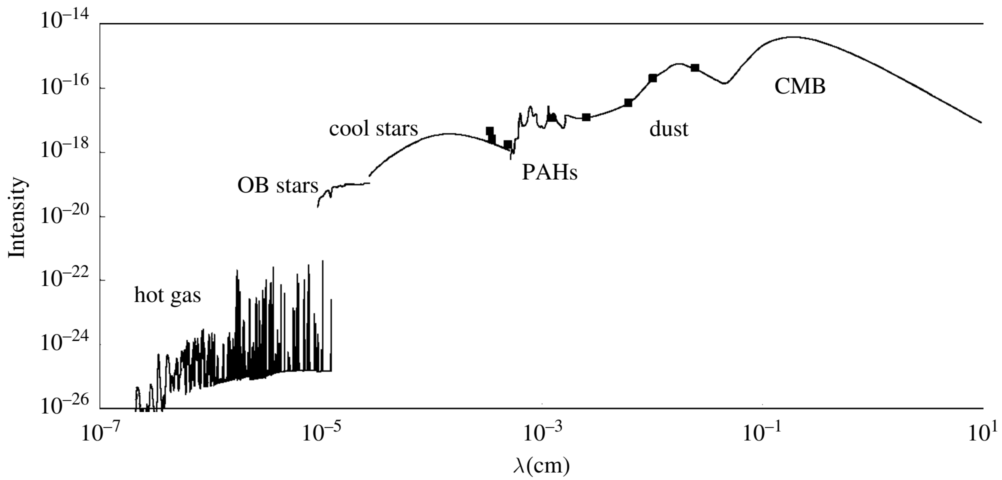

Figure from Tielens, Physics and Chemistry of the ISM (Cambridge University Press)

interstellar medium (ISM)

Abundances, scaled to 1.000.000 H atoms

element		atomic number	abundance
hydrogen	H	1	1.000.000
deuterium	$_1H^2$	1	16
helium	He	2	68.000
carbon	C	6	420
nitrogen	N	7	90
oxygen	O	8	700
neon	Ne	10	100
sodium	Na	11	2
magnesium	Mg	12	40
aluminium	Al	13	3
silicium	Si	14	38
sulfur	S	16	20
calcium	Ca	20	2
iron	Fe	26	34
nickel	Ni	28	2

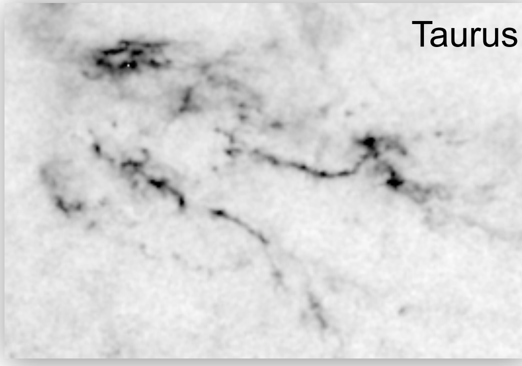

hydrogen is by far the most abundant element (more than 90% in number).

phases of the ISM

Because hydrogen is the dominating element, the classification scheme is based on its chemical state:

ionized atomic hydrogeN	*HII (H^+)*
neutraler atomic hydrogen	*HI (H)*
molecular hydrogen	*H_2*

different regions consist of almost 100% of the appropriate phase, the transition regions between HII, H and H_2 are very thin.

star formation always takes place in dense and cold molecular clouds.

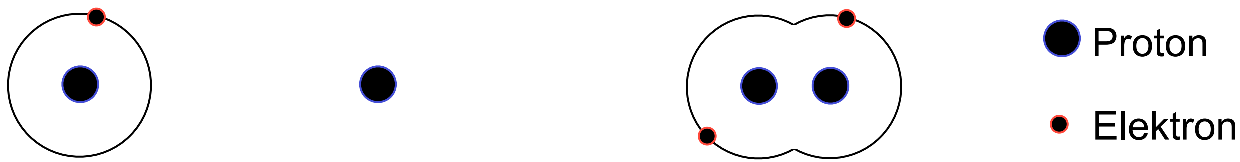

phases of the ISM

Because hydrogen is the dominating element, the classification scheme is based on its chemical state:

ionized atomic hydrogeN	HII (H^+)
neutraler atomic hydrogen	HI (H)
molecular hydrogen	H_2

different regions consist of almost 100% of the appropriate phase, the transition regions between HII, H and H_2 are very thin.

star formation always takes place in dense and cold molecular clouds.

NGC 3324, Hubble Heritage Site

phases of the ISM

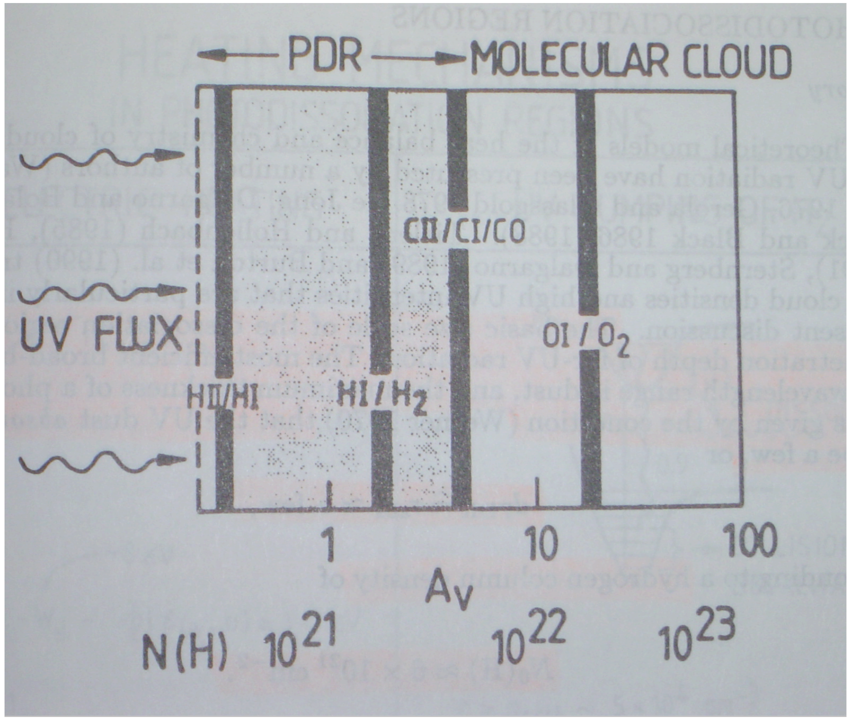

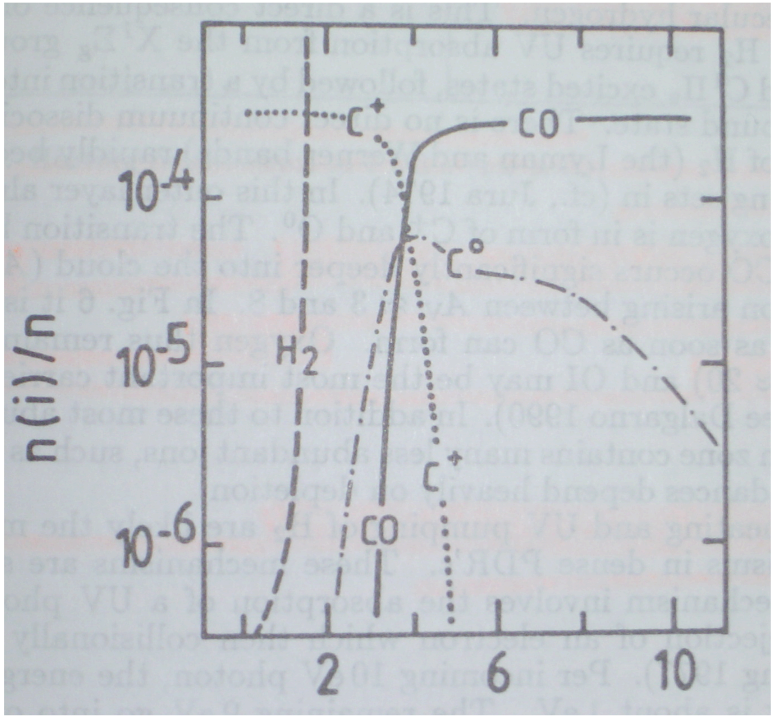

A_V

HII HI H_2

density / column density increases

A_V denotes the extinction, the attenuation of radiation due to absorption (mostly on dust grains)

multi-phase ISM

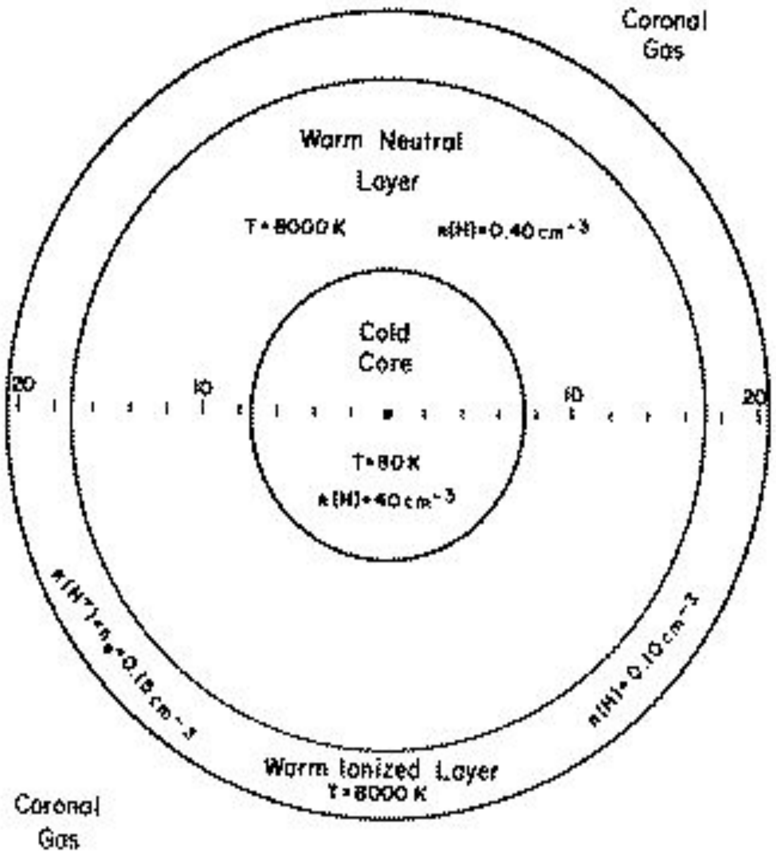

Fig. 8. Structure of a composite cloud. Values of $n(H)$, the neutral hydrogen density, and temperature T are indicated for the cold central core and the two warm envelopes; the electron density n_e is also specified for the outer envelope. The horizontal scale shows radii in light years.

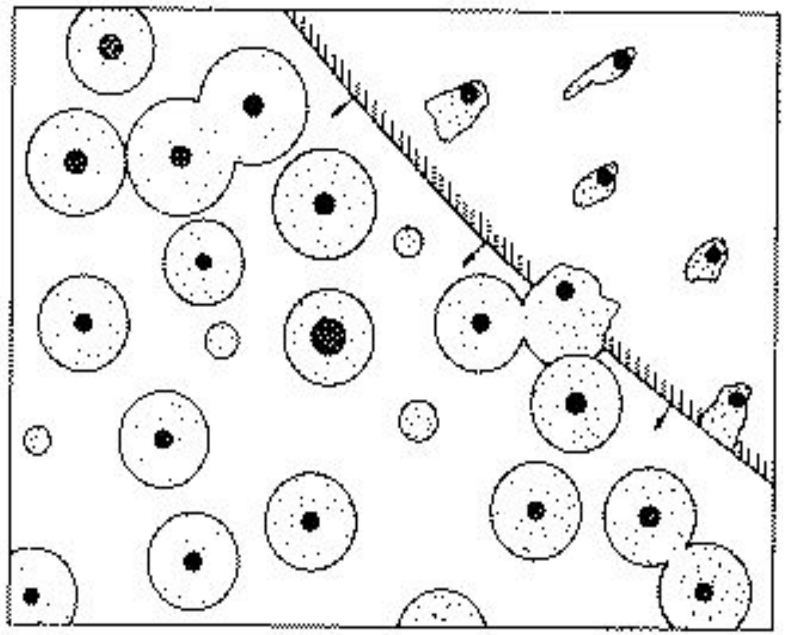

Fig. 9. Clouds in the galactic disc. Each cloud intersecting the galactic plane is represented by its cross-section through the cloud center. The dark central cores represent cold diffuse clouds, while the surrounding dotted circles represent envelopes of warm gas. The hot coronal gas fills the space between the clouds. An expanding supernova remnant advances in the upper right [50].

life cycle of the ISM

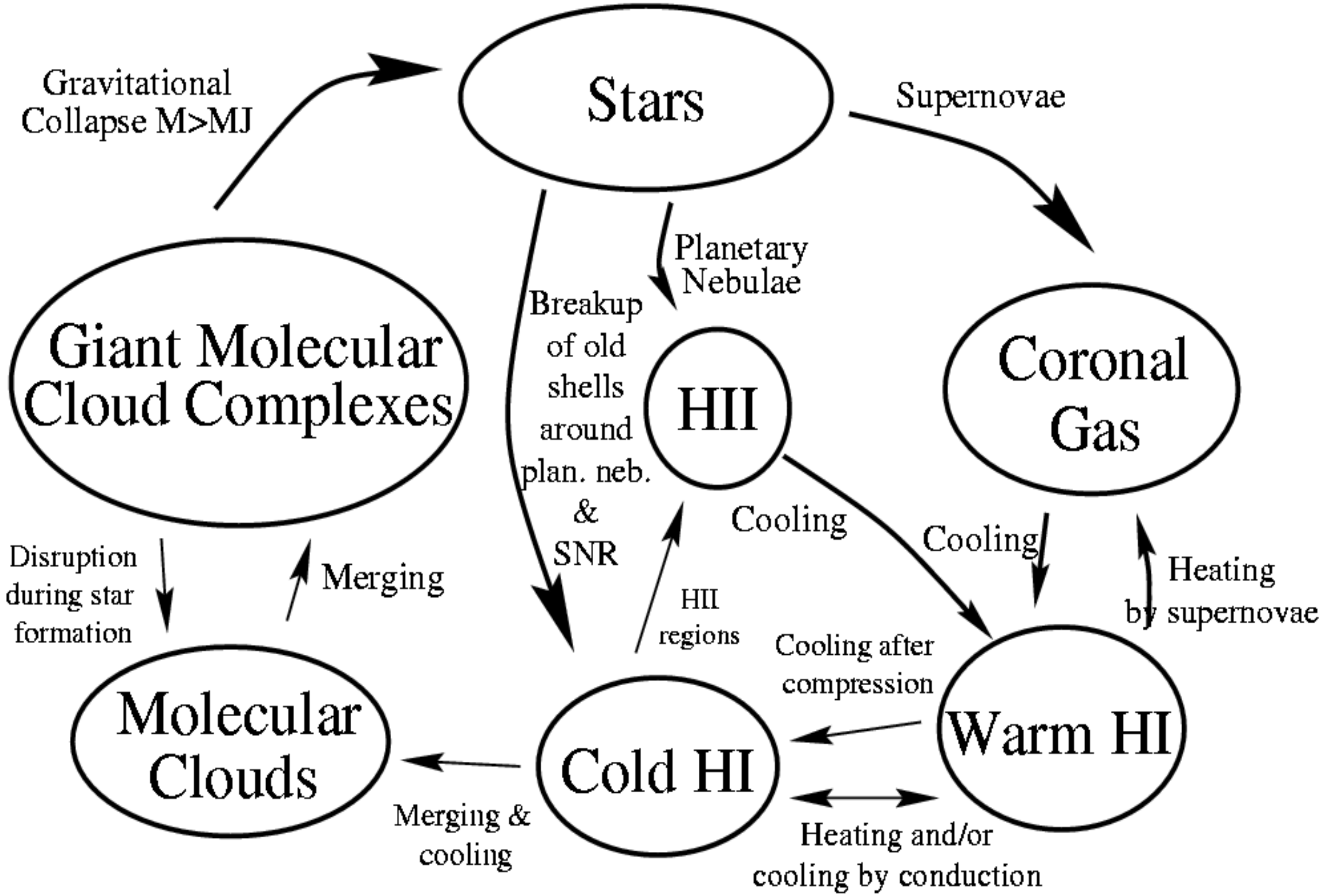

dust

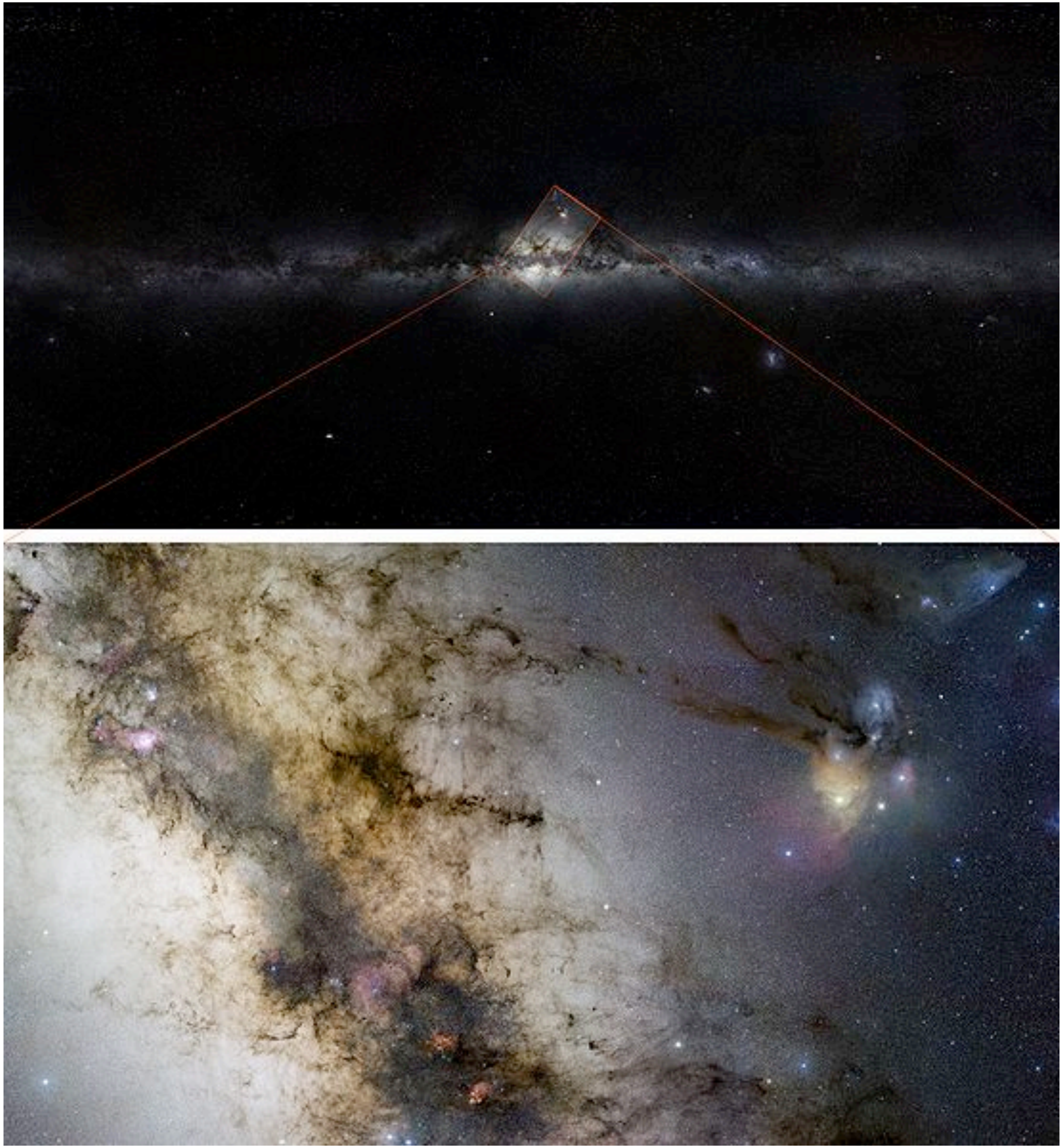

Milky way starscape taken from Paranal.(ESO)

Milky way starscape taken from Paranal.(ESO)

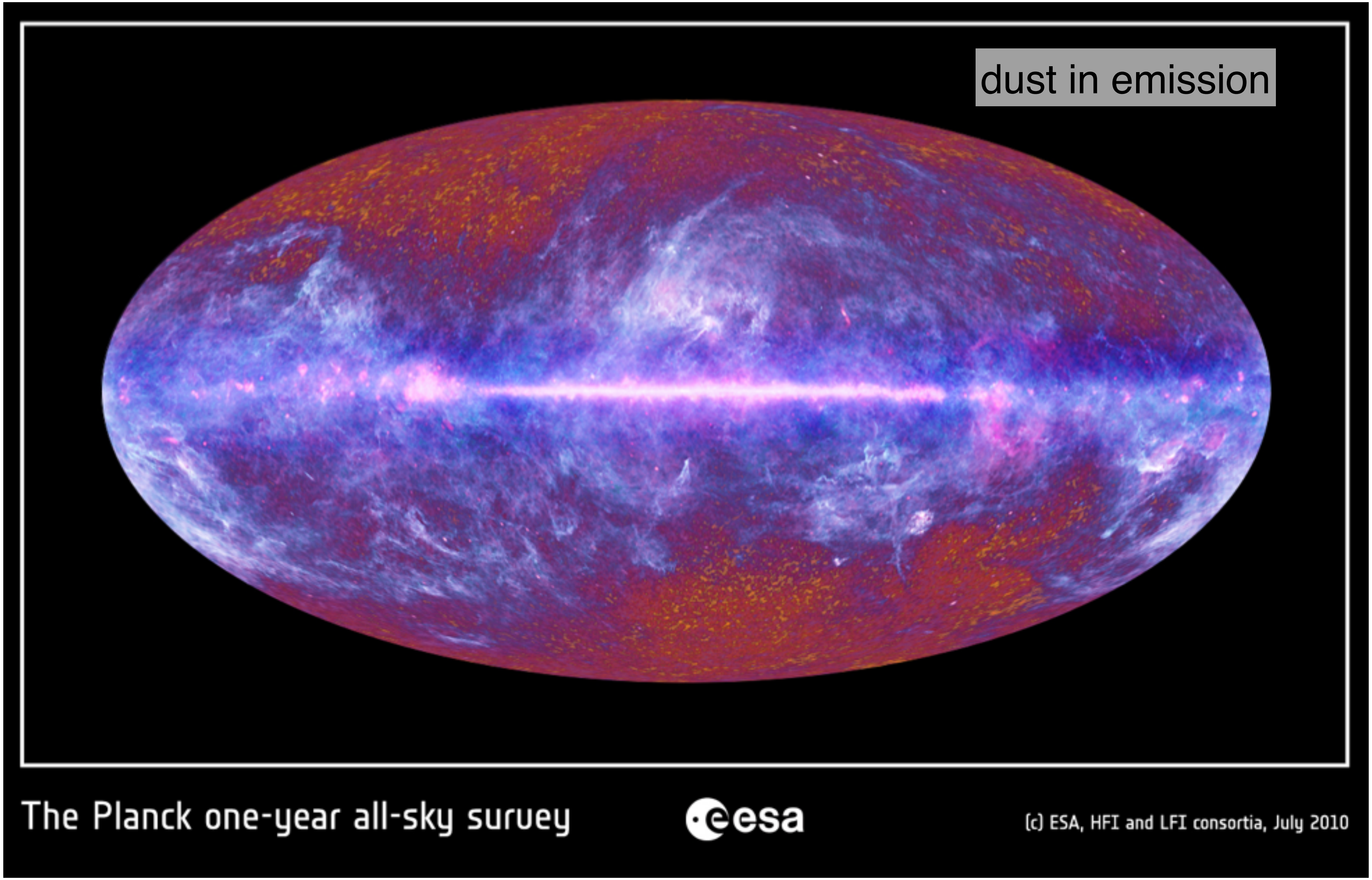
dust in emission
The Planck one-year all-sky survey
(c) ESA, HFI and LFI consortia, July 2010

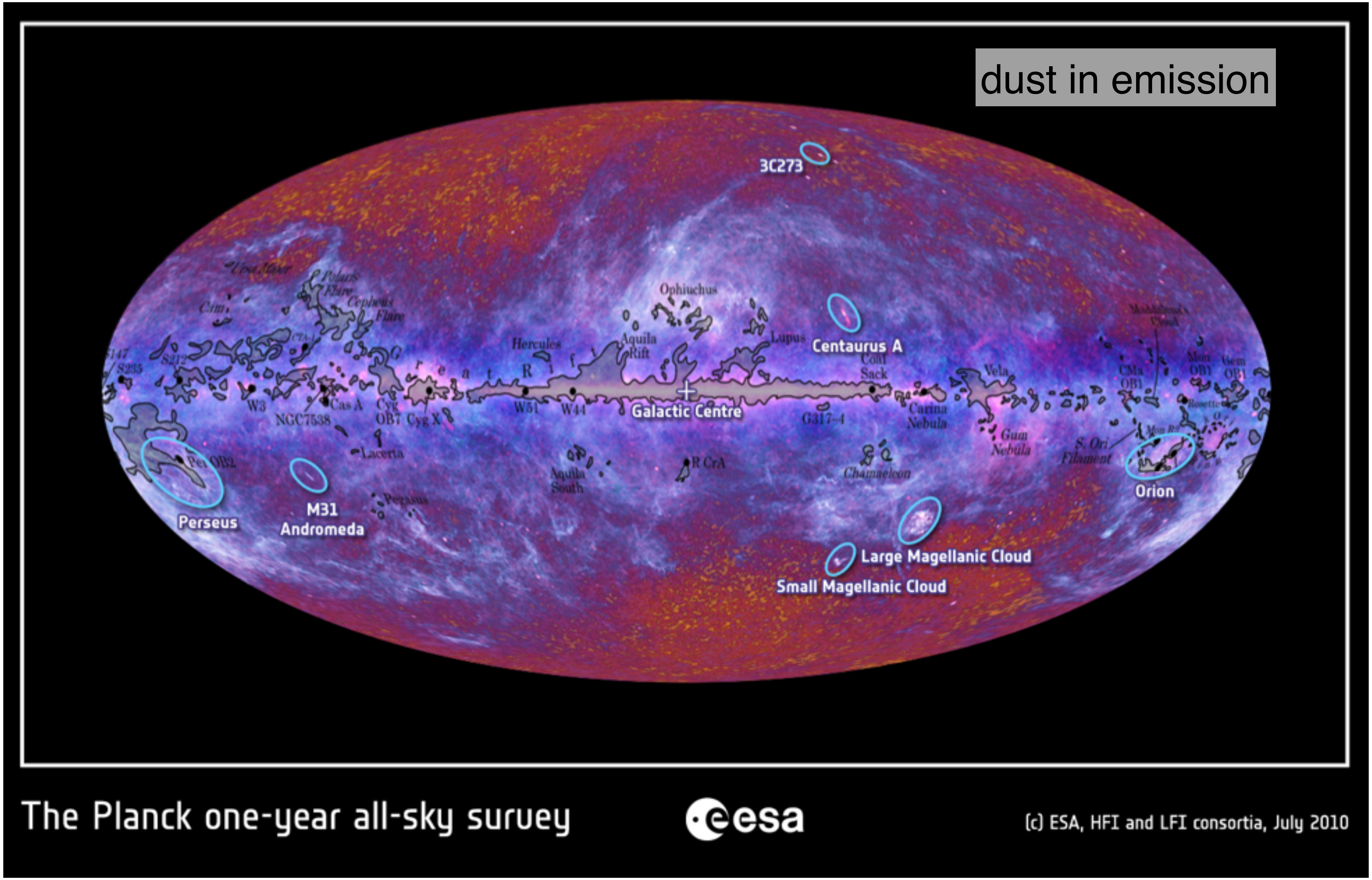

dust in emission
3C273
Ophiuchus
Centaurus A
Hercules
Aquila Rift
Lupus
Coal Sack
Vela
W51
W44
Galactic Centre
G317-4
Carina Nebula
Gum Nebula
W3
NGC7538
Cas A
Cyg OB7
Cyg X
Lacerta
Per OB2
Perseus
M31
Andromeda
Pegasus
Aquila South
R CrA
Chamaeleon
Large Magellanic Cloud
Small Magellanic Cloud
Orion
S. Ori Filament
CMa OB1
Mon OB1
Gem OB1
Polaris Flare
Cepheus Flare
Ursa Major
S235
S212
The Planck one-year all-sky survey
esa
(c) ESA, HFI and LFI consortia, July 2010

interstellar dust

- large variations in size and composition: from a few dozens of molecules (PAHs) to little kernels of a few micrometer diameter
- typically complex, fractal structure with large surface compared to the volume (ßen Oberfläche im Vergleich zum Volumen
- dust is important catalyst for chemical reactions in the ISM (example: formation of H_2 on surface of dust grains)

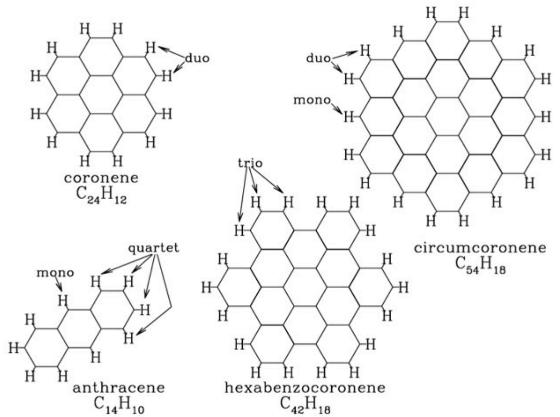

PAH: Polyaromatische Hydrokarbonate

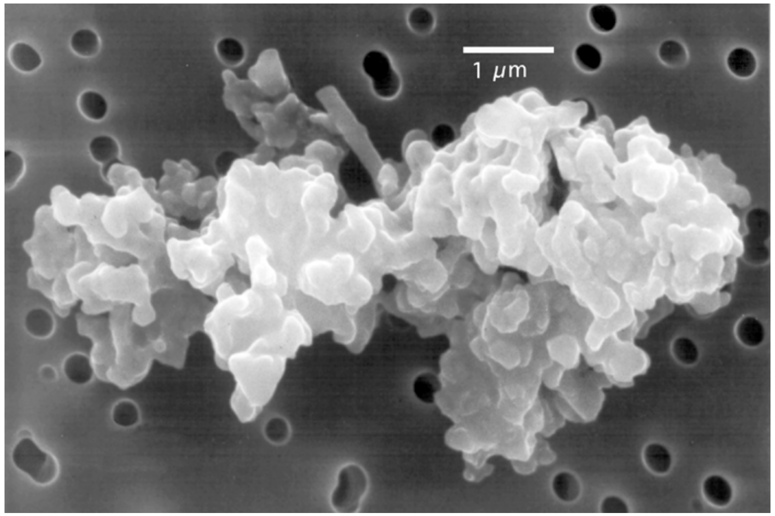

Quelle: Brownlee & Jessberger (in Jessberger et al, 2001, in Interstellar Dust), im Netz: Wikipedia

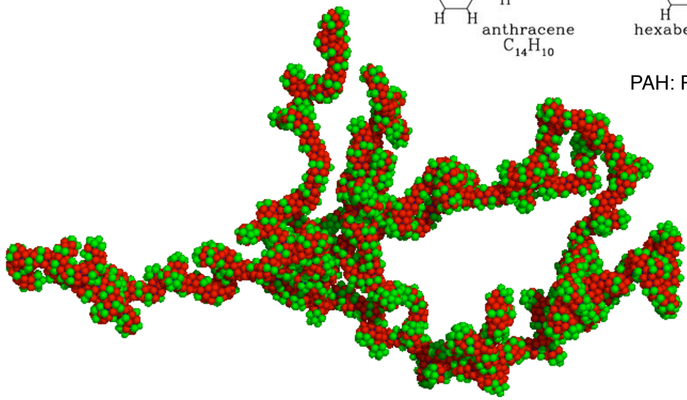

Quelle: E. L. Wright (UCLA), im Netz: Wikepedia

interstellar dust

- dust and gas are well mixed (dust to gas ratio ~ 1% by mass)
- dust absorbs short-wavelength light and re-emits the energy as thermal spectrum at IR frequencies
- extinction depends on wavelength
- relation between extincion A_V and reddening E_{B-V}: $A_V = R_V\, E_{B-V}$ (B=blue, V=visible)
  mit $A_\lambda = 2.5 \log_{10} (F_{\lambda,0}/F_\lambda)$ und $E_{B-V} = A_B - A_V = (B-V)-(B-V)_0$ und $R_V = 3.1$
- on average A_V=0.3 mag/kpc (much higher in dark clouds: Av up to several 10^2)

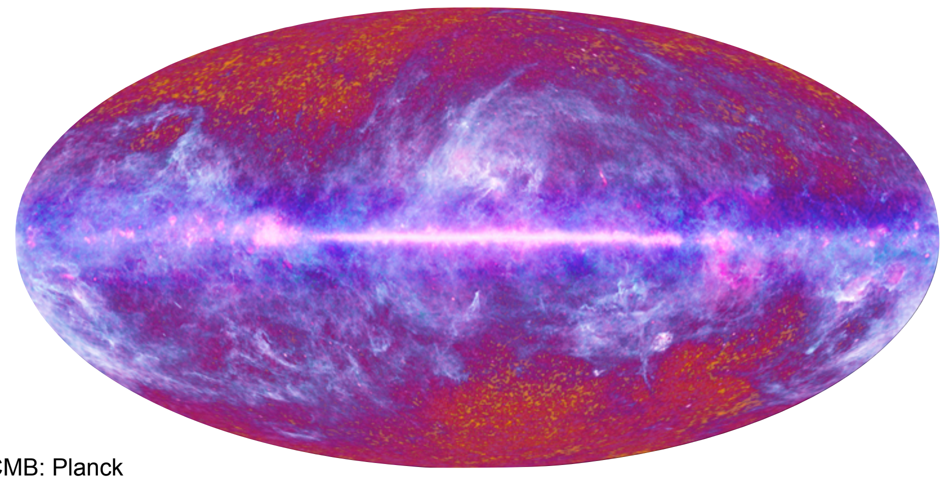

CMB: Planck

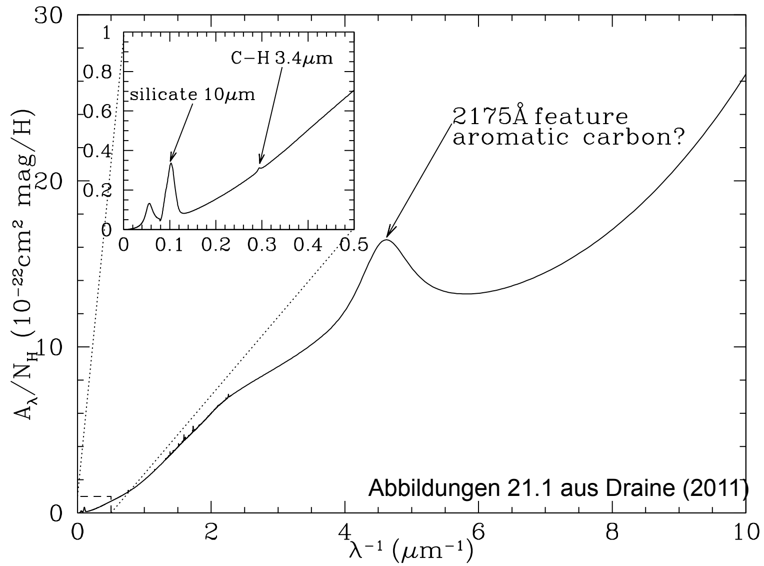

Abbildungen 21.1 aus Draine (2011)

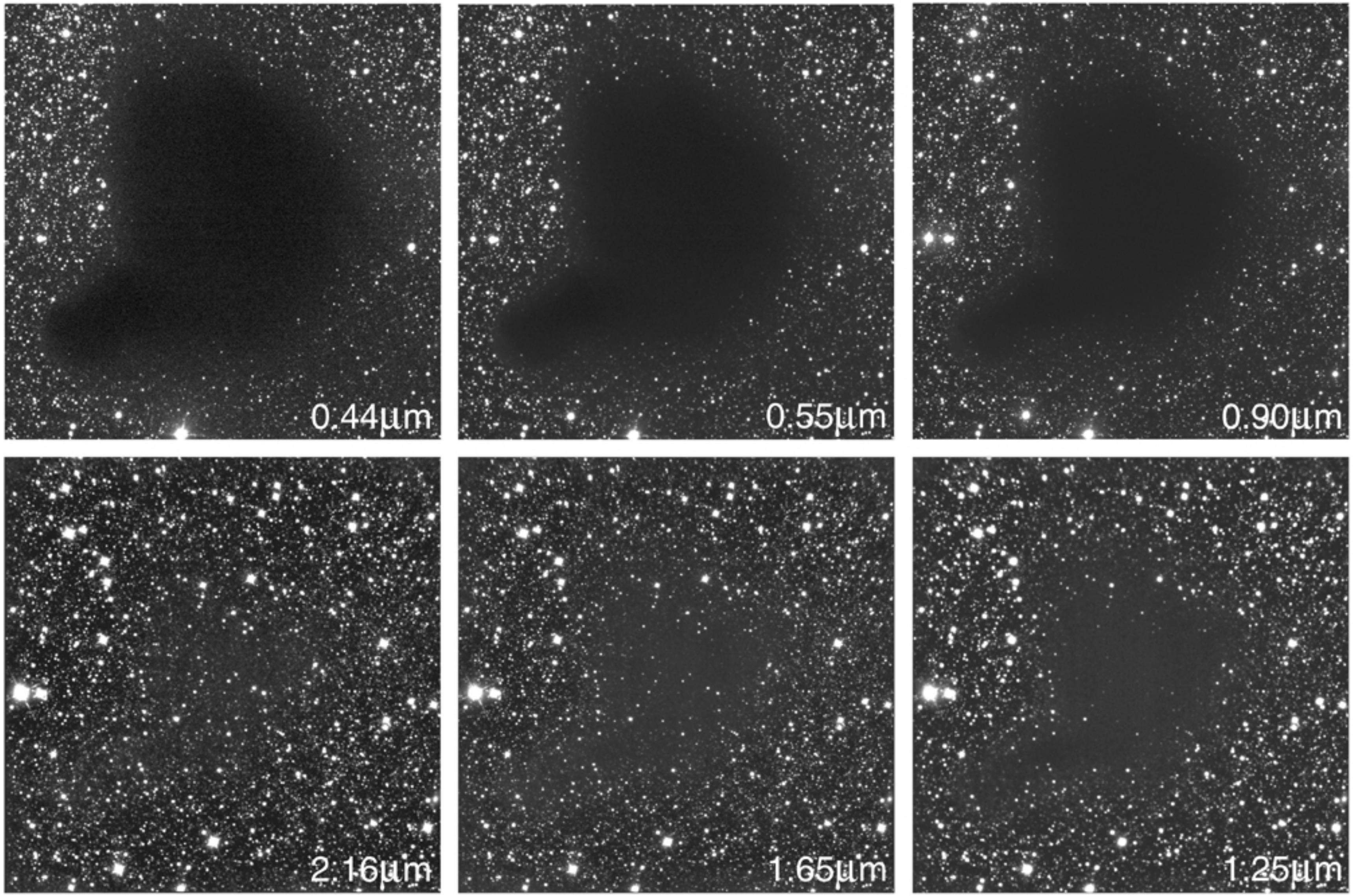

The Dark Cloud B68 at Different Wavelengths (NTT + SOFI)

ESO PR Photo 29b/99 (2 July 1999)

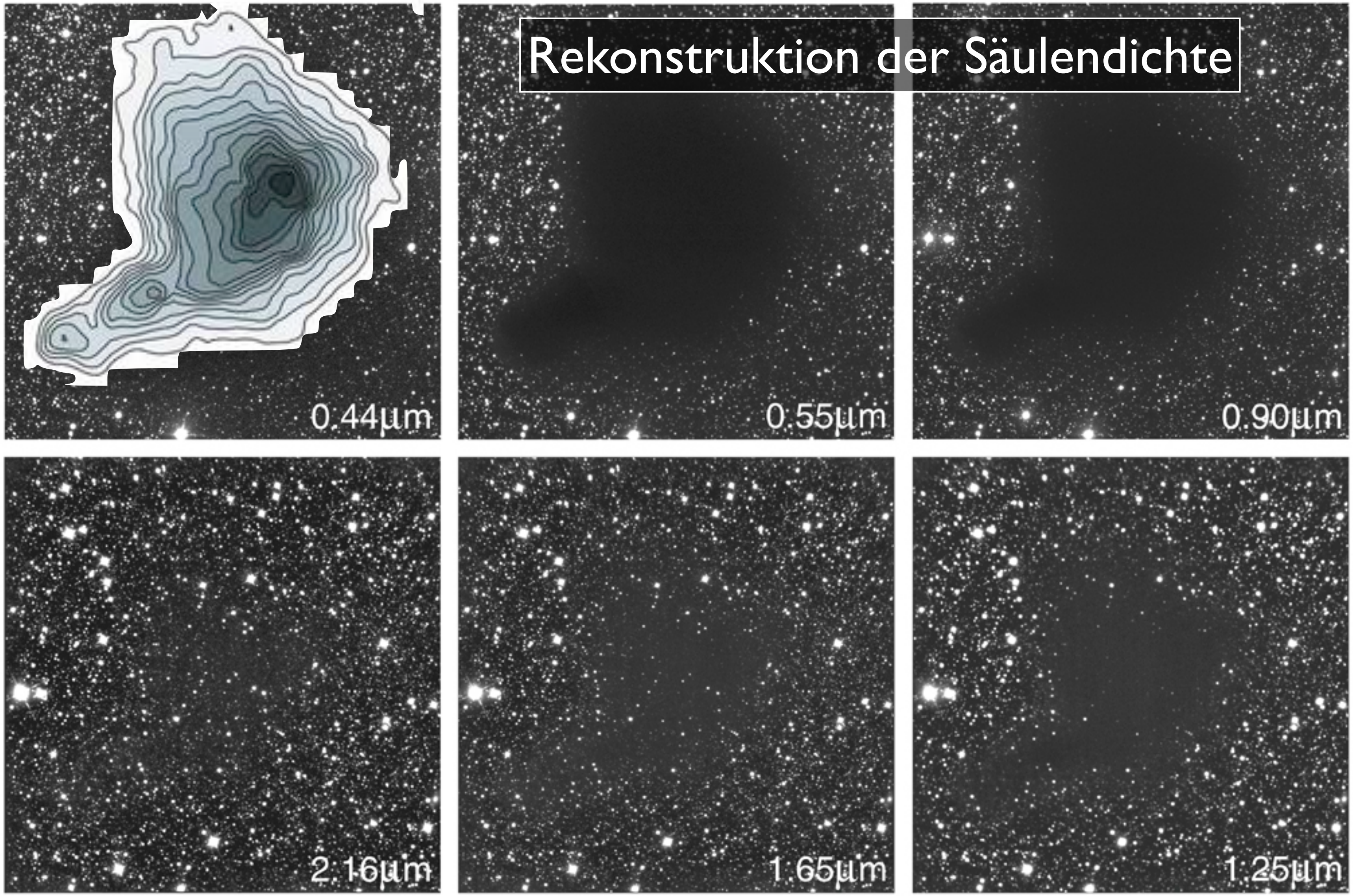

The Dark Cloud B68 at Different Wavelengths (NTT + SOFI)

ESO PR Photo 29b/99 (2 July 1999)

Barnard 68: a well-studied isolated prestellar core

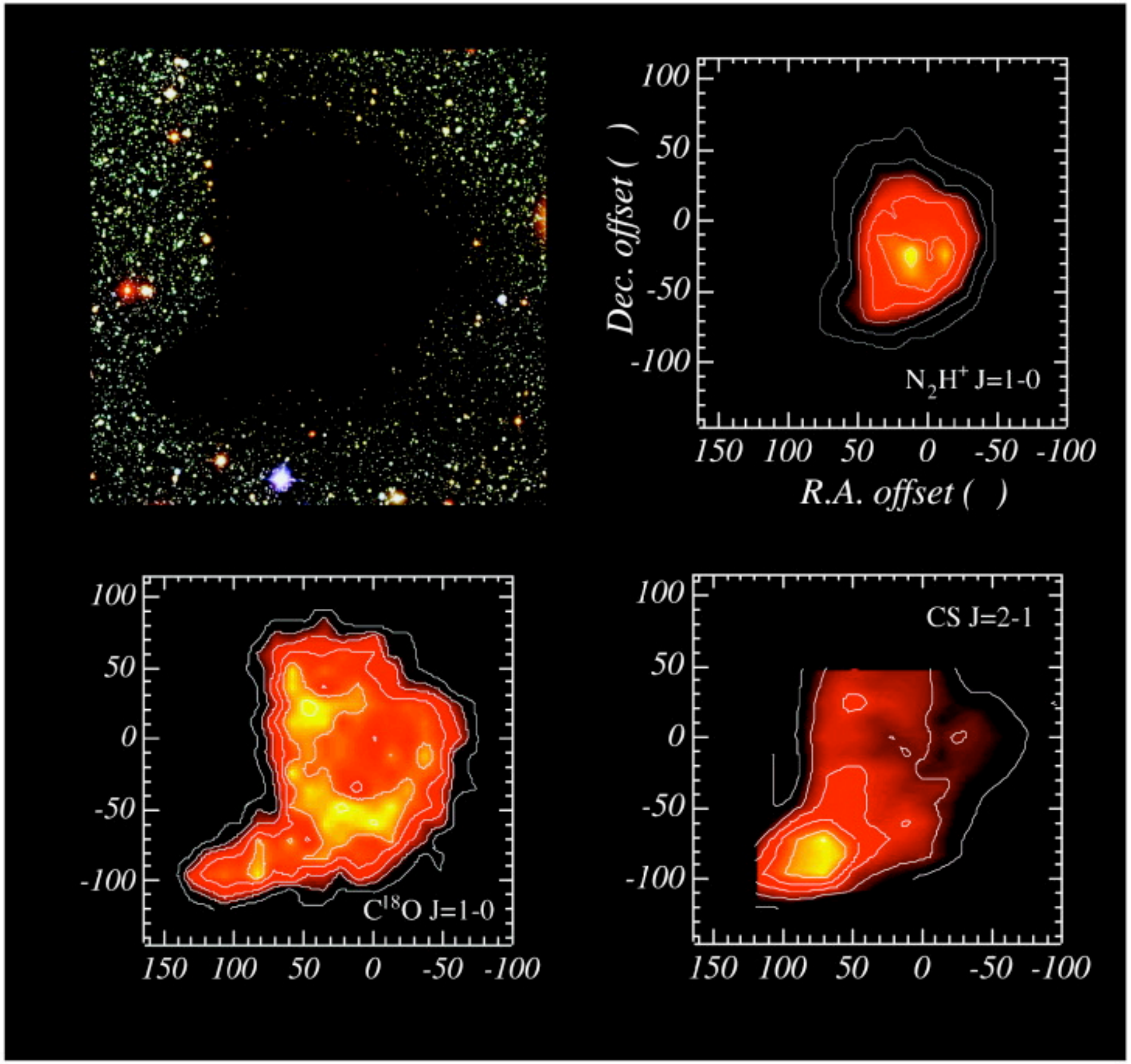

(Lada et al. 2003)

dust and magnetic fields

- dust leads to polarization of star light
- polarization degrees up to 5%
- reason: elongated dust particles aligned with B-field (typically semi-minor axis parallel to field line) and rotate around field lines
- important information about Galactic B-fields

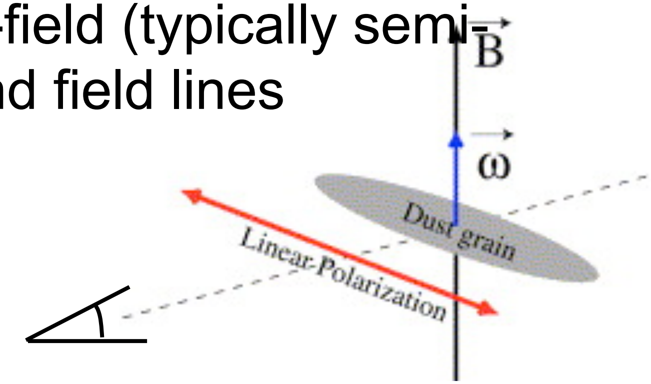

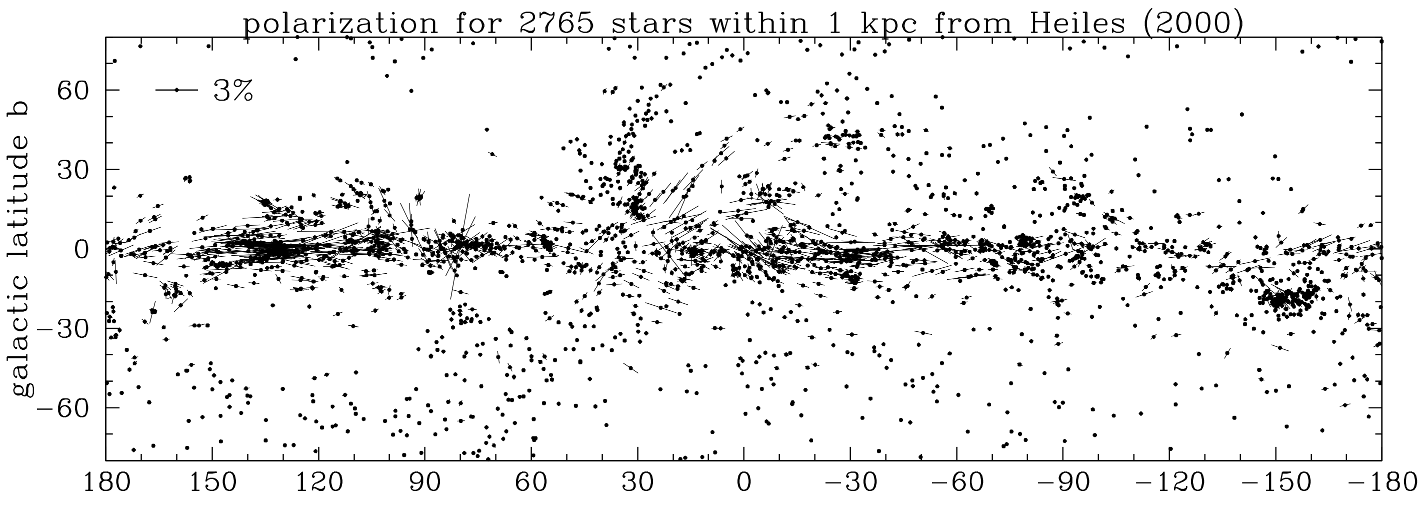

Abbildungen 21.3 aus Draine (2011)

dust and magnetic fields

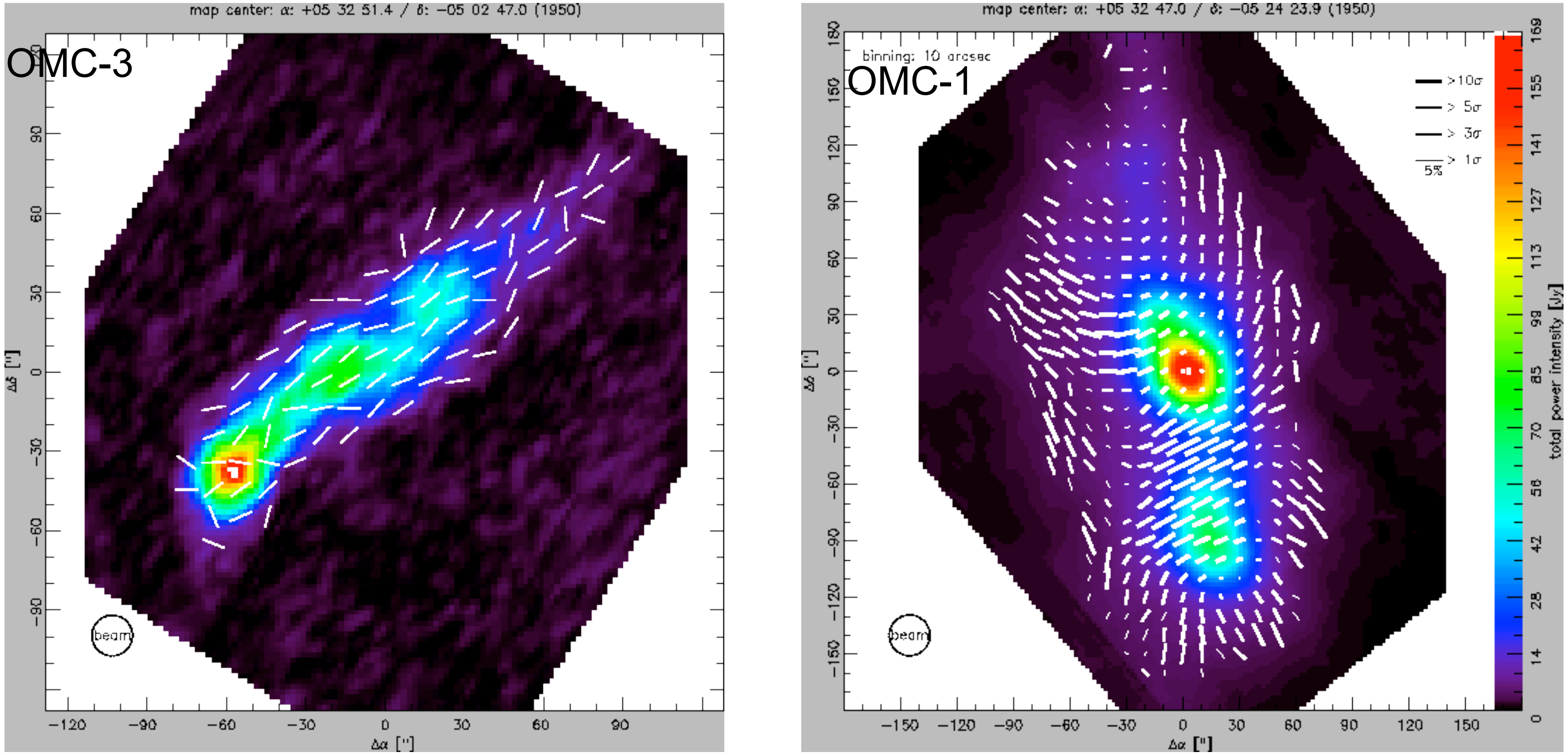

dust polarization maps of nearby molecular cloud cores

(Quelle: Max Planck Institut für Radioastronomie, Bonn) cosmic rays

cosmic rays

- cosmic rays are highly relativistic particles
- mostly proton, also electrons
- sources: hot stars, supernova remnants, quasars
- additional acceleration in expanding supernova shells (multiple "scattering" on magnetic field lines, Fermi effect)
- energy range E = 10^8 - 10^{20} eV
- move along magnetic field lines (also some diffusion ⊥ to B) with gyro radius

$$r_G = 10^{-6} pc \frac{E[GeV]}{B[\mu G]}$$

- up to 10^{16} eV confined to Milky Way
- lifetime ~ 2 Myr

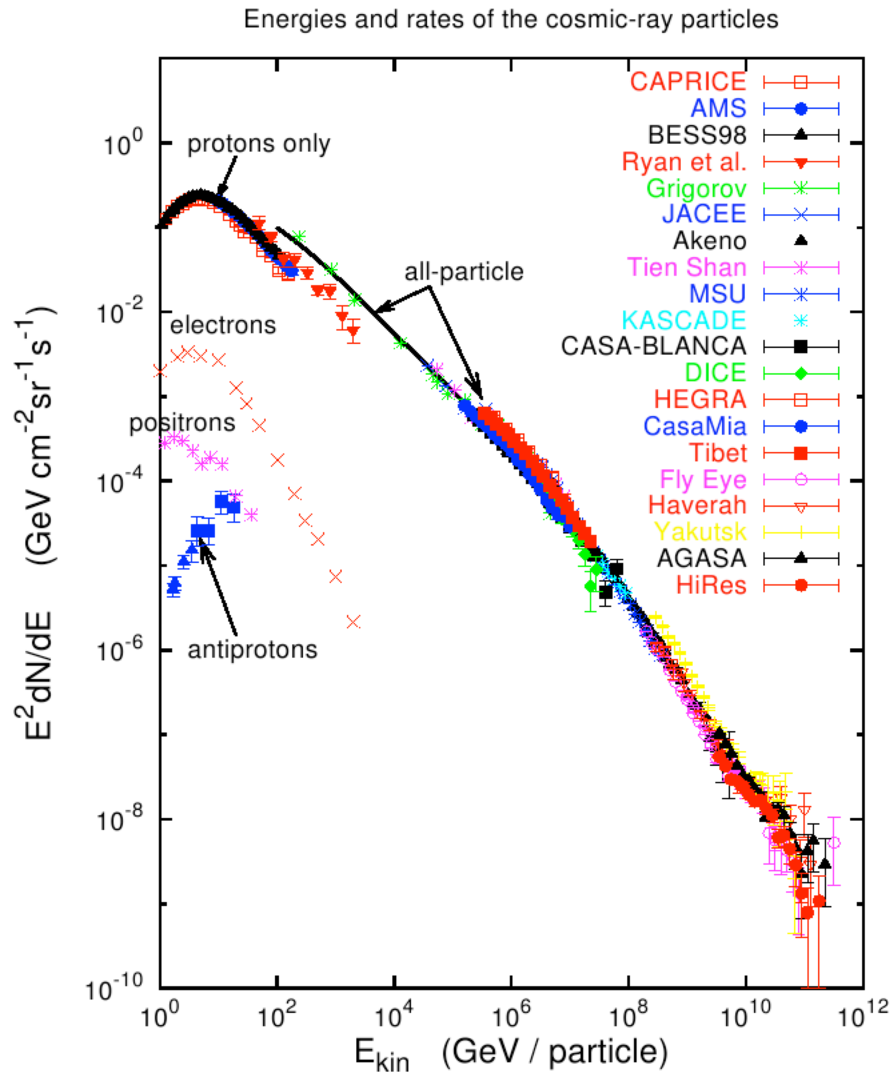

Abbildung: Hillas (2006, arXiv:astro-ph/0607109)

cosmic rays

- cosmic rays are highly relativistic particles
- mostly proton, also electrons
- sources: hot stars, supernova remnants, quasars
- additional acceleration in expanding supernova shells (multiple “scattering” on magnetic field lines, Fermi effect)

- Fermi mechanism: acceleration of charged particles in magnetized shocks
- particles can be reflected in inhomogeneities of the magnetic field and gain energy

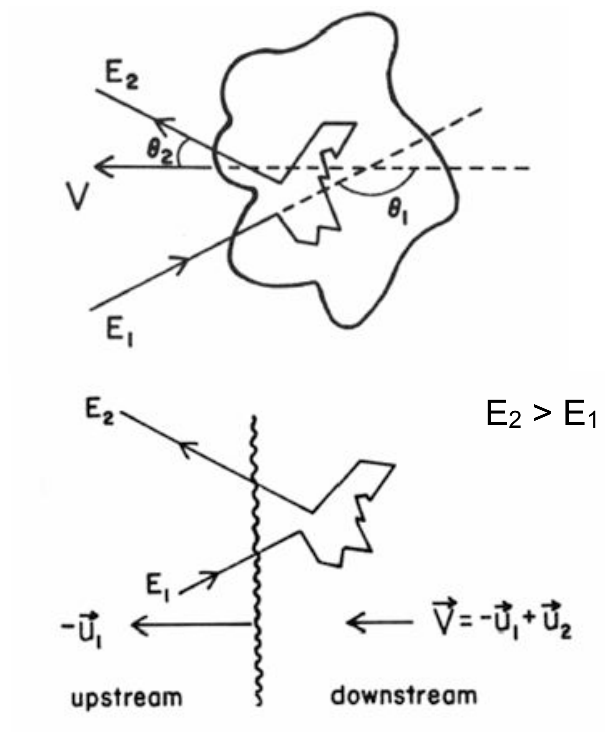

$E_2 > E_1$

Gaisser, T. (1990, COSMIC RAY AND PARTICLE PHYSICS (CAMBRIDGE UNIV. PRESS 1990)

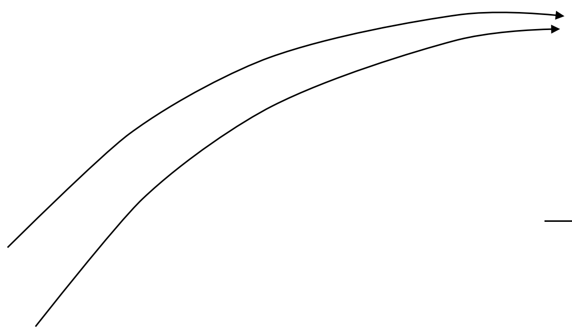

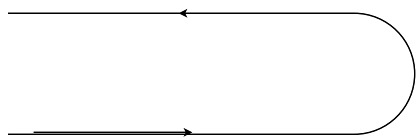

cosmic rays

- detection via particle shower experiments on Earth

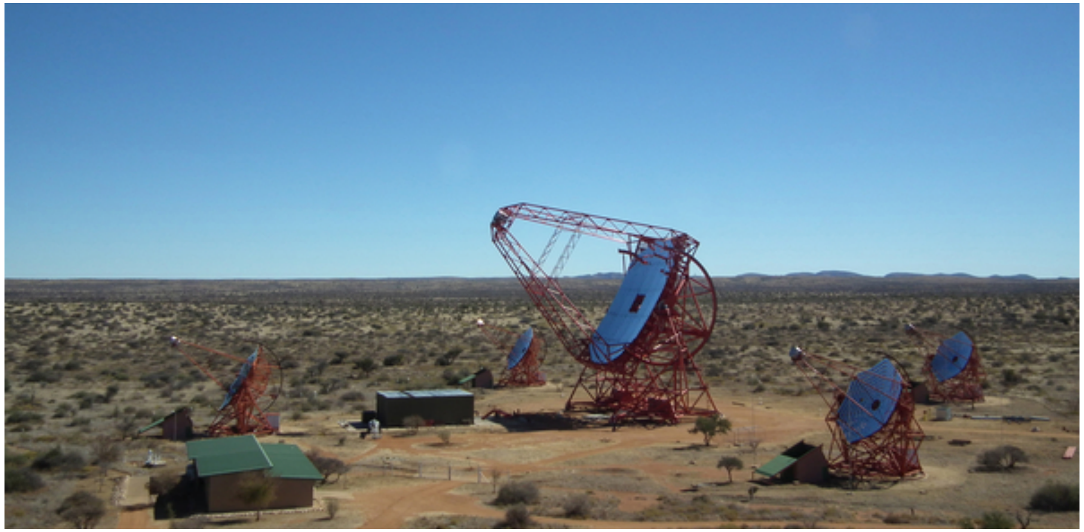

H.E.S.S. Teleskope in Namibia (PI: W. Hofmann, MPI-K)

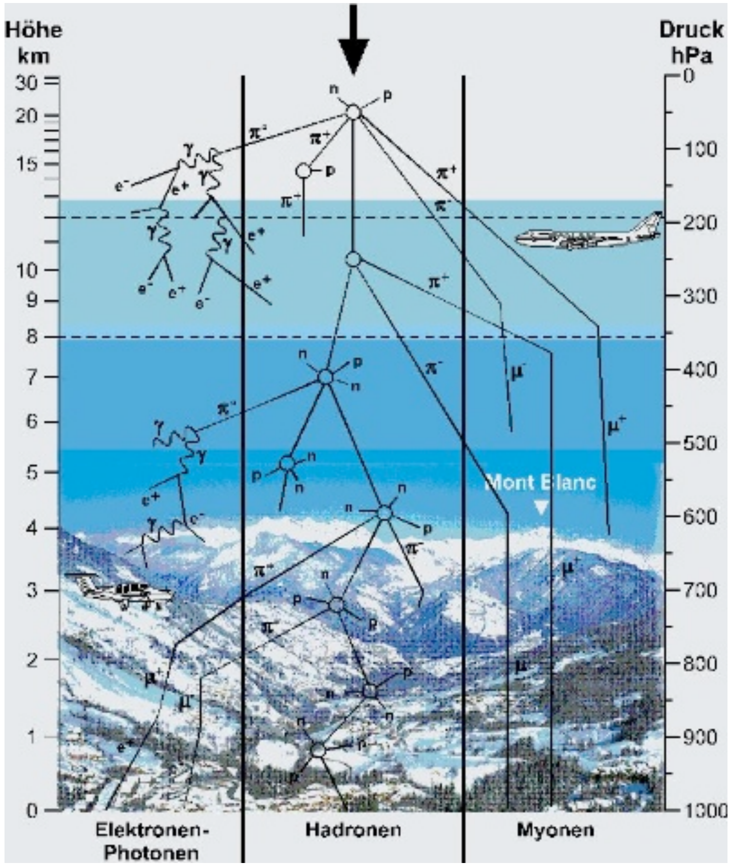

Roland Kotte, Forschungszentrum Rossendorf


Trifid Nebel: MPG/ESO 2.2 Teleskop La Silla


Carina with HST


Orion Nebula Cluster (ESO, VLT, M. McCaughrean)

photoionized gas 1

We consider gas that becomes ionized by UV radiation above *hv* > 13.6 eV.

- example: 32% of the photons coming from a O8 star with T~35.000 K are about the ionization energy of H.

Strömgren sphere:

- high-mass star embedded in homogeneous gas cloud
- rate Q_0 of UV photons = number of photons with *hv* > 13.6 eV per second
- in equilibrium: number of recombinations = number of ionization events in considered volume

$$H^+ + e^- \rightarrow H + h\nu \quad = \quad H + h\nu \rightarrow H^+ + e^-$$

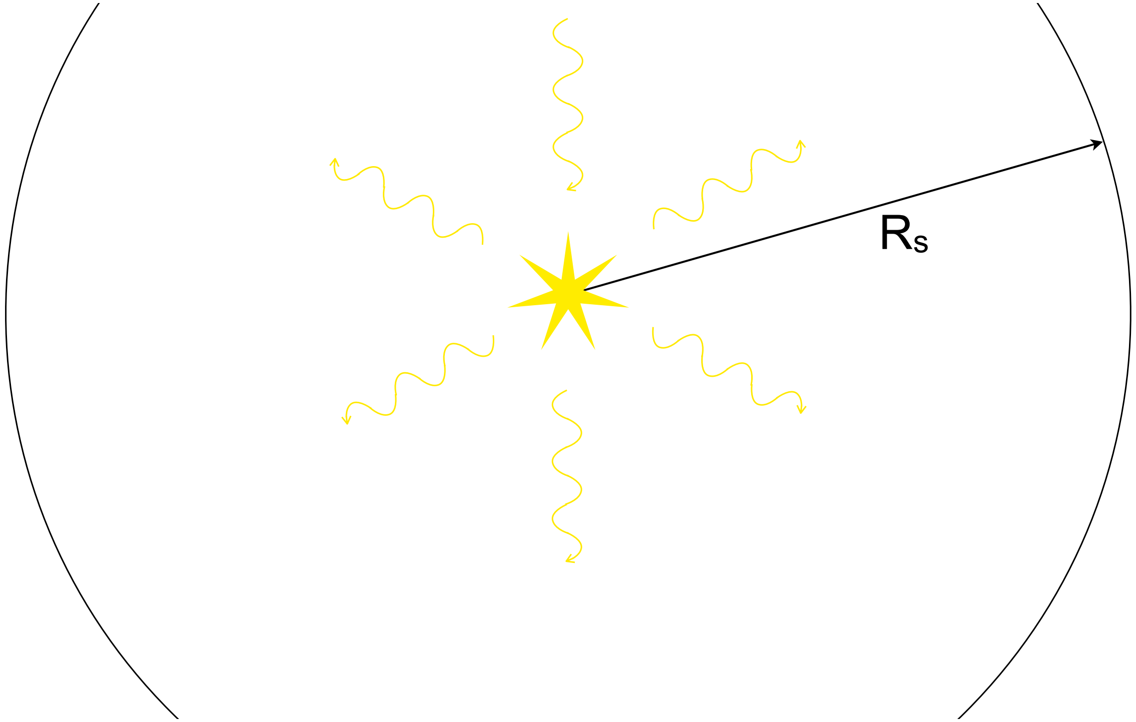

photoionized gas 2

We consider gas that becomes ionized by UV radiation above *hv* > 13.6 eV.

- example: 32% of the photons coming from a O8 star with T~35.000 K are about the ionization energy of H.

Strömgren sphere:

- high-mass star embedded in homogeneous gas cloud
- rate Q_0 of UV photons = number of photons with *hv* > 13.6 eV per second
- in equilibrium: number of recombinations = number of ionization events in considered volume

$$H^+ + e^- \rightarrow H + h\nu \quad = \quad H + h\nu \rightarrow H^+ + e^-$$

- with recombination rate α we get the number of recombination events as $\frac{4\pi}{3} R_S^3 \, \alpha \, n_{H^+} n_{e^-}$
- thus: $Q_0 = \frac{4\pi}{3} R_S^3 \, \alpha \, n_{H^+} n_{e^-}$
- the star ionizes a sphere with radius

$$R_S = \left(\frac{3 Q_0}{4\pi \, \alpha \, n_{H^+} n_{e^-}} \right)^{1/3}$$

- the transition between ionized and neutral material is extremely sharp (the mean free path of photons is much smaller than radius of Strömgren sphere)

photoionized gas 3

How long does it take to ionize the Strömgren Volume?

- we know rate Q_0 and number of H atoms therefore

$$\tau_{\rm ion} = \frac{(4\pi/3)R_{\rm S}^3 n_H}{Q_0} = \frac{1}{\alpha n_H} \approx \frac{10^3\,{\rm Jahre}}{n_H/100{\rm cm}^{-3}}$$

- if we "switch off" the star, we get the same

$$\tau_{\rm rec} = \frac{1}{\alpha n_H} \approx \frac{10^3\,{\rm Jahre}}{n_H/100{\rm cm}^{-3}}$$

- the temperature of the ionized gas is very high, about 10^4 K. the pressure within the Strömgren sphere therefore is much larger than the on in the surrounding atomic ISM. the sphere begins to expand. what are the timescales for this?
- to estimate this time, let us compute the sound crossing time:

speed of sound : $c_{\rm s} = (2kT/m_H)^{1/2} \approx 12.8\,{\rm km/s}$ at 10^4 K

thus: $\tau_{\rm dyn} = \frac{R_{\rm S}}{c_{\rm s}} \ll \tau_{\rm ion}$ with typical values of ~10^5 years

- that means, the Strömgren sphere is "instantaneously" ionized and then begins to expand on timescales of a few 10^5 years atomic gas

atomic gas

atomic hydrogen ***HI***

- most important observations: 21 cm line (1420 MHz, 6x10-6 eV)
- hyperfine structure transition

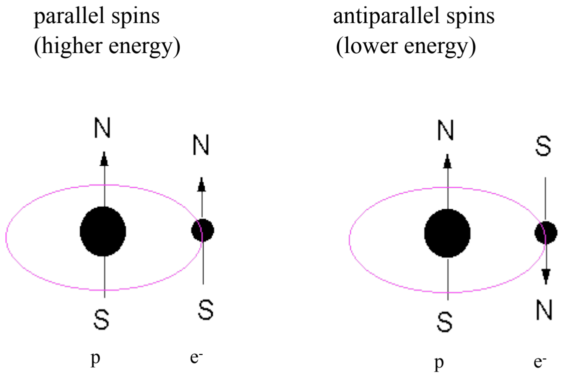

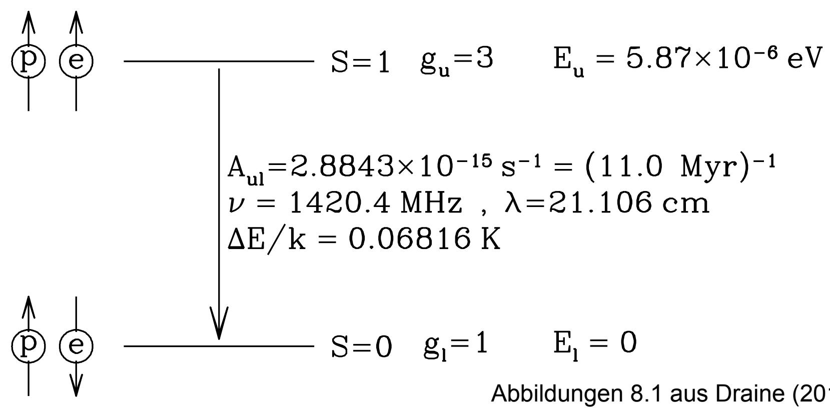

Abbildungen 8.1 aus Draine (2011)

typical timescales
- collisional excitation (t_c ~ 500 yr)
- radiative de-exitation (t_r ~ $1\text{x}10^7$ yr)

optically thin, works well to study Galactic structure

well described by 2-level model

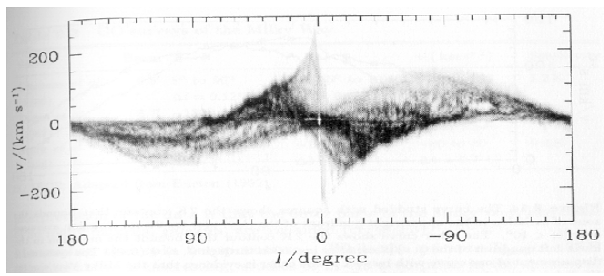

21 cm Survey of Milky Way
(Leiden/Dwingeloo Survey)

HI sky

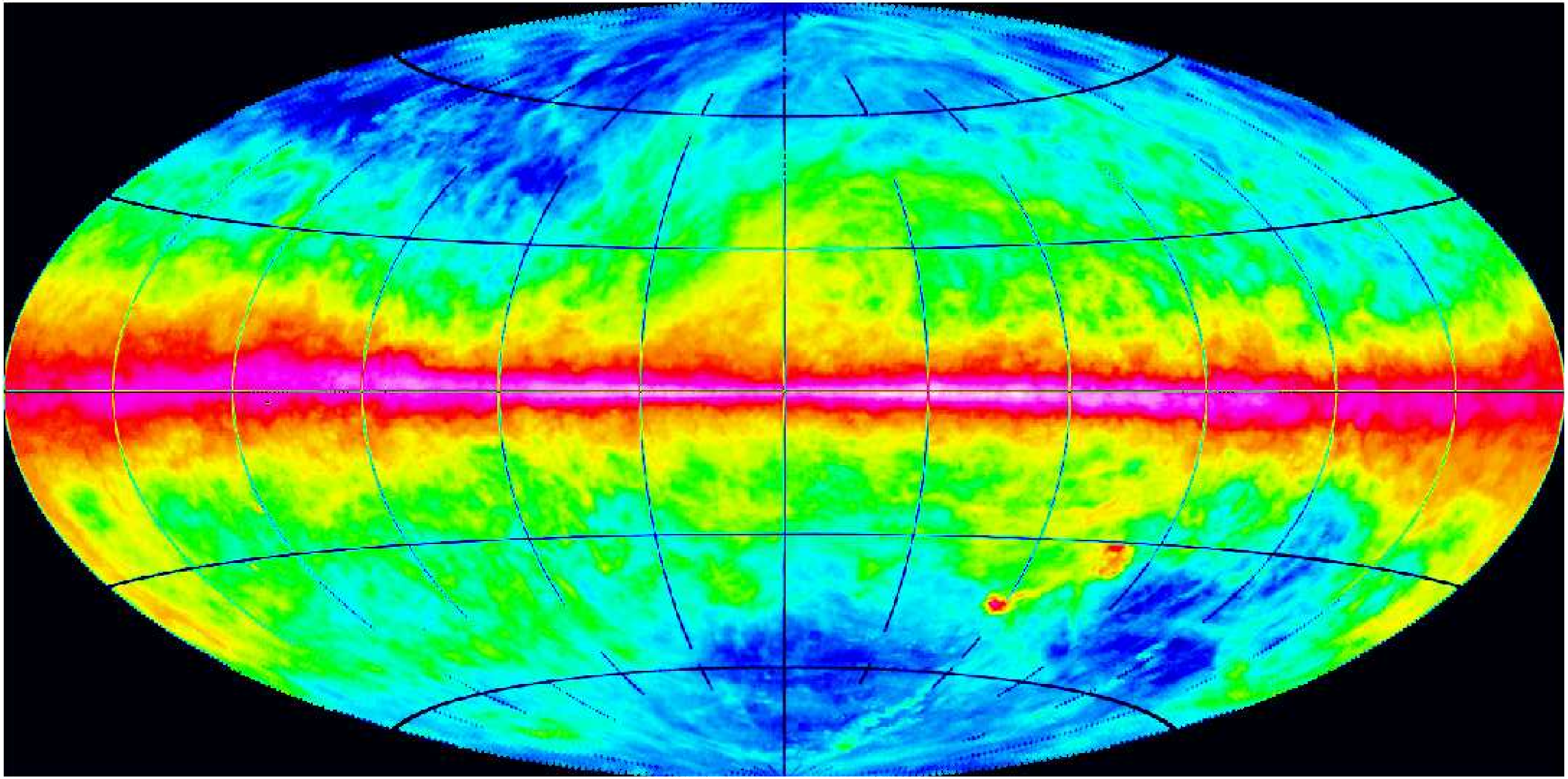

Source: P. Kalberla et al. (Leiden/Argentine/Bonn (LAB) HI Survey) radio sky in 21cm wave

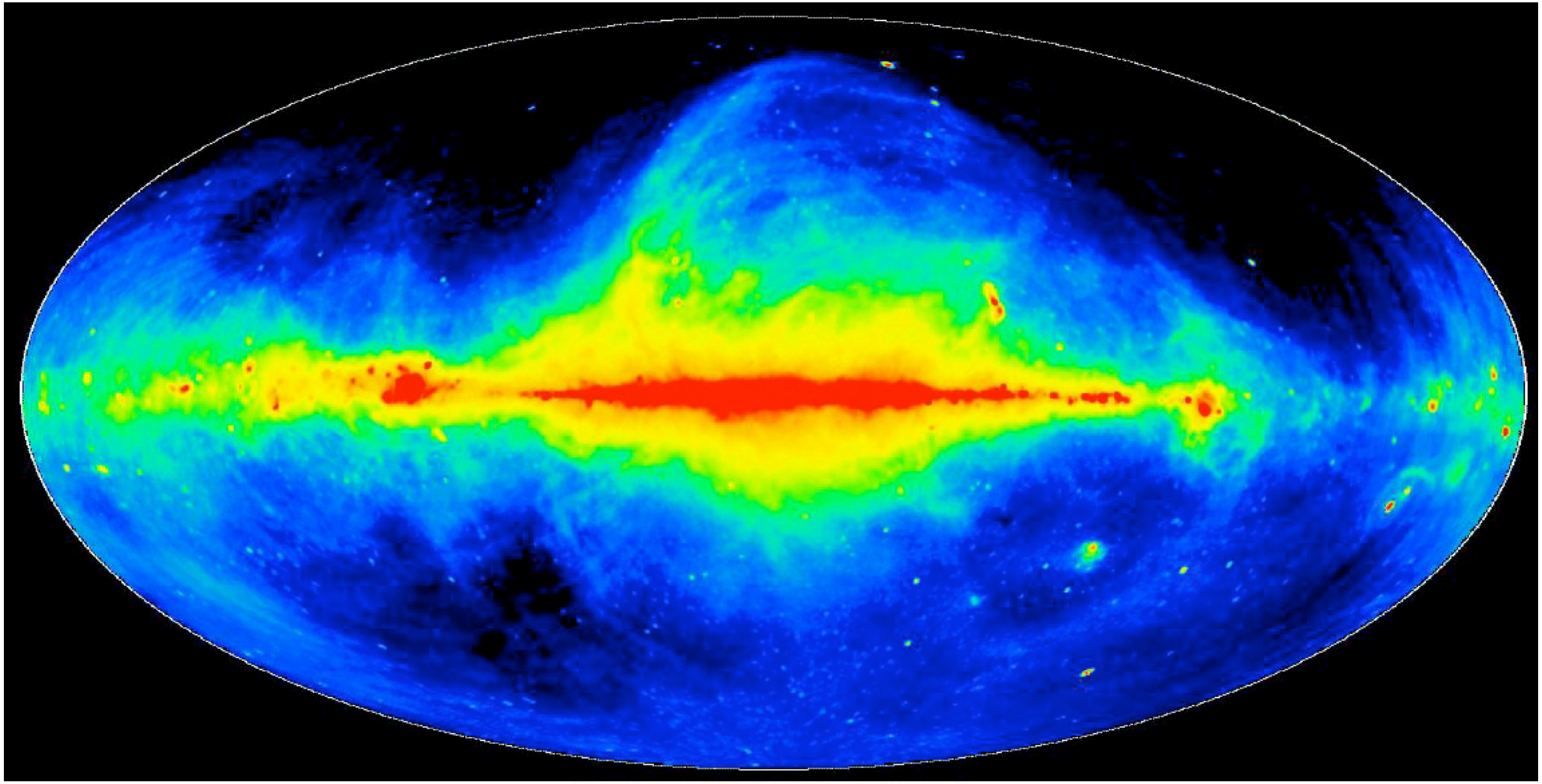

Source: Max-Planck-Institut für Radioastronomie
P. Reich et al. 2001, A&A 376, 861

Corrected for HI emission in Galactic disk

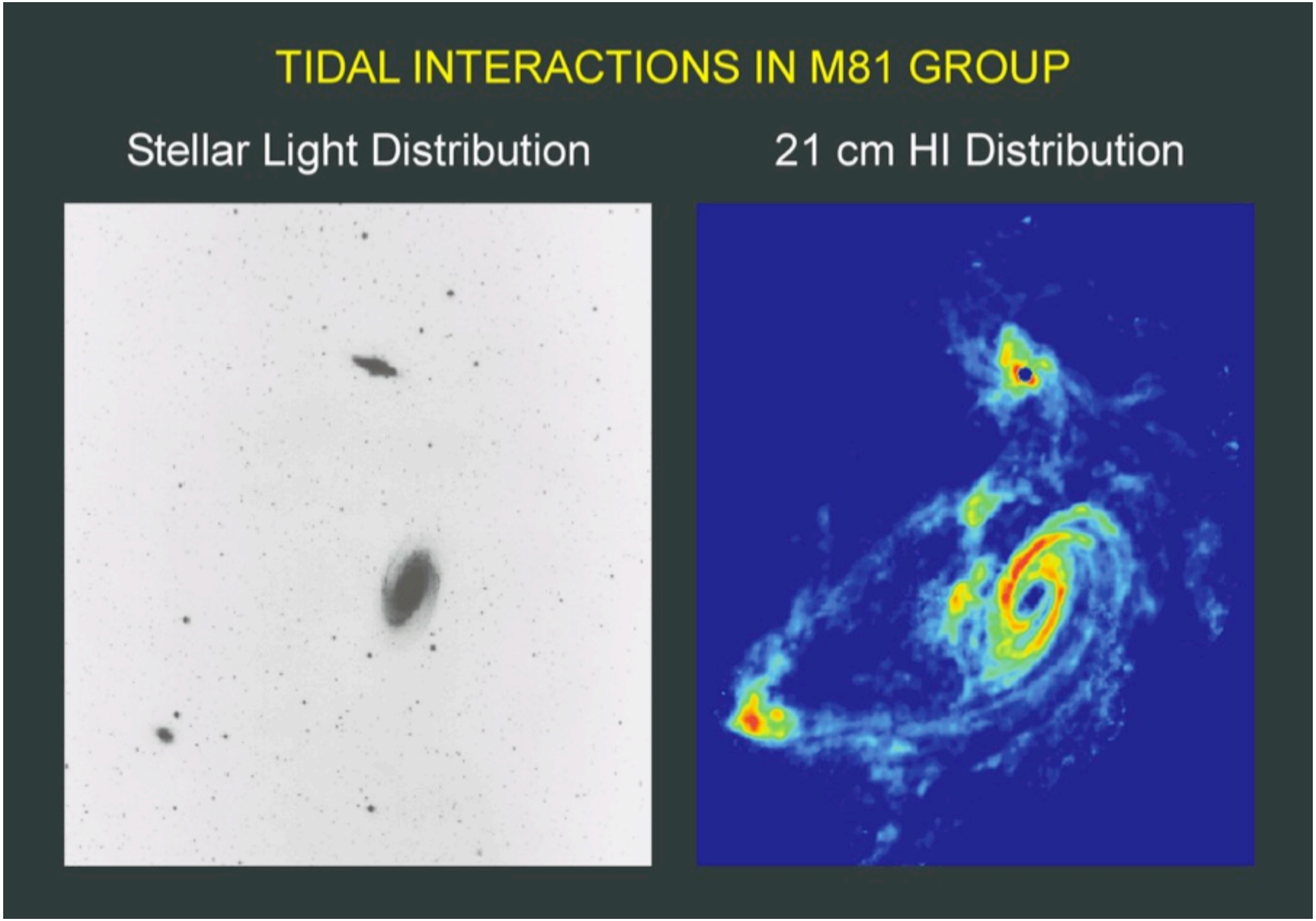

Source: National Radio Astronomy Observatory (NRAO) molecular clouds

molecular clouds

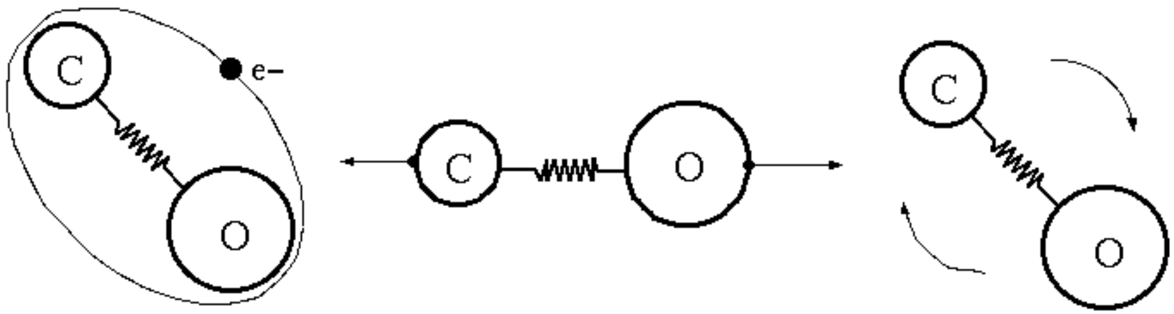

transitions in diatomic molecules

- rotational transitions (needs dipole moment, otherwise “forbidden” quadrupole transition) energy: *~10⁻³ eV*
- vibrational transitions, energy: *~10⁻¹ - 10⁻² eV*
- electronic transitions, energy: *~1 eV*

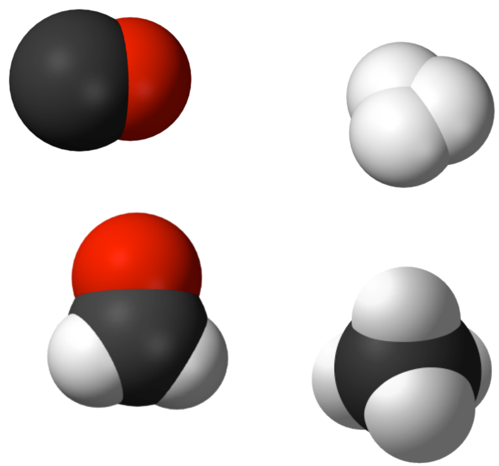

lowes rotational and vibrational transitions

	J = 1 – 0			n = 1 - 0		
	Frequenz	Wellenlänge	T	Frequenz	Wellenlänge	T
H_2	3,87 THz	77 μm	185 K	131 THz	2,28 μm	6300 K
^{12}CO	115 GHz	2,6 mm	5,5 K	64 THz	4,63 μm	3100 K

usually only lowest transitions are excited in the ISM

molecular clouds

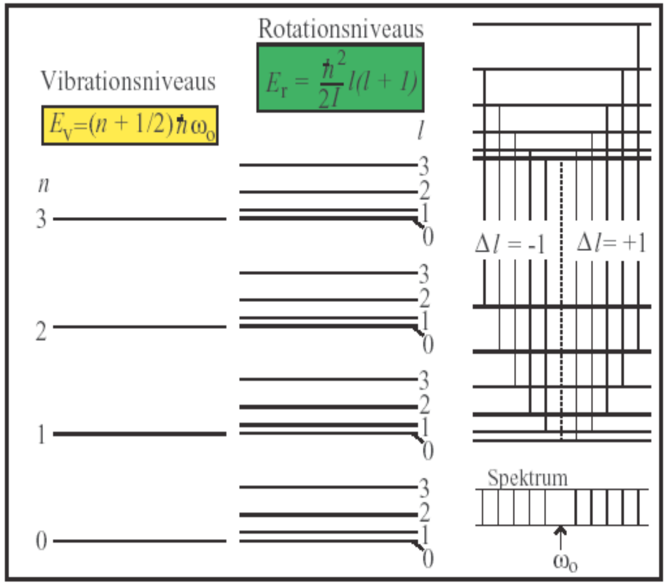

Abbildung 7.3: *Rotations- und Vibrationsniveaus eines zweiatomigen Moleküls mit den nach den Auswahlregeln möglichen Übergängen.*

Aus: Ryder: Quantenphysik und statistische Physik

because of $E_r = \frac{\hbar^2}{2I}\ell(\ell+1)$

and $\Delta l = \pm 1$ we get for the transition energy:

$$\Delta E_{\ell+1\to\ell} = \frac{\hbar^2}{I}\ell$$

where I is the moment of inertia

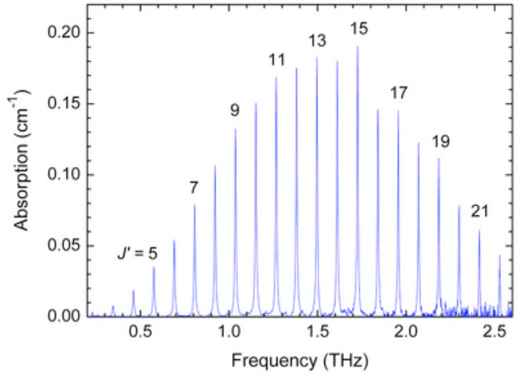

lowes rotational and vibrational transitions

	J = 1 – 0			n = 1 - 0		
	Frequenz	Wellenlänge	T	Frequenz	Wellenlänge	T
H_2	3,87 THz	77 µm	185 K	131 THz	2,28 µm	6300 K
^{12}CO	115 GHz	2,6 mm	5,5 K	64 THz	4,63 µm	3100 K

usually only lowest transitions are excited in the ISM

Table 2.4 *Characteristics of molecular cooling lines*

Species	Transition	ν_{ul}(GHz)	E_u(K)	A_{ul} (s^{-1})	n_{cr} (cm^{-3})
CO	1–0	115.3	5.5	7.2×10^{-8}	1.1×10^{3}
	2–1	230.8	16.6	6.9×10^{-7}	6.7×10^{3}
	3–2	346.0	33.2	2.5×10^{-6}	2.1×10^{4}
	4–3	461.5	55.4	6.1×10^{-6}	4.4×10^{4}
	5–4	576.9	83.0	1.2×10^{-5}	7.8×10^{4}
	6–5	691.2	116.3	2.1×10^{-5}	1.3×10^{5}
	7–6	806.5	155.0	3.4×10^{-5}	2.0×10^{5}
CS	1–0	49.0	2.4	1.8×10^{-6}	4.6×10^{4}
	2–1	98.0	7.1	1.7×10^{-5}	3.0×10^{5}
	3–2	147.0	14.0	6.6×10^{-5}	1.3×10^{6}
	5–4	244.9	35.0	3.1×10^{-4}	8.8×10^{6}
	7–6	342.9	66.0	1.0×10^{-3}	2.8×10^{7}
	10–9	489.8	129.0	2.6×10^{-3}	1.2×10^{8}
HCO^+	1–0	89.2	4.3	3.0×10^{-5}	1.7×10^{5}
	3–2	267.6	26.0	1.0×10^{-3}	4.2×10^{6}
	4–3	356.7	43.0	2.5×10^{-3}	9.7×10^{6}
HCN	1–0	88.6	4.3	2.4×10^{-5}	2.6×10^{6}
	3–2	265.9	26.0	8.4×10^{-4}	7.8×10^{7}
	4–3	354.5	43.0	2.1×10^{-3}	1.5×10^{8}
H_2CO	2_{12}–1_{11}	140.8	6.8	5.4×10^{-5}	1.1×10^{6}
	3_{13}–2_{12}	211.2	17	2.3×10^{-4}	5.6×10^{6}
	4_{14}–3_{13}	281.5	30	6.0×10^{-4}	9.7×10^{6}
	5_{15}–4_{14}	351.8	47	1.2×10^{-3}	2.6×10^{7}
NH_3	(1,1) inversion	23.7	1.1	1.7×10^{-7}	1.8×10^{3}
	(2,2) inversion	23.7	42	2.3×10^{-7}	2.1×10^{3}
H_2	2–0	1.06×10^{4} [a]	510	2.9×10^{-11}	10
	3–1	1.76×10^{4} [b]	1015	4.8×10^{-10}	300

[a] $\lambda = 28.2\,\mu m$.
[b] $\lambda = 17.0\,\mu m$.

A. Tielens: Physics and Chemistry of the ISM (Cambridge University Press)

interstellar molecules

so far more than 100 interstellar molecules identified

Liste interstellarer Moleküle (2000)

Wasserstoff-Moleküle

H_2	*HD*	H_3^+	**H_2D^+**		

Wasserstoff- und Kohlenstoff-Moleküle

CH	***CH^+***	*C_2*	CH_2	C_2H	*C_3
CH_3	C_2H_2	C_3H(lin)	c-C_3H	*CH_4	c-C_3H_2
H_2CCC(lin)	C_4H	*C_5	*C_2H_4	C_5H	H_2C_4(lin)
CH_3C_2H	C_6H*	H_2C_6	C_7H	CH_3C_4H	*C_8H

Wasserstoff-, Kohlenstoff- (möglich) und Sauerstoff-Moleküle

OH	*CO*	***CO^+***	H_2O	HCO	**HCO^+**
HOC^+	C_2O	CO_2	**H_3O^+**	**$HOCO^+$**	H_2CO
C_3O	CH_2CO	HCOOH	**H_2COH+**	CH_3OH	HC_2CHO
C_5O	CH_3CHO	c-C_2H_4O	CH_3OCHO	CH_2OHCHO	CH_3COOH**?**
CH3OCH3	CH3CH2OH	(CH3)2CO			

Wasserstoff-, Kohlenstoff- (möglich) und Stickstoff-Moleküle

NH	*CN*	*NH_2*	HCN	HNC	**N^2H^+**
NH_3	**$HCNH^+$**	H_2CN	HCCN	C_3N	CH_2CN
CH_2NH	HC_2CN	HC_2NC	NH_2CN	C_3NH	CH_3CN
CH_3NC	**HC_3NH+**	C_5N	CH_3NH_2	CH_2CHCN	HC_5N
CH_3C_3N	CH_3CH_2CN	HC_7N	CH_3C_5N?	HC_9N	$HC_{11}N$

Wasserstoff-, Kohlenstoff- (möglich), Stickstoff- und Sauerstoff-Moleküle

NO	HNO	N2O	HNCO	NH2CHO	

Andere Moleküle

more http://en.wikipedia.org/wiki/List_of_interstellar_and_circumstellar_molecules

what information do we get?

Molecular Gas

CO as tracer of molecular H_2

(analysis of density and velocity structure)

Observations in mm and sub-mm

ESO Swedish European
Sub-mm Telescope SEST

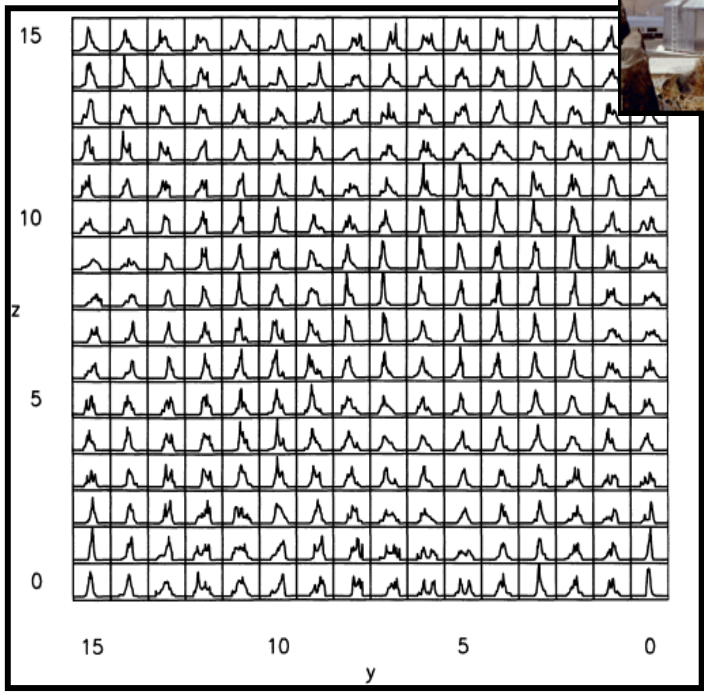

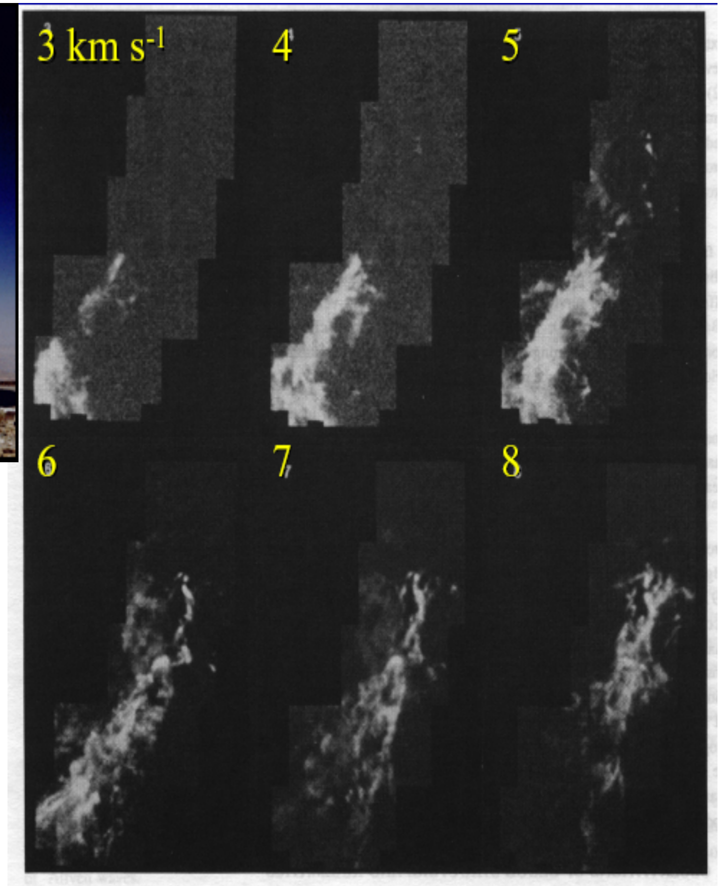

Surface density maps of emision from Orion A (in ^{13}CO) at different velocities (velocity bandwidth is 1 km/s). The size of the region is ~2º x 5º.

Chart of CO spectra at different locations in a MC. With this type of survey one obtains **position-position-velocity cubes** (i.e. surface density at different velocity bands). Velocity information allows for separation of different clouds or cloud components (which are thought to have different relative velocities. *BUT:* **problems with deprojection** (i.e. solutions are not unique and interpretation often misled)

Adopted from B. Stecklum: Physik der Sternentstehung

Phases of interstellar matter

Molecular Gas

Global properties of molecular clouds

	Temperature	Density	Radius	Mass	velocity gradient	E_{rot}/E_{pot}
diffuse molecular clouds (10 ... 50% of total H_2 mass)	T = 40 ... 80 K	n = 100 cm^{-3}				
Dark clouds/globules	T = 20 ... 40 K	n = 10^3 ... 10^4 cm^{-3}	R = 0,1 ... 5 pc	1 ... 10 $M_\odot$	0,5 ... 4 km/s/pc	10^{-3}... 0.3
Giant molecular clouds	T = 10 ... 50 K	n = 10^4 ... 10^6 cm^{-3}	R = 10 ... 100 pc	10^3 ... 10^6 $M_\odot$	0,1 ... 0,2 km/s/pc	10^{-4}... 0.1
Hot cores in MCs	T = 100 ... 300 K	n > 10^7 cm^{-3}	R < 0,1 pc	10 ... 100 $M_\odot$		

Giant molecular clouds are strongly concentrated in the galactic plane and towards the center of the Galaxy (similar holds for external galaxies)

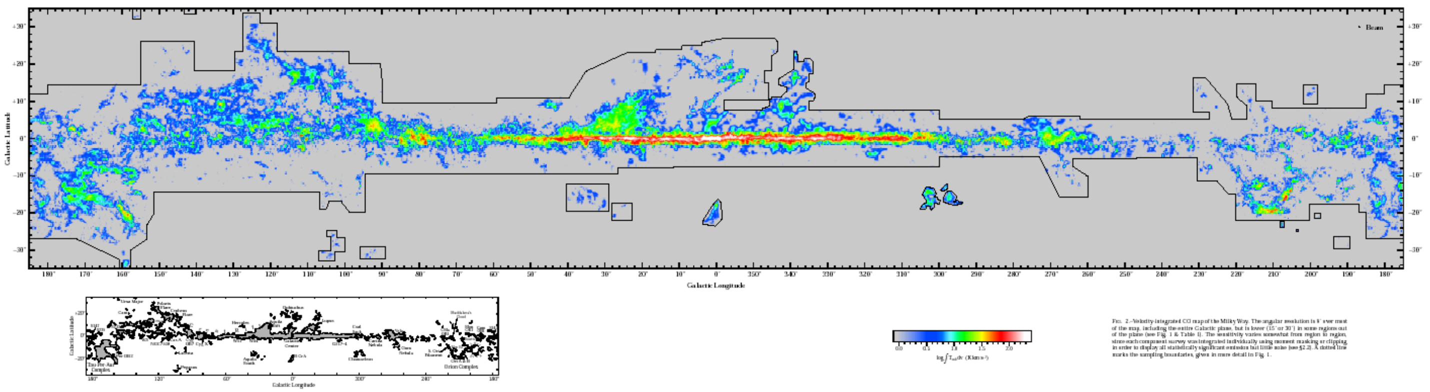

CO Survey of Milky Way
(Dame et al. 2001)

Data from Thomas Dame, CfA Harvard

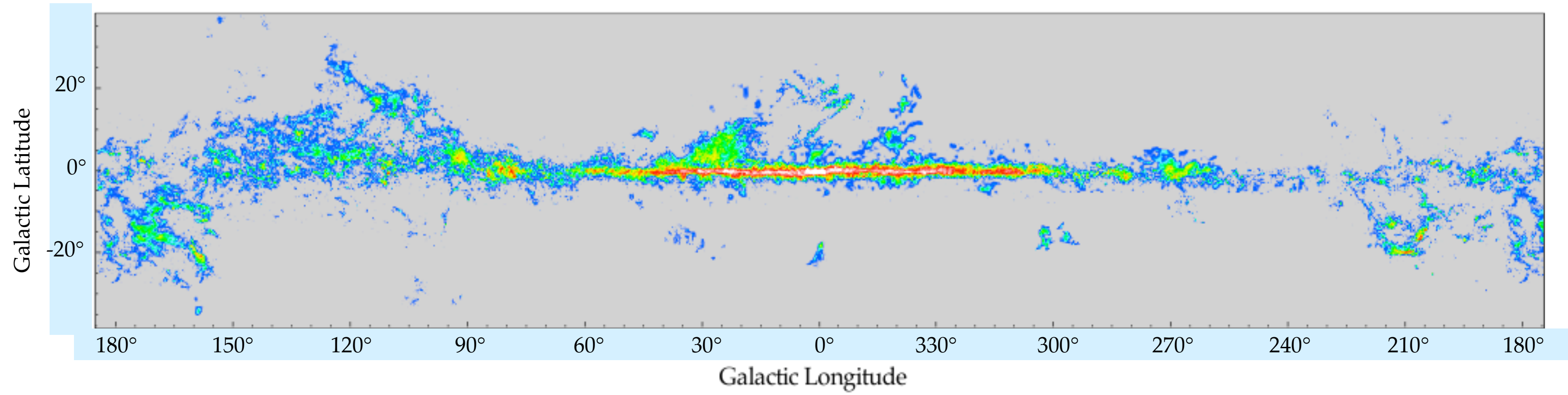

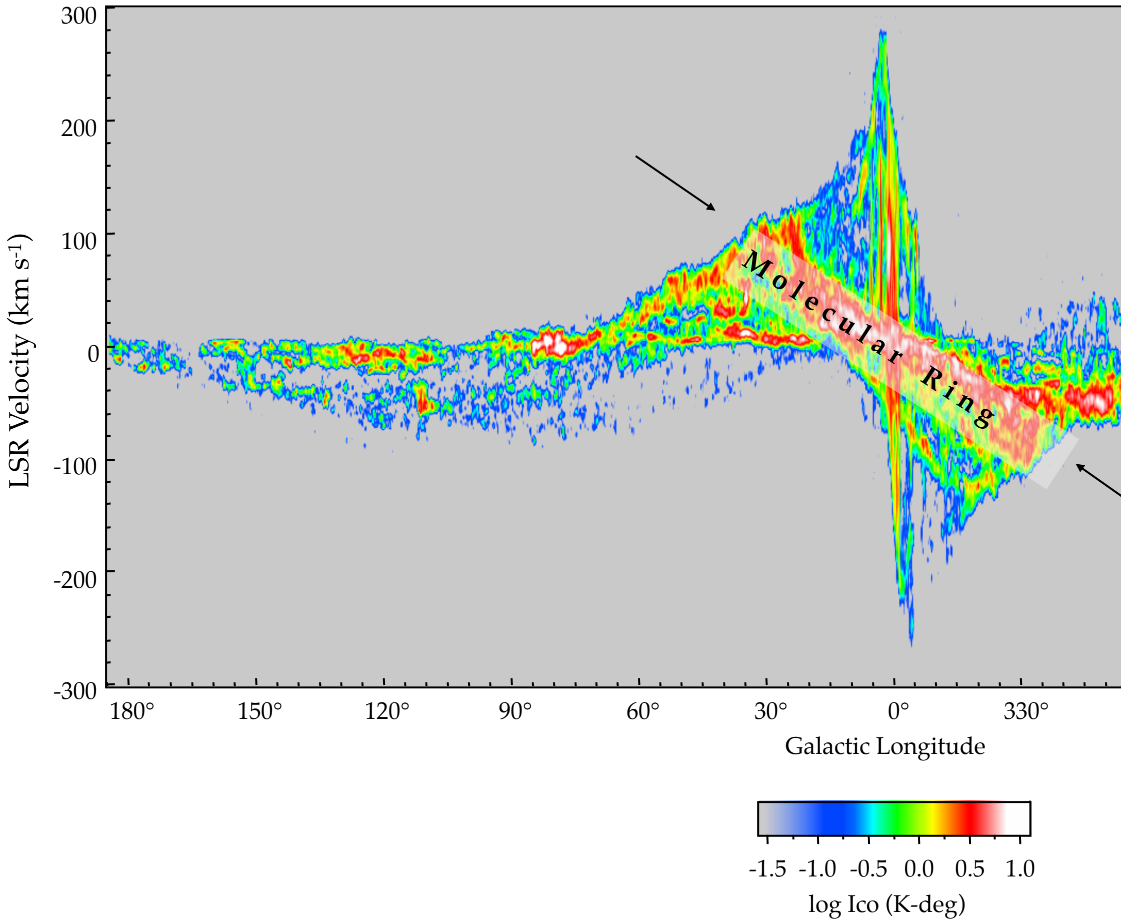

M_{tot} (H_2) ~ 2 x 10^9 M_o

M_{tot} (HI) ~ 6 x 10^9 M_o

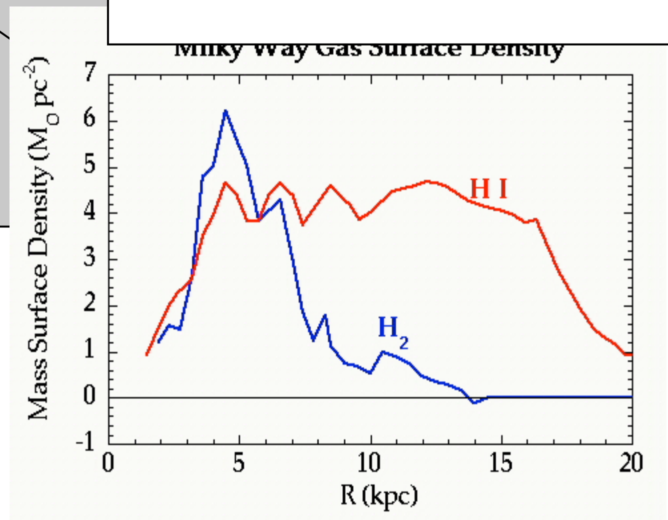

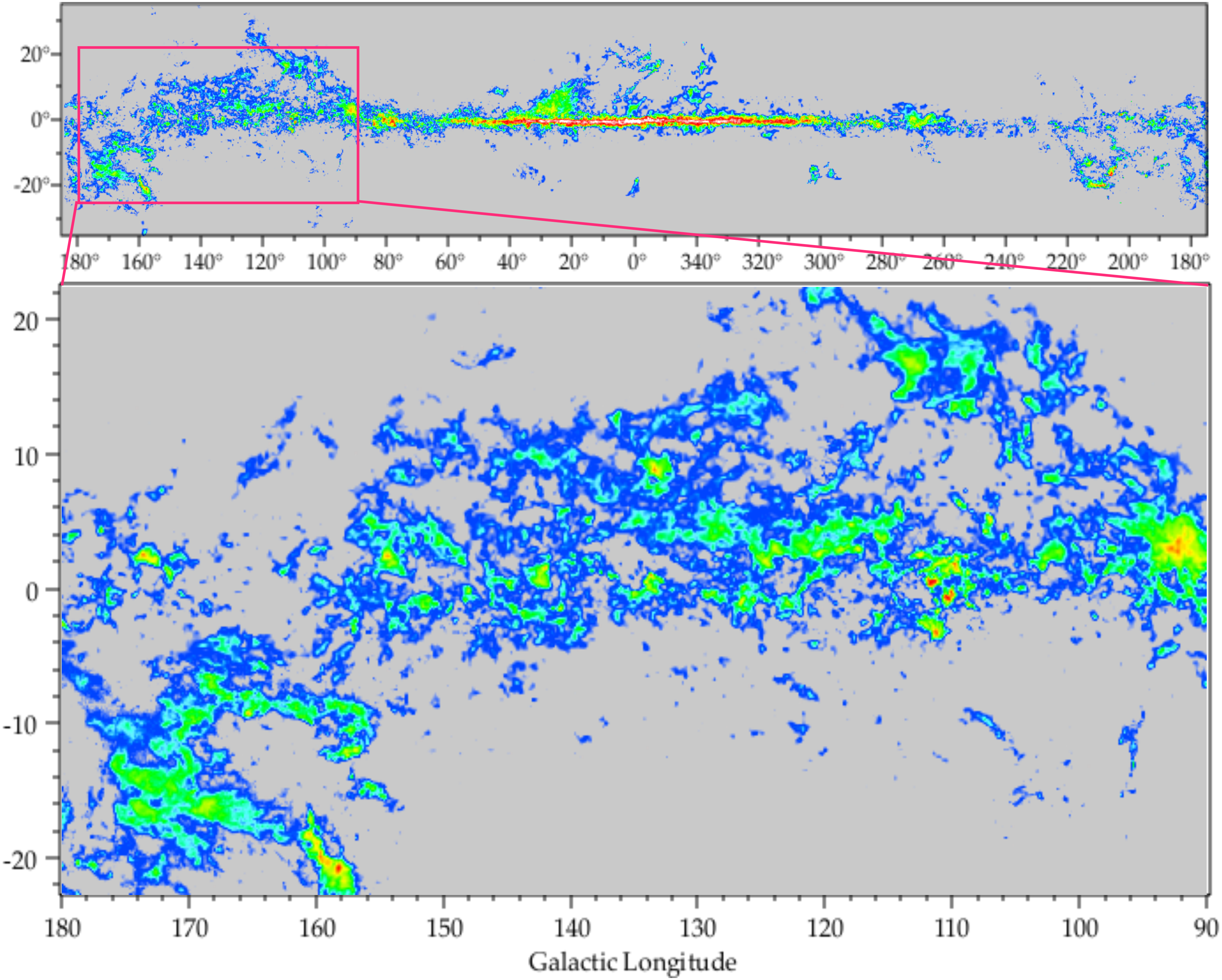

ata from Thomas Dame, CfA Harvard

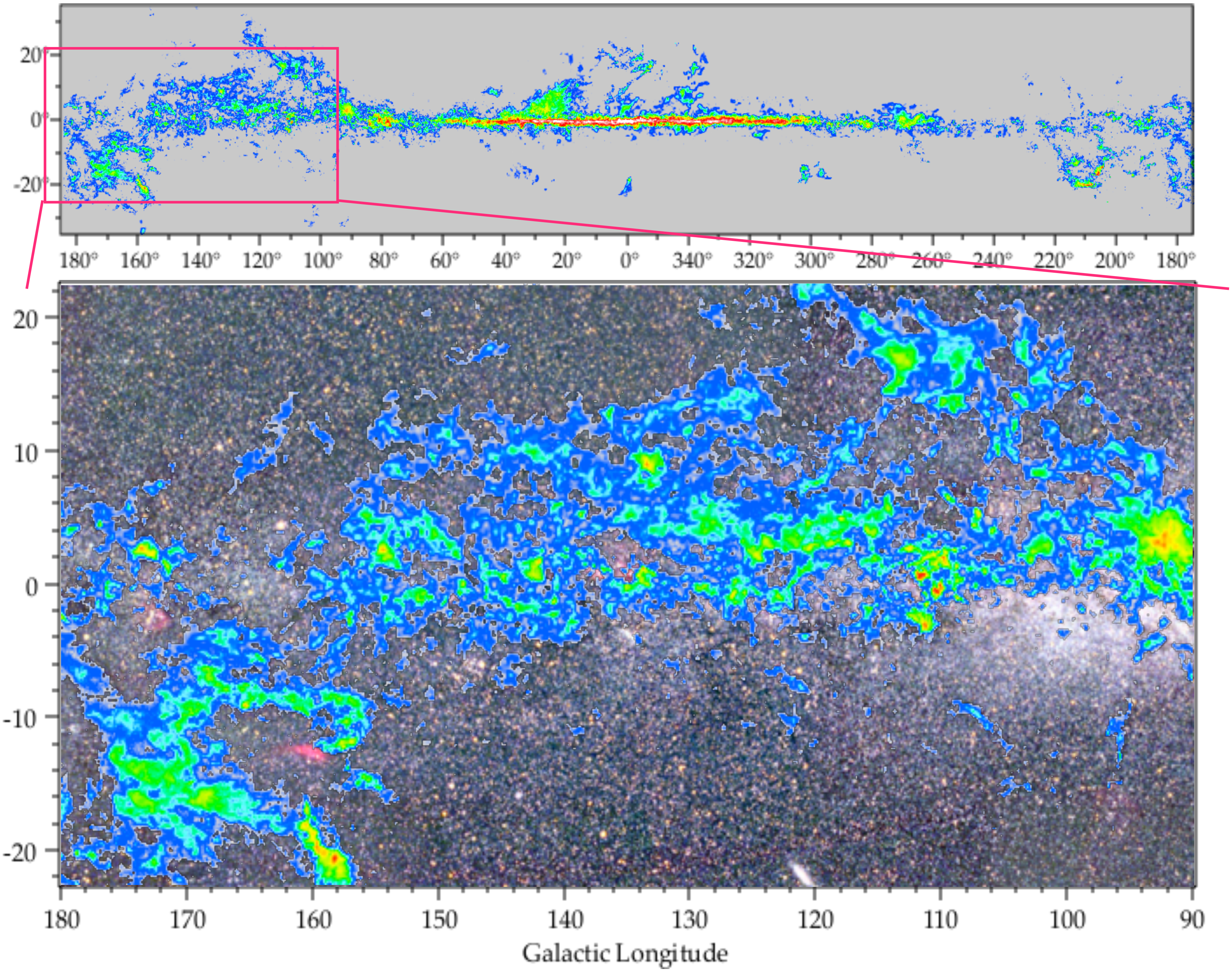

ata from Thomas Dame, CfA Harvard

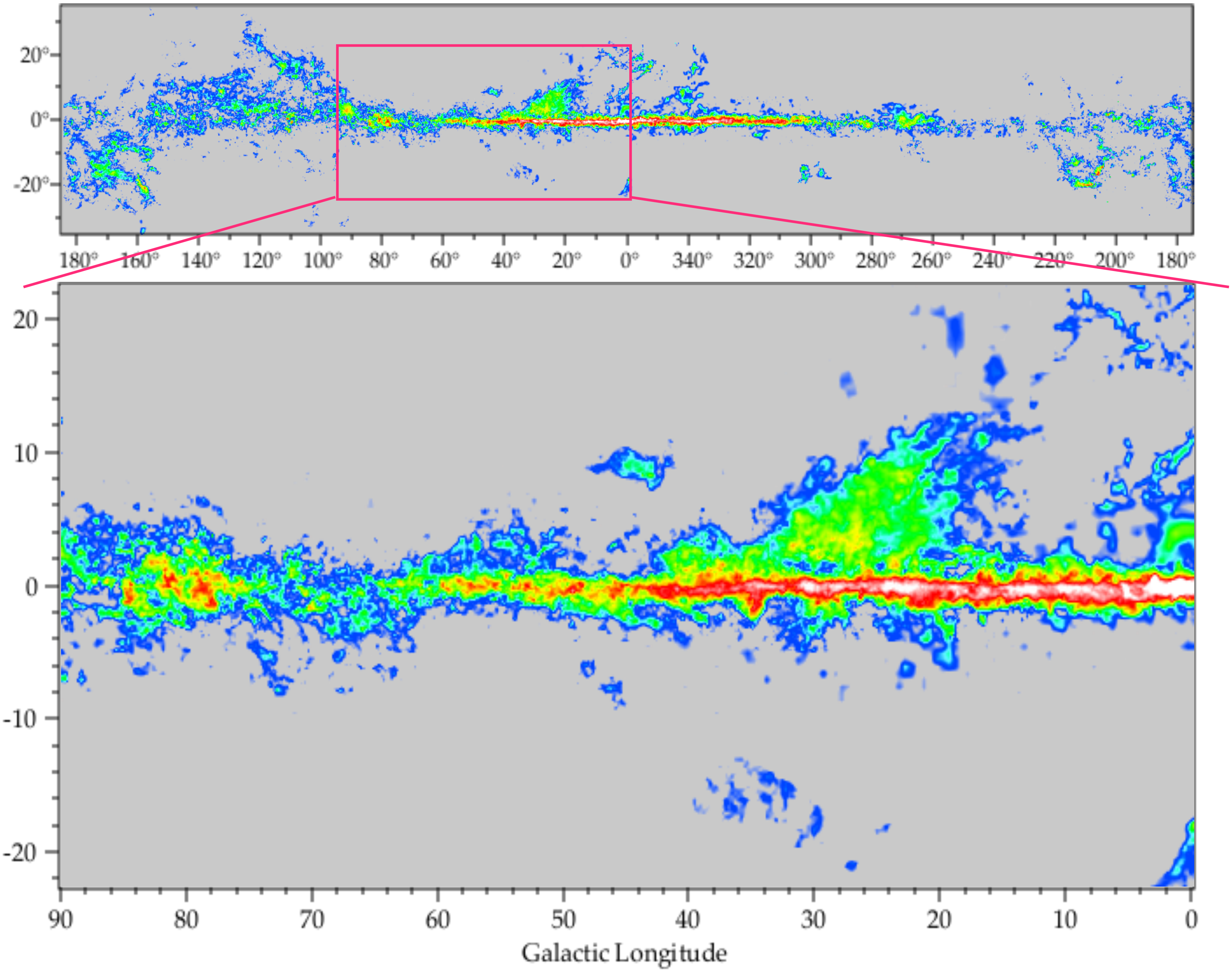

ata from Thomas Dame, CfA Harvard

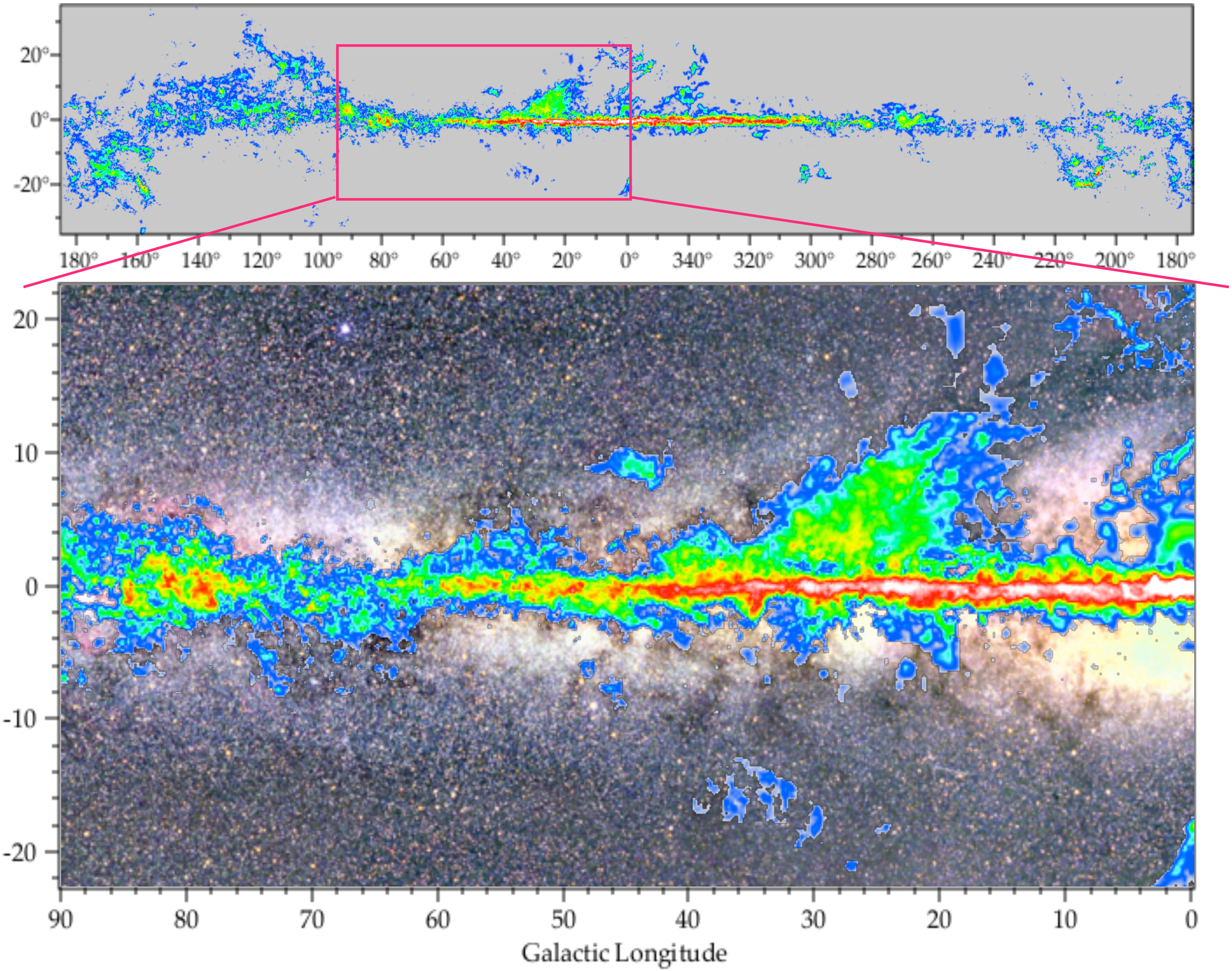

ata from Thomas Dame, CfA Harvard

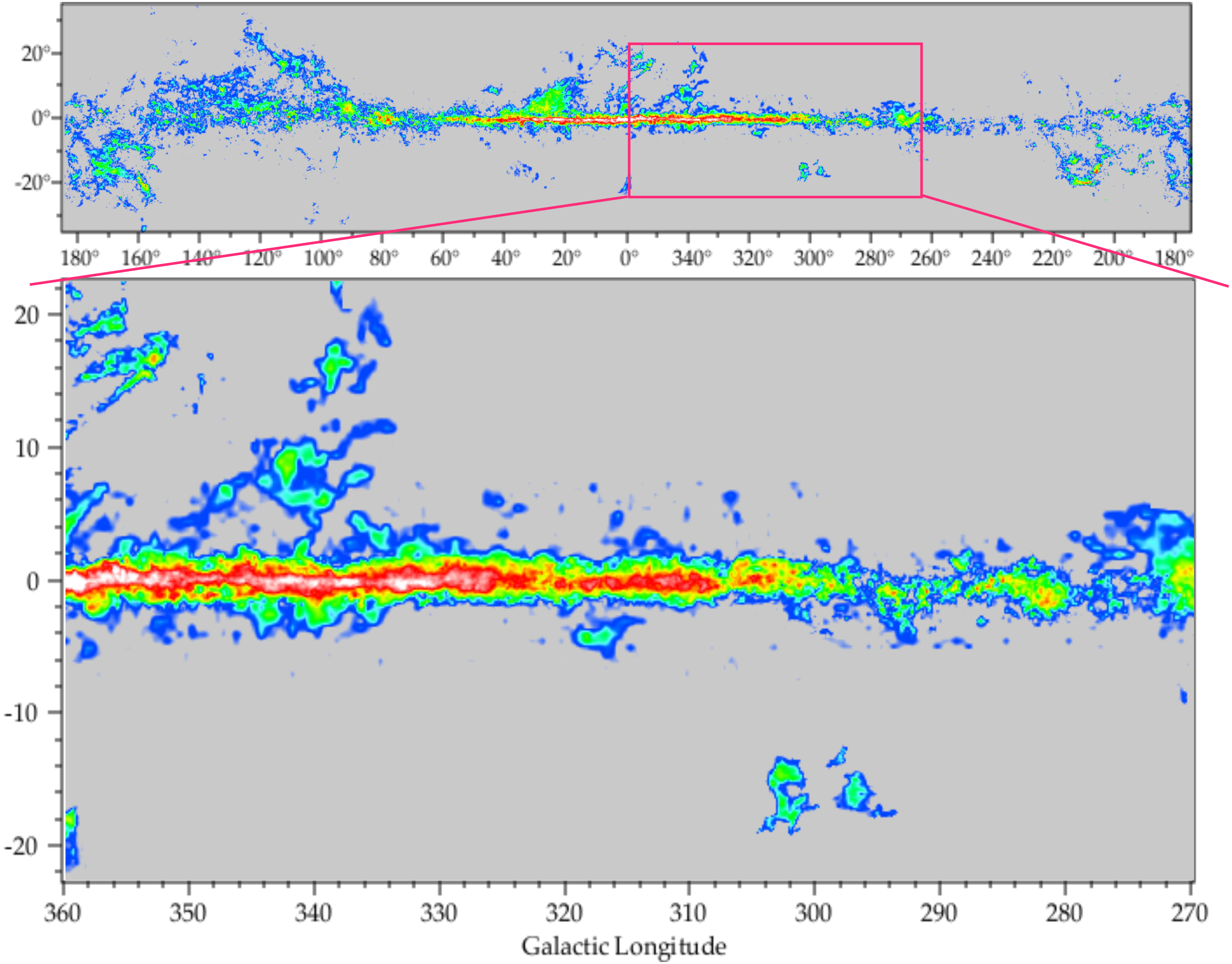

ata from Thomas Dame, CfA Harvard

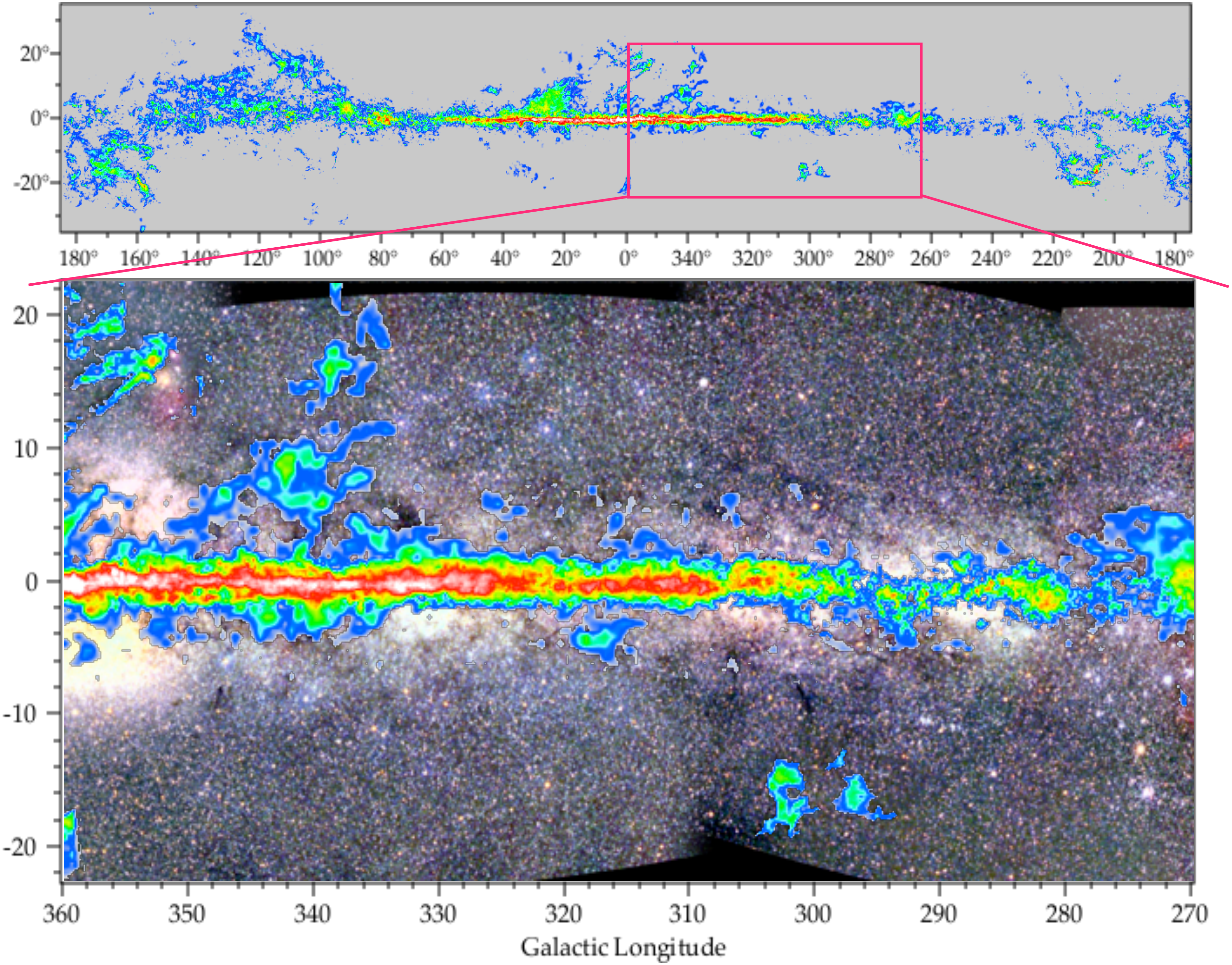

ata from Thomas Dame, CfA Harvard

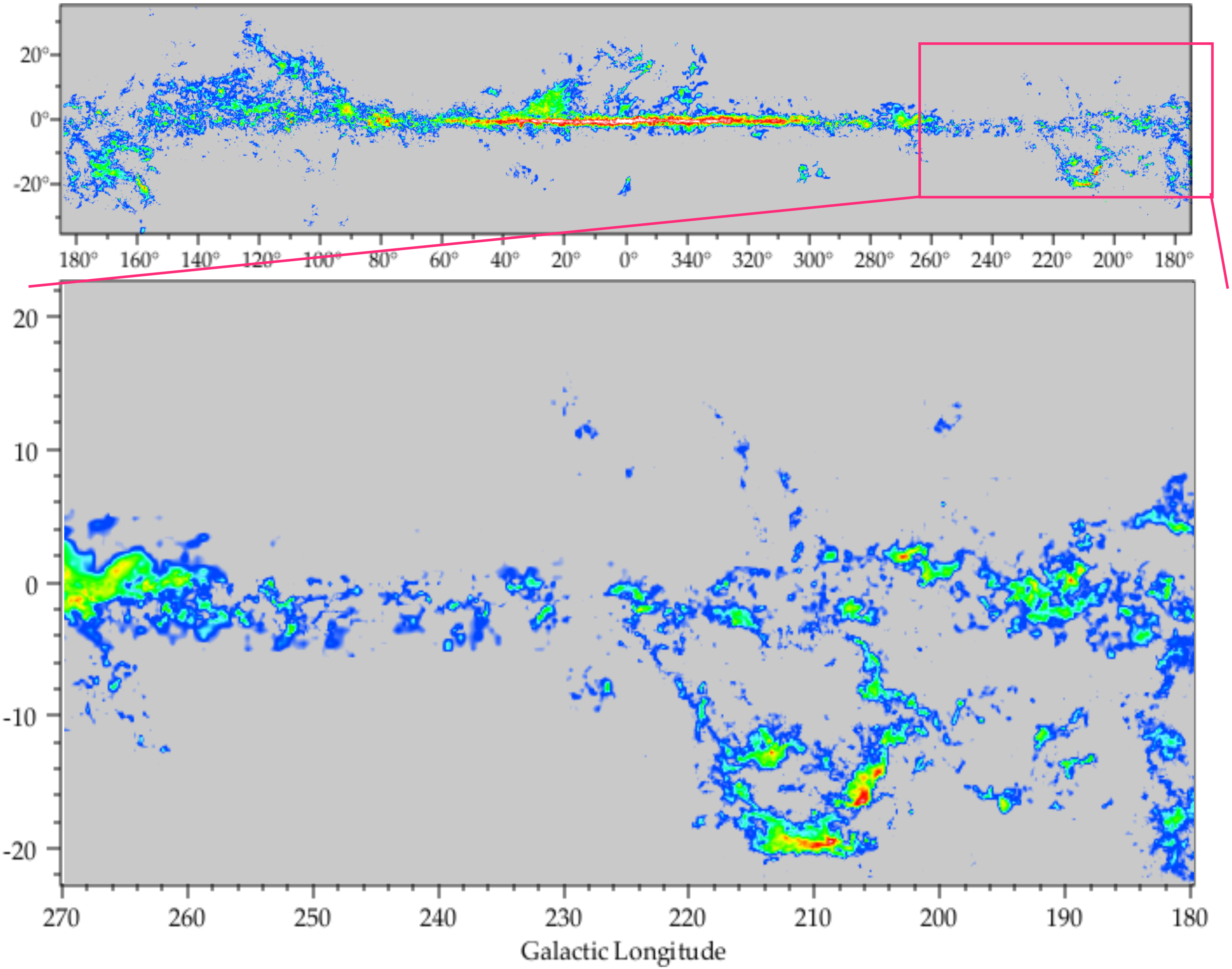

ata from Thomas Dame, CfA Harvard

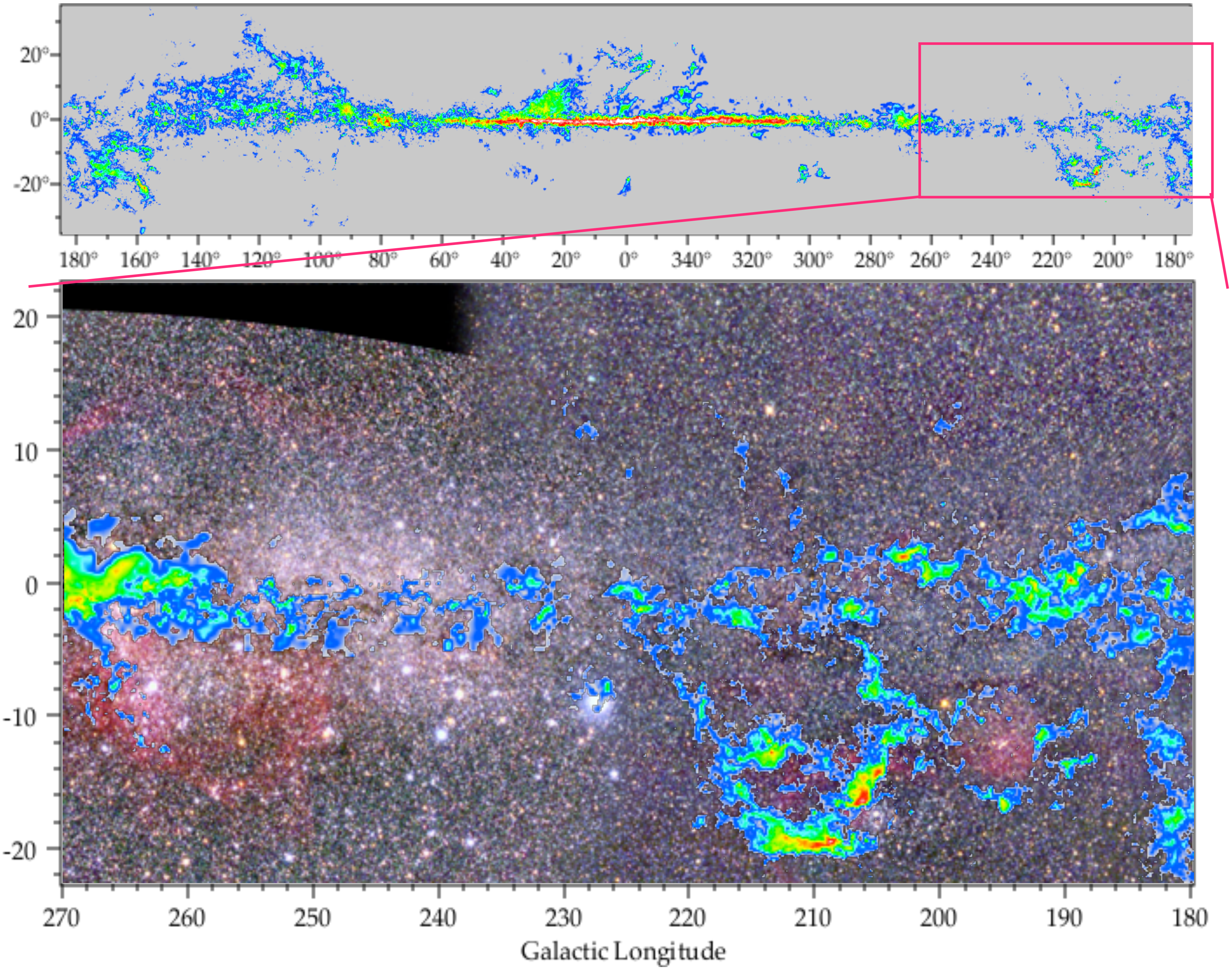

ata from Thomas Dame, CfA Harvard

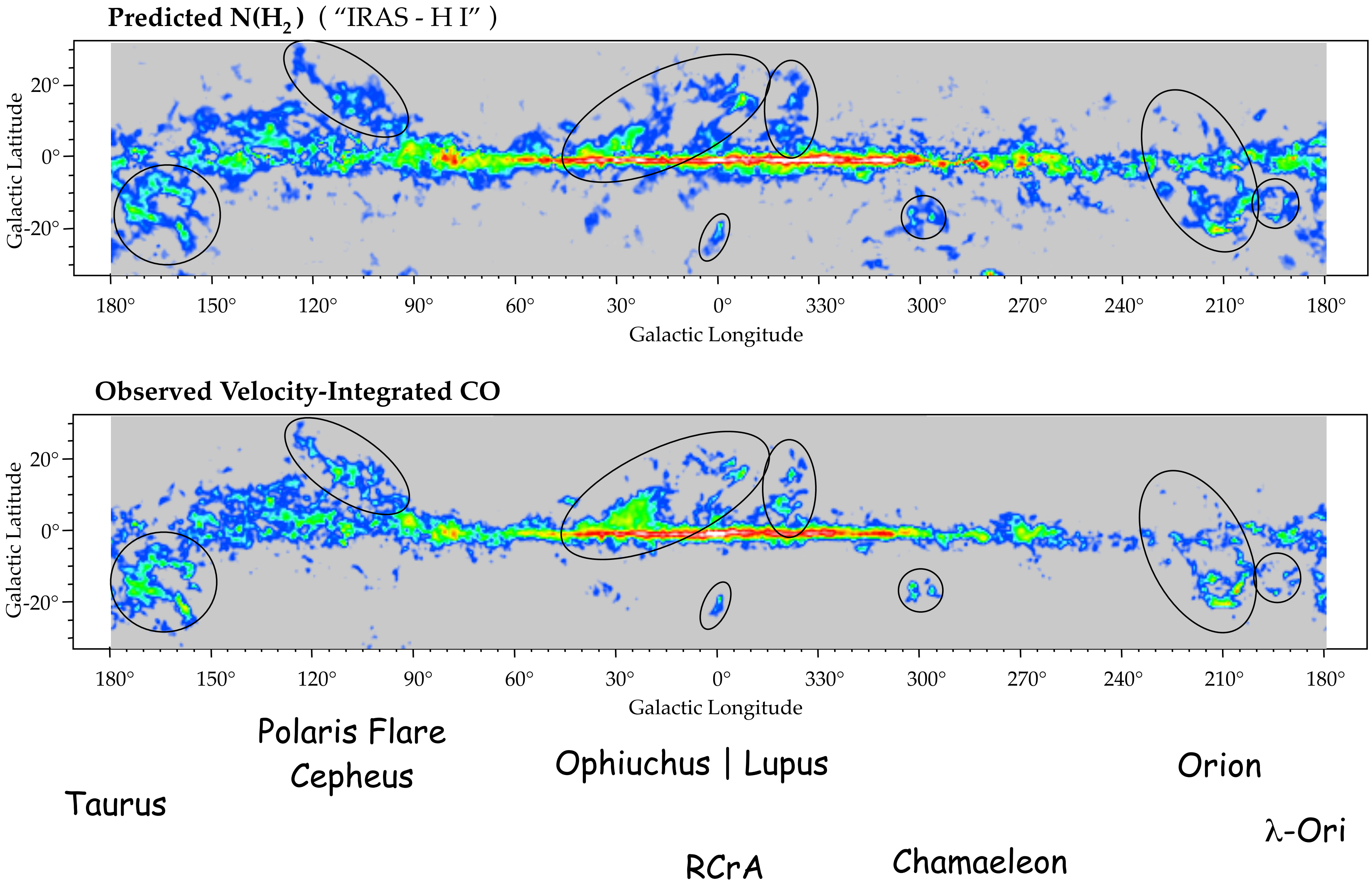

ata from Thomas Dame, CfA Harvard

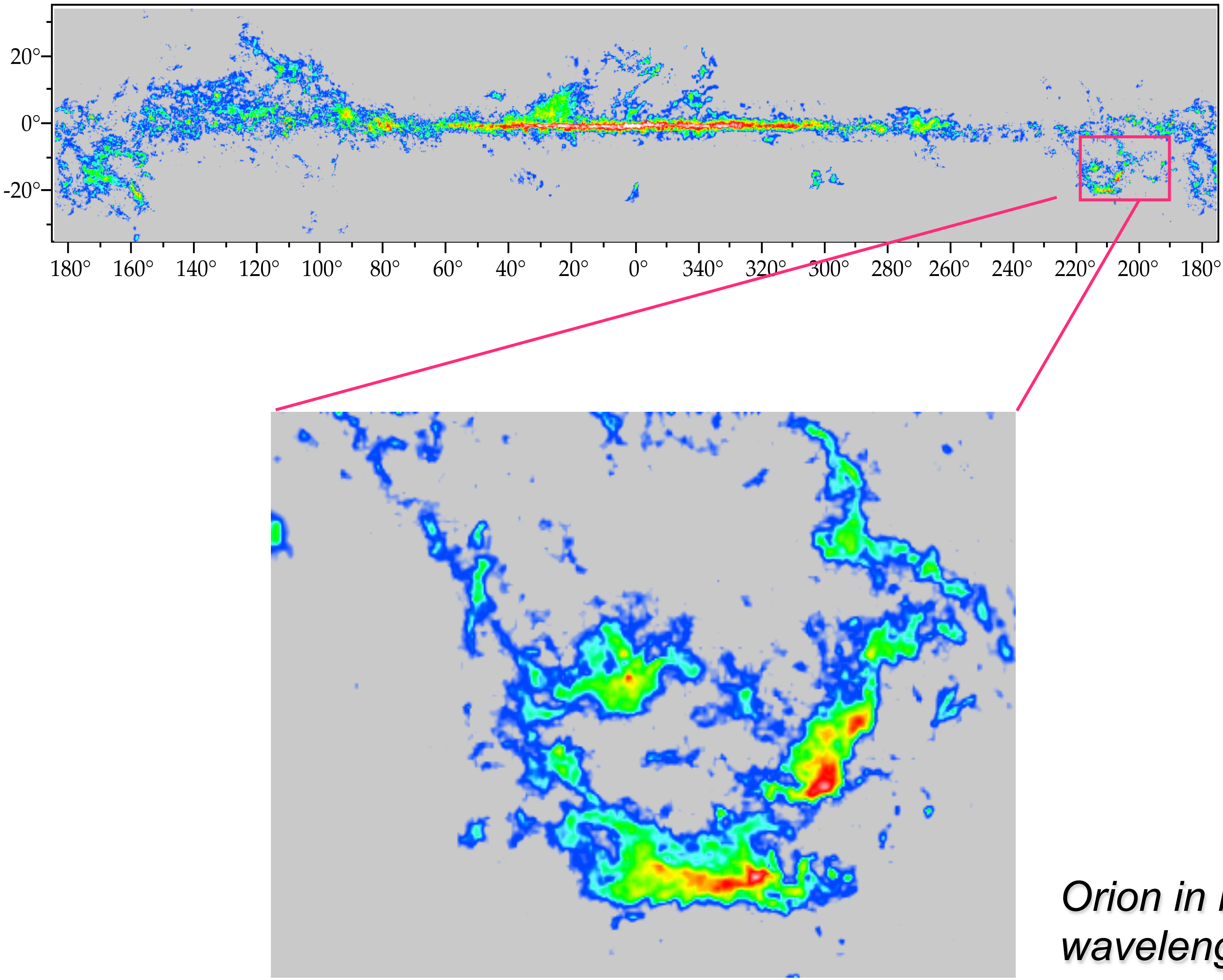

Orion in radio wavelengths

ata from Thomas Dame, CfA Harvard

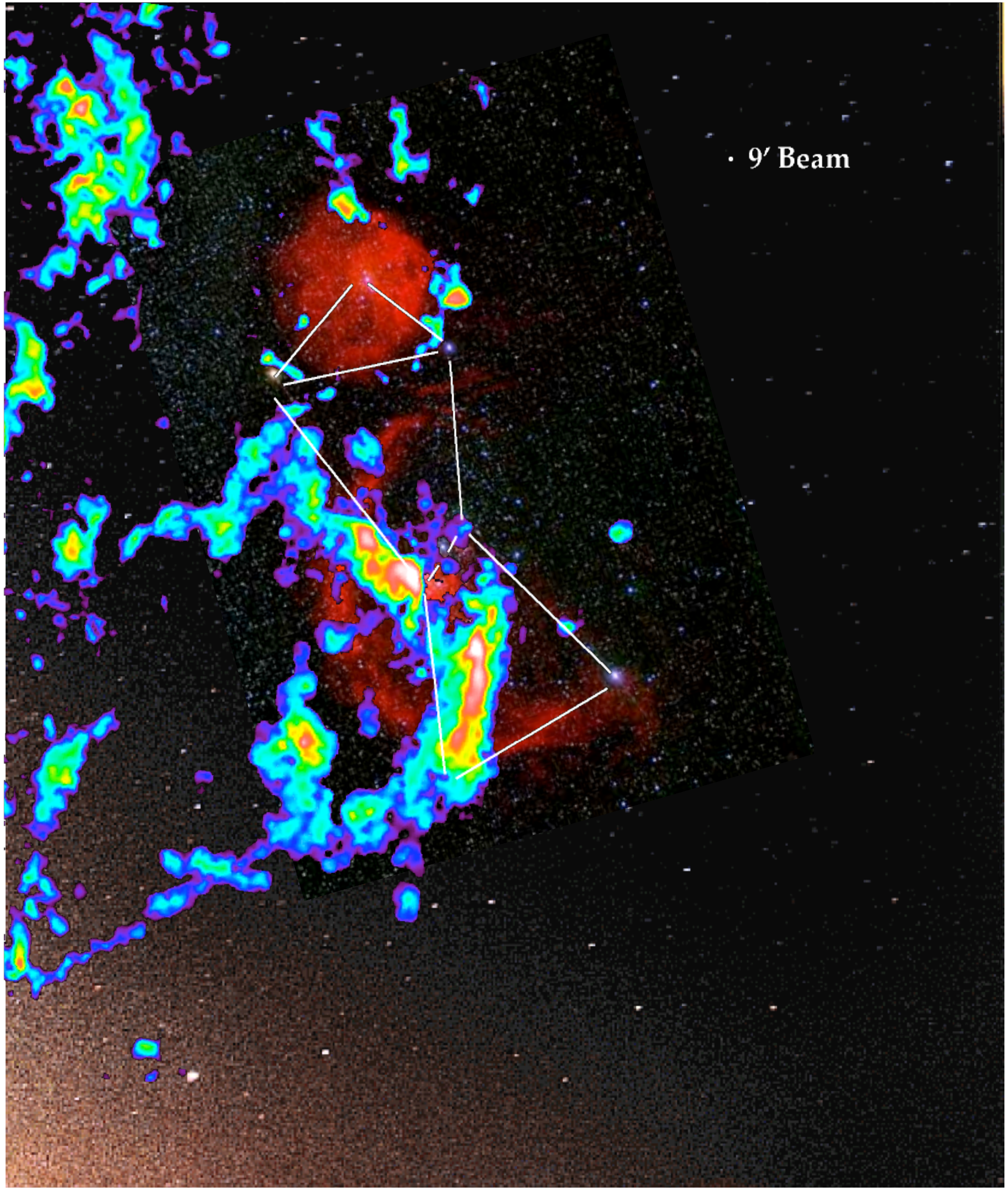

We see

- *stars* (in optical light)
- *atomic hydrogen* (in Hα -- red)
- *molecular hydrogen* H_2 (radio -- color coded)

molecular clouds

- high-density regions in the ISM
- consist mostly of H_2
- cold
- extremely complex velocity and density structure (turbulence, fractal dimension?)
- all stars form in molecular clouds (cause or tracer?)
- mass spectrum $dN/dM \sim M^{-2}$

turbulence statistics

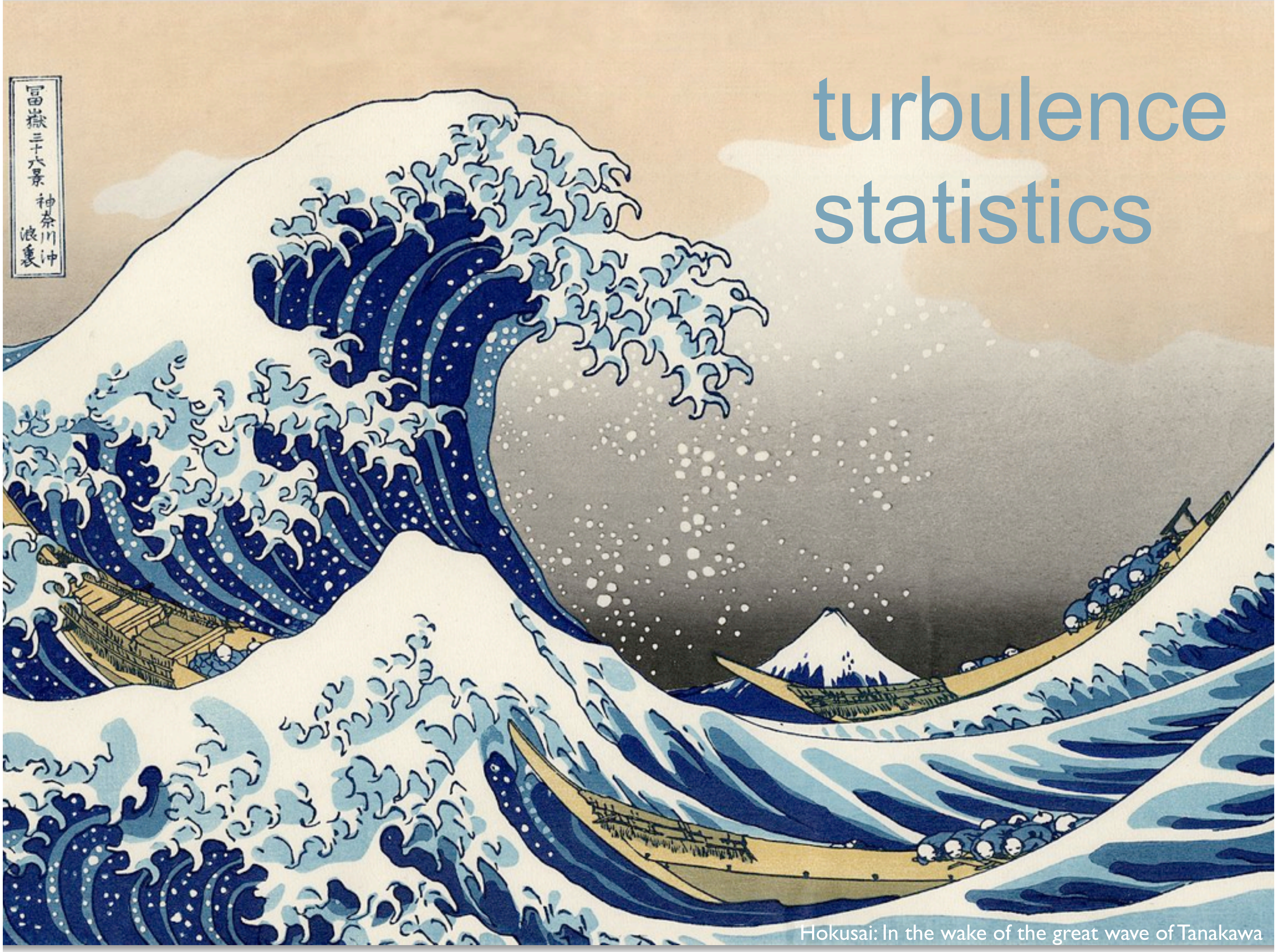

Hokusai: In the wake of the great wave of Tanakawa

COMPLETE = COordinated Molecular Probe Line Extinction Thermal Emission Survey of Star-Forming Regions

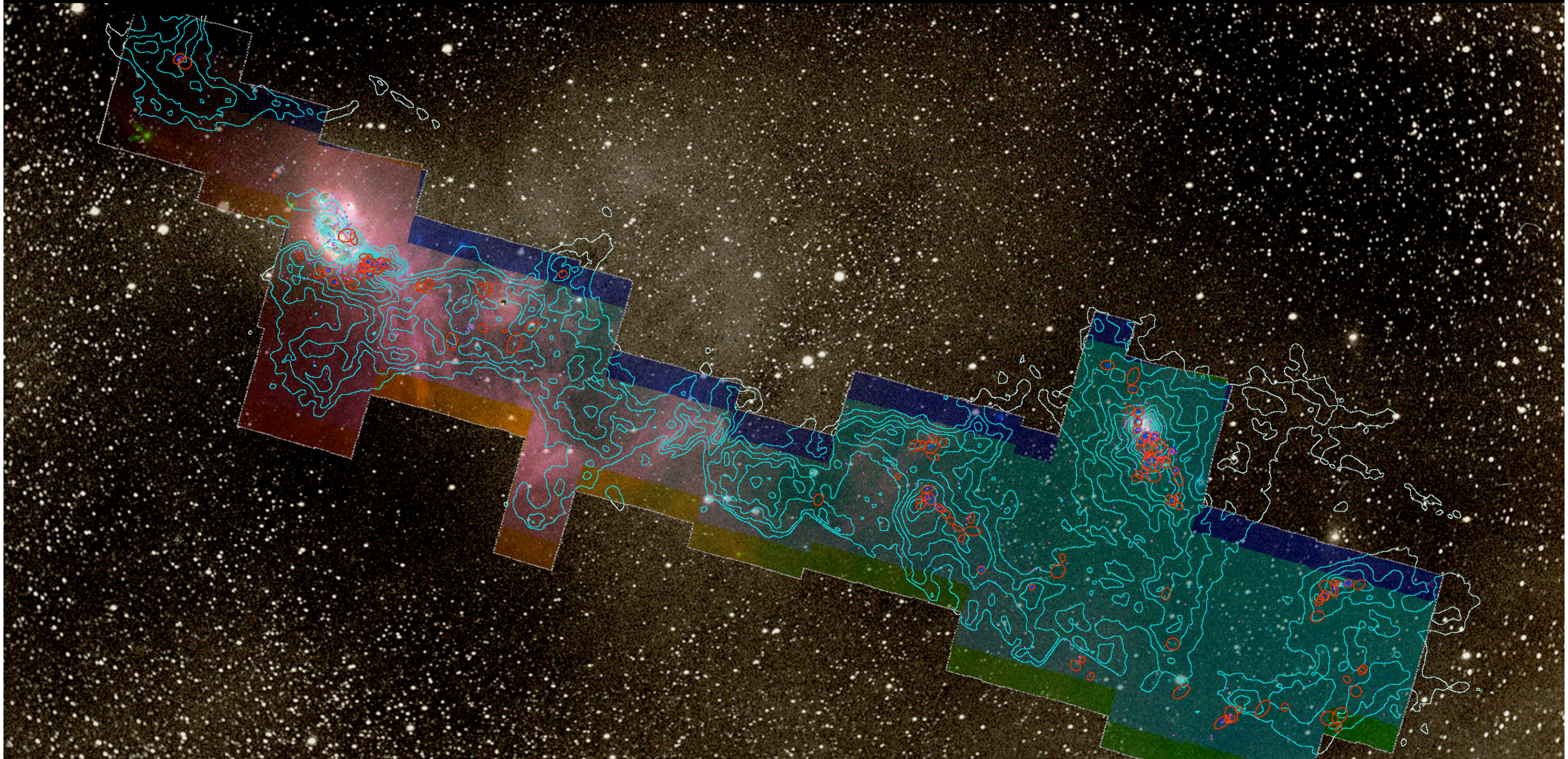

COMPLETE Collaborators, Summer 2008:

Alyssa A. Goodman (CfA/IIC)

João Alves (Calar Alto, Spain)

Héctor Arce (Yale)

Michelle Borkin (IIC)

Paola Caselli (Leeds, UK)

James DiFrancesco (HIA, Canada)

Jonathan Foster (CfA, PhD Student)

Katherine Guenthner (CfA/Leipzig)

Mark Heyer (UMASS/FCRAO)

Doug Johnstone (HIA, Canada)

Jens Kauffmann (CfA/IIC)

Helen Kirk (HIA, Canada)

Di Li (JPL)

Jaime Pineda (CfA, PhD Student)

Erik Rosolowsky (UBC Okanagan)

Rahul Shetty (CfA)

Scott Schnee (Caltech)

Mario Tafalla (OAN, Spain)

COMPLETE Perseus

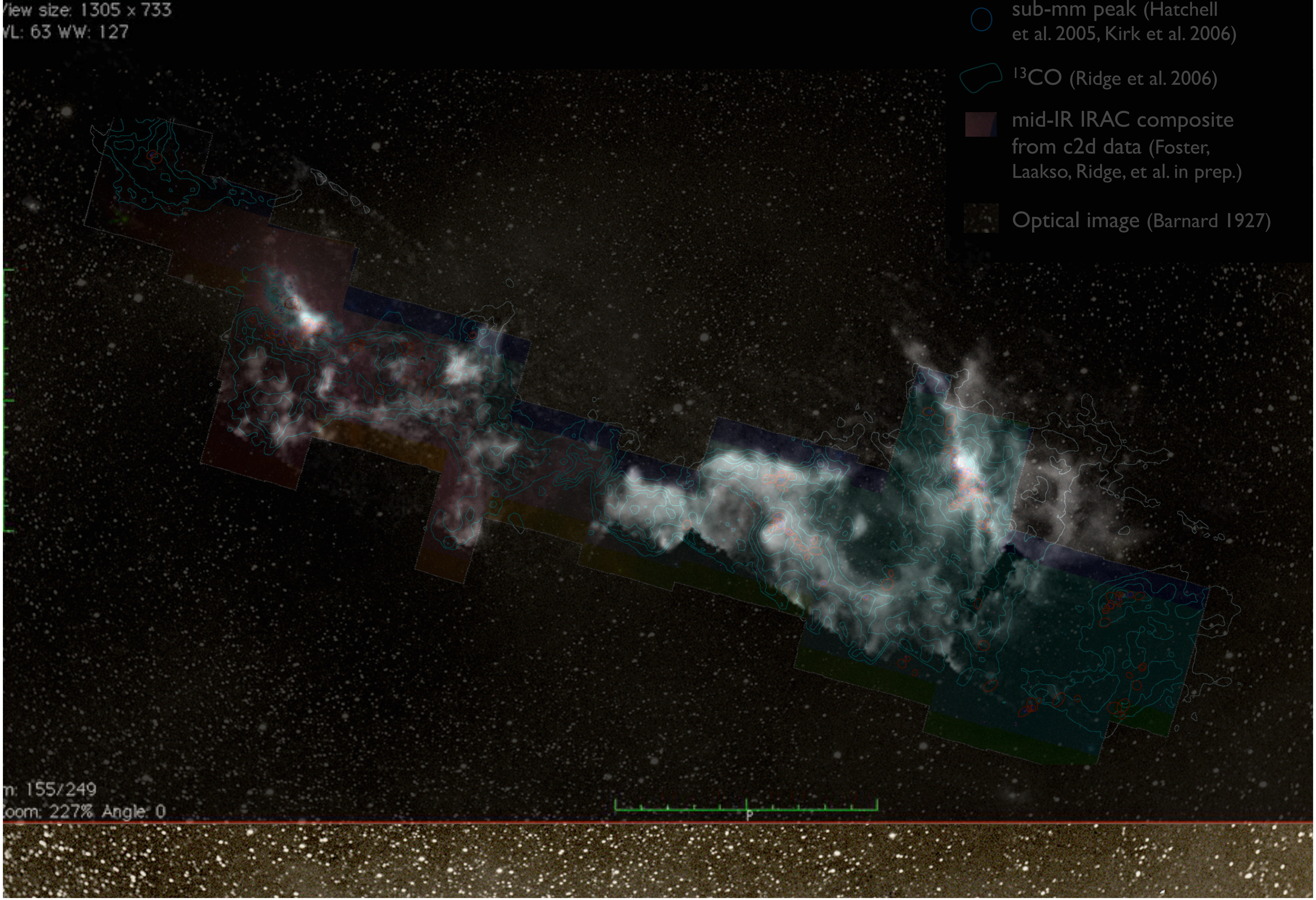

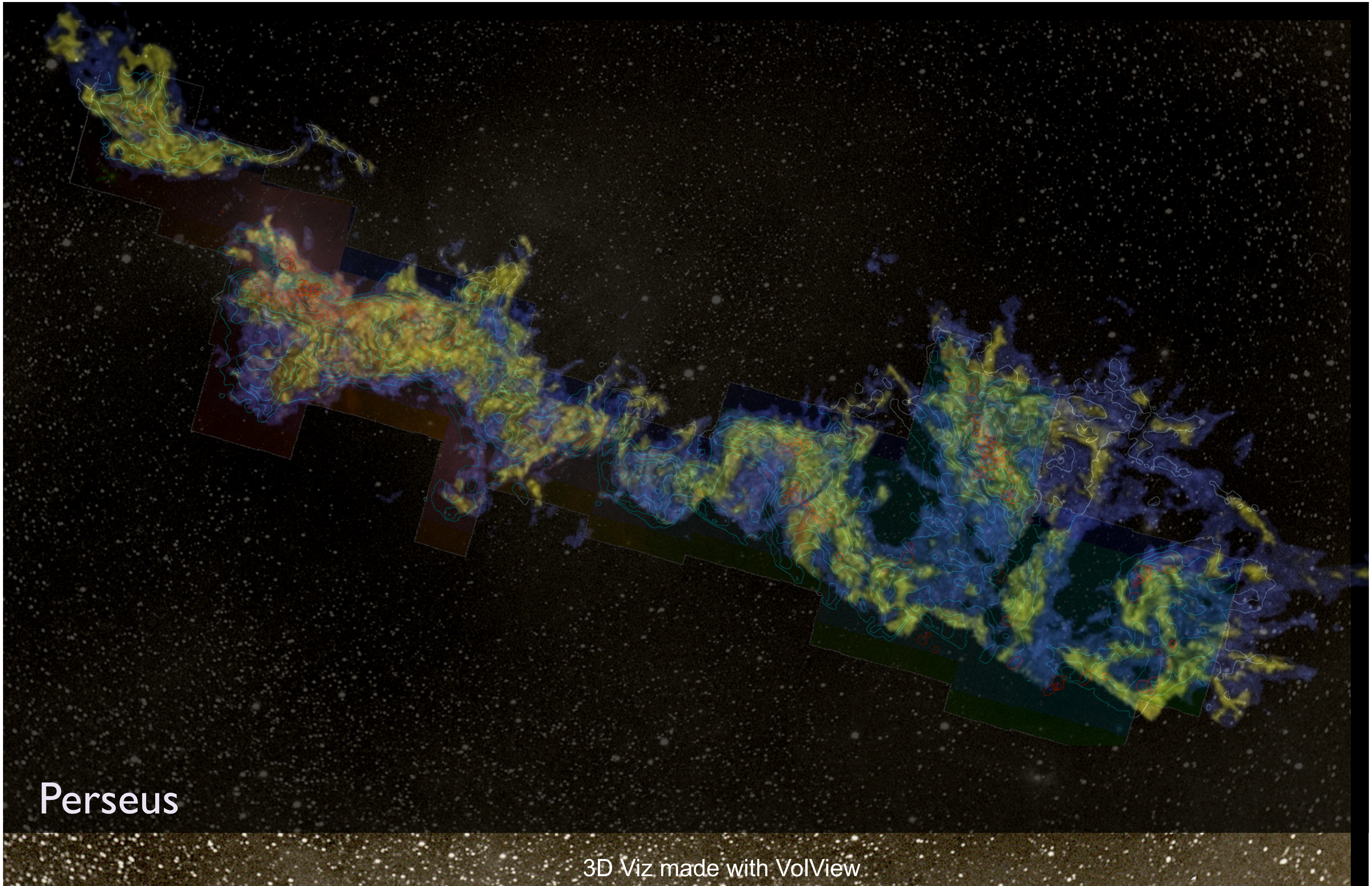

AstroMed@IIC

COMPLETE

Properties of turbulence

- laminar flows turn *turbulent* at *high Reynolds* numbers

$$Re = \frac{\text{advection}}{\text{dissipation}} = \frac{VL}{\nu}$$

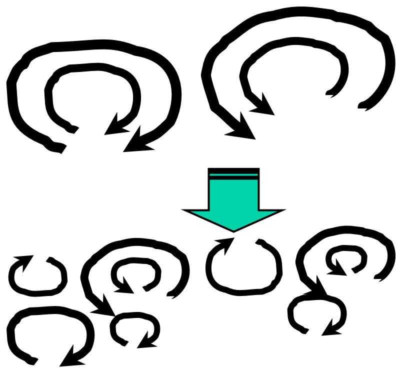

V= typical velocity on scale L, $\nu = \eta/\rho$ = kinematic viscosity,
turbulence for Re > 1000

- Navier-Stokes equation (transport of momentum)

$$\rho\frac{d\vec{v}}{dt} = \rho\left(\frac{\partial\vec{v}}{\partial t} + (\vec{v}\cdot\vec{\nabla})\vec{v}\right) = -\vec{\nabla}P + \eta\,\vec{\nabla}^2\vec{v} + \left(\frac{\eta}{3} + \zeta\right)\vec{\nabla}(\vec{\nabla}\cdot\vec{v})$$

shear viscosity

bulk viscosity

$$\sigma_{ij} \equiv \eta\left(\frac{\partial v_i}{\partial x_j} + \frac{\partial v_j}{\partial x_i} - \frac{2}{3}\,\delta_{ij}\frac{\partial v_k}{\partial x_k}\right) + \zeta\delta_{ij}\frac{\partial v_k}{\partial x_k}$$

viscous stress tensor

Properties of turbulence

- laminar flows turn *turbulent* at *high* *Reynolds* numbers

$$Re = \frac{\text{advection}}{\text{dissipation}} = \frac{VL}{\nu}$$

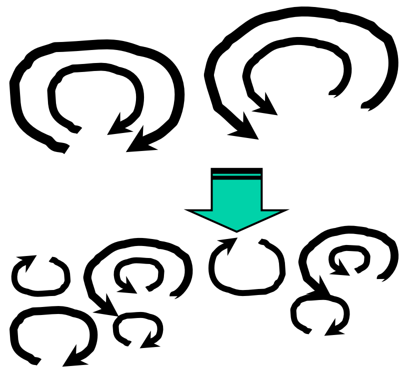

V= typical velocity on scale L, $\nu = \eta/\rho$ = kinematic viscosity,
turbulence for Re > 1000

- vortex streching --> turbulence is intrinsically anisotropic
(only on large scales you may get
homogeneity & isotropy in a statistical sense;
see Landau & Lifschitz, Chandrasekhar, Taylor, etc.)

(ISM turbulence: shocks & B-field
cause additional inhomogeneity)

classical picture of vortex formation

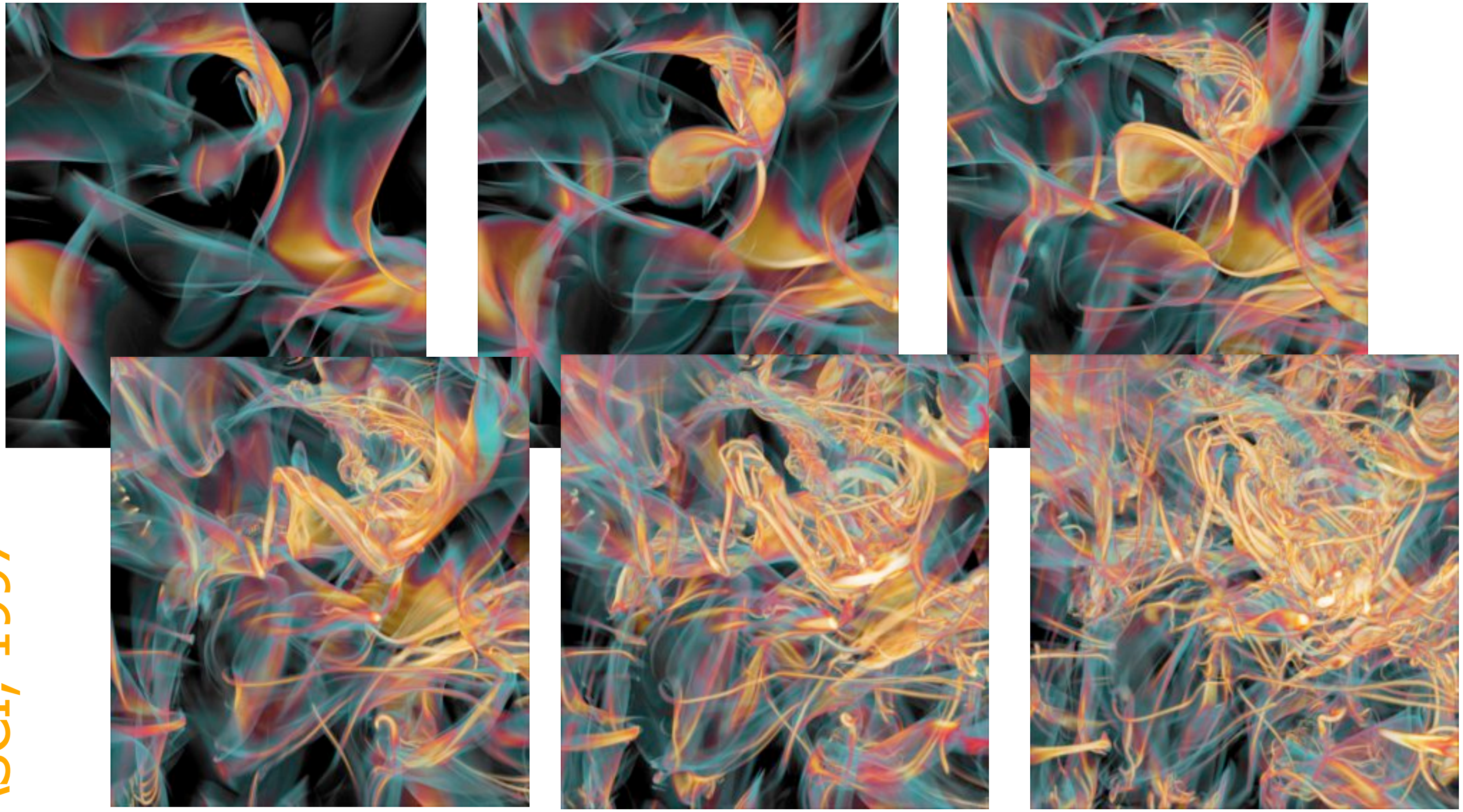

Porter et al.
ASCI, 1997

Vortices are streched and folded in three dimensions

turbulent cascade

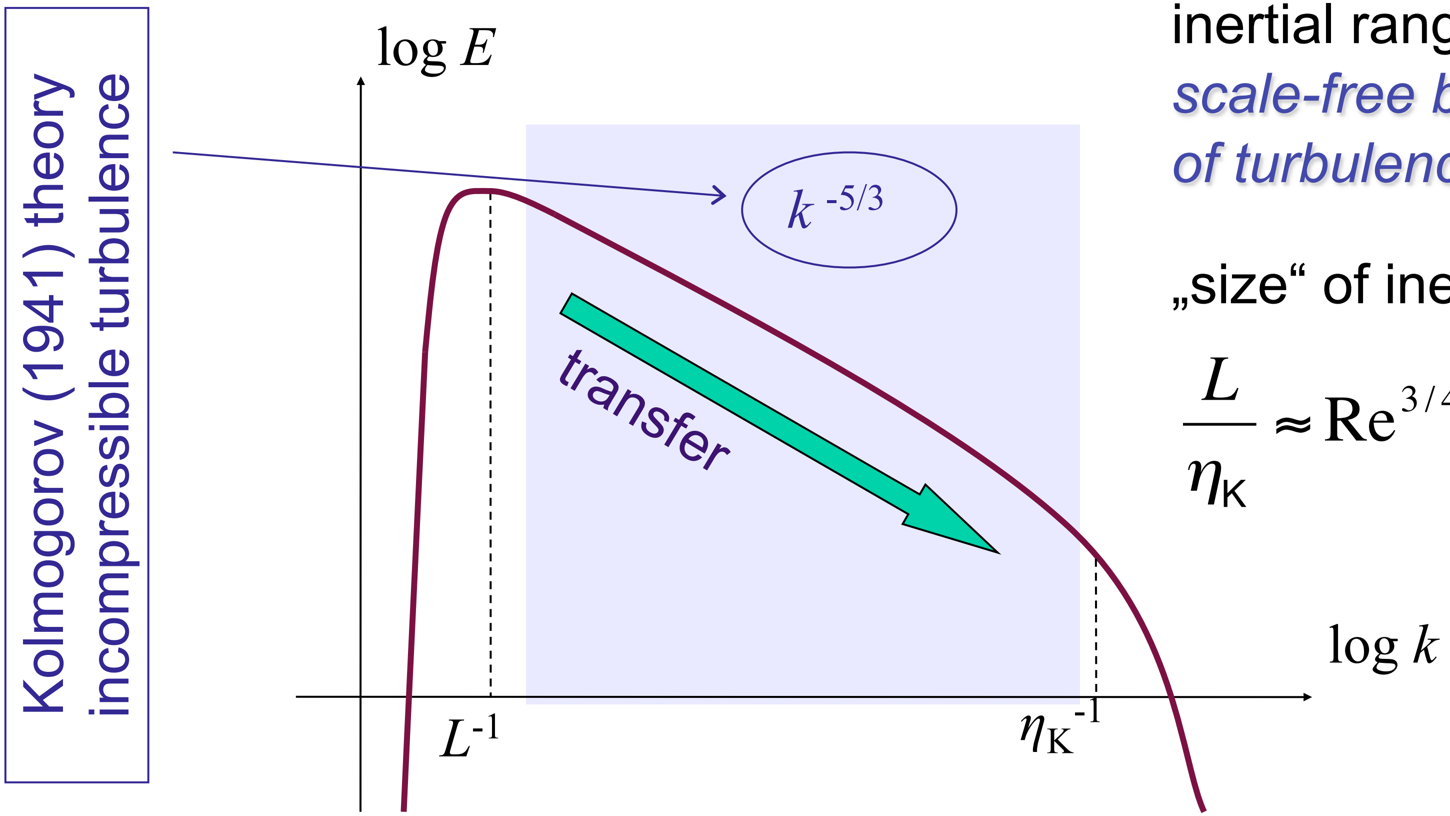

energy
input
scale

energy
dissipation
scale

inertial range:
scale-free behavior of turbulence

„size“ of inertial range:

$$\frac{L}{\eta_K} \approx \mathrm{Re}^{3/4}$$

turbulent cascade in ISM

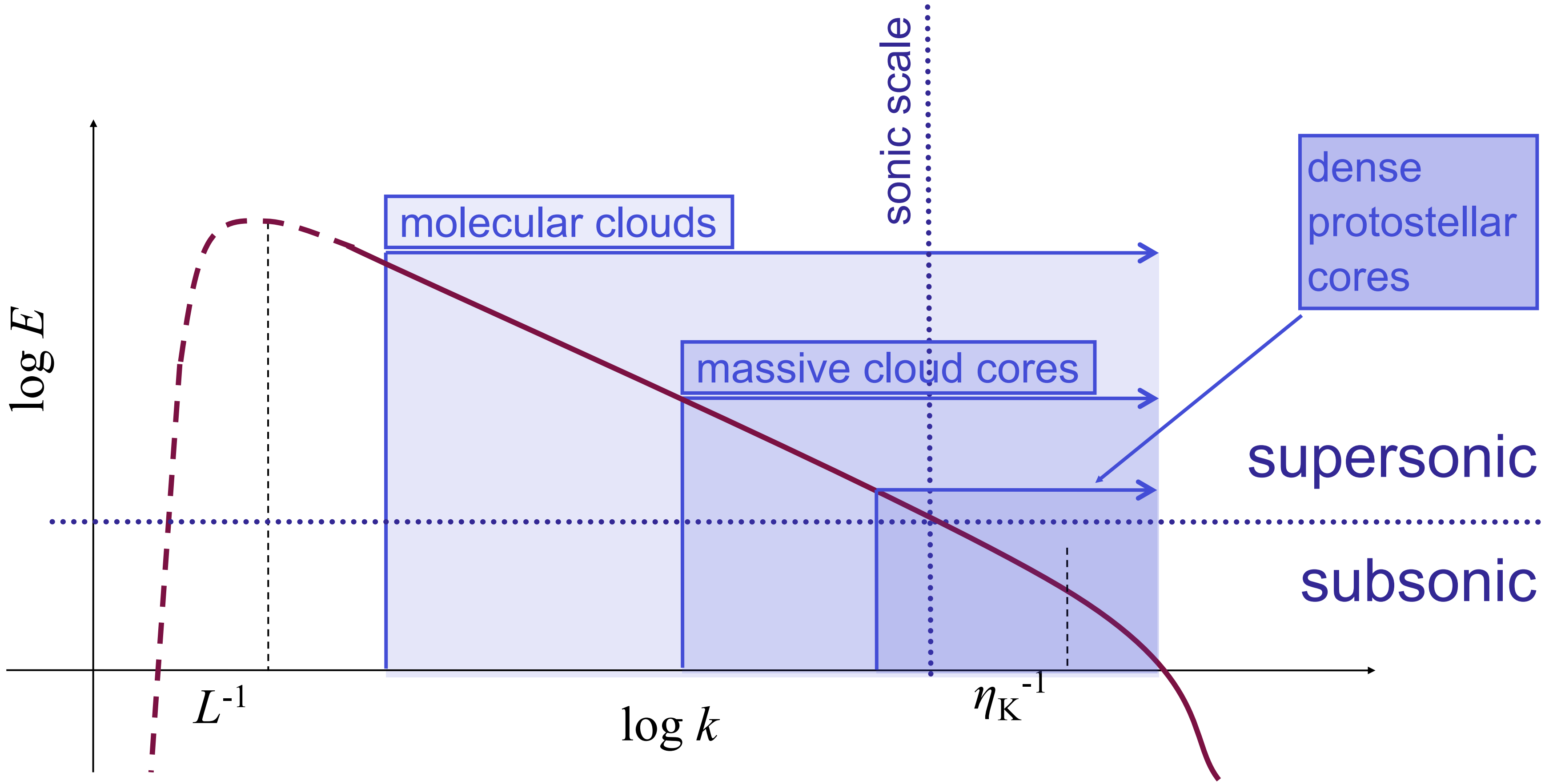

energy source & scale
NOT known
(supernovae, winds, spiral density waves?)

$\sigma_{rms} << 1$ km/s

$\mathcal{M}_{rms} \lesssim 1$

$L \approx 0.1$ pc

dissipation scale not known (ambipolar diffusion, molecular diffusion?)

statistical characteristics of turbulence

- two point statistics
  - power spectrum of velocity (in Fourier space)
  - structure function of velocity (note: compare v, $\rho^{1/2}v$, $\rho^{1/3}v$ at two different locations)
  - PCA: principle component analysis (e.g. Heyer & Schloerb 1997, Heyer et al. 2006, Roman-Duval et al. 2011)
  - CVI: centroid velocity increment (e.g. Lis et al. 1996, Klessen 2000, Hily-Blant et al. 2008, Federrath et al. 2010)
  - Δ variance: wavelet analysis of density (e.g. Stutzki et al. 1998, Bensch et al. 2001, Ossenkopf et al. 2008)

- one point statistics
  - probability distribution function (PDF) of density
  - observations: only *column* density PDF
  - probability distribution function (PDF) of velocity

power spectrum 1

- power spectrum measures the fluctuation strength on different scales
- example: power spectrum of the specific kinetic energy density $\boldsymbol{u}^2/2$

$$\tilde{\boldsymbol{u}}(\boldsymbol{k}) = \frac{1}{(2\pi)^3} \int_{\mathcal{V}} \boldsymbol{u}(\boldsymbol{x}) e^{-2\pi i \boldsymbol{k} \cdot \boldsymbol{x}} \, d\boldsymbol{x}$$

velocity in wave number space

$$\mathcal{E}(\boldsymbol{k}) \equiv \frac{1}{2} \left| \tilde{\boldsymbol{u}}(\boldsymbol{k}) \right|^2$$

specific kinetic energy in Fourier space

$$\mathcal{E}(k) \equiv \int_{\tilde{\mathcal{V}}} \mathcal{E}(\boldsymbol{k}) \delta(|\boldsymbol{k}| - k) d\boldsymbol{k}$$

as function of $\boldsymbol{k}$

- in inertial range: power-law behavior $\boxed{\mathcal{E}(k) \sim k^{-\beta}}$

power spectrum 2

- power-law behavior in inertial range as seen in numerical simulations

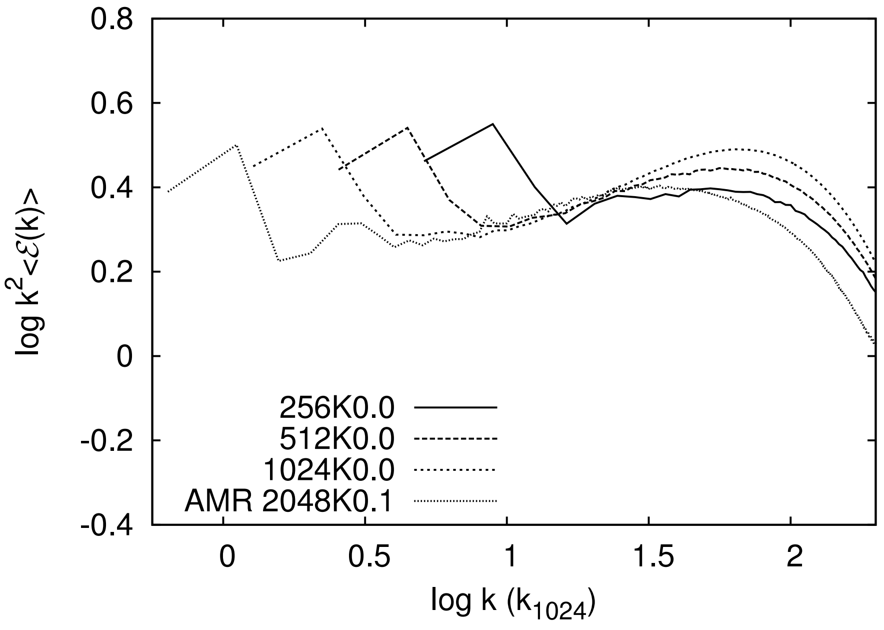

compensated power spectrum $\mathcal{E}(k)$

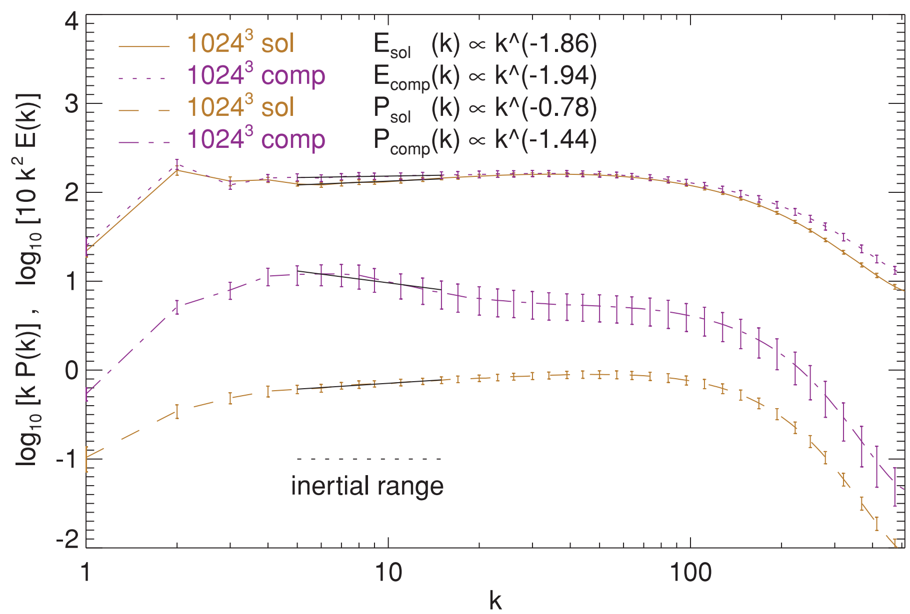

top: compensated power spectrum kinetic energy density $\mathcal{E}(k)$
bottom: compensated power spectrum of density $P(k)$

Kritsuk et al. (2007, ApJ, 665, 416)

Federrath et al. (2009, ApJ, 692, 364)

power spectrum 2

- power-law behavior in inertial range as seen in numerical simulations

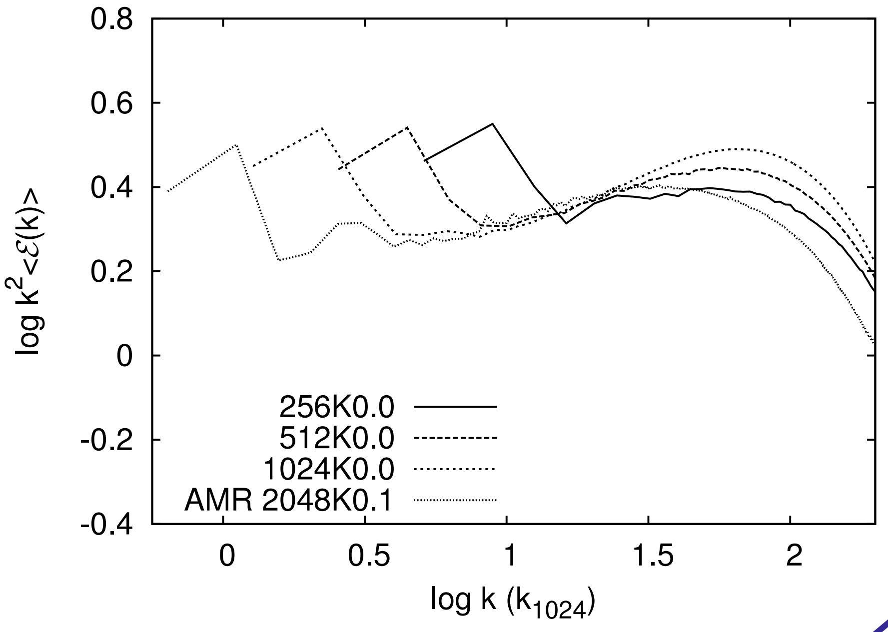

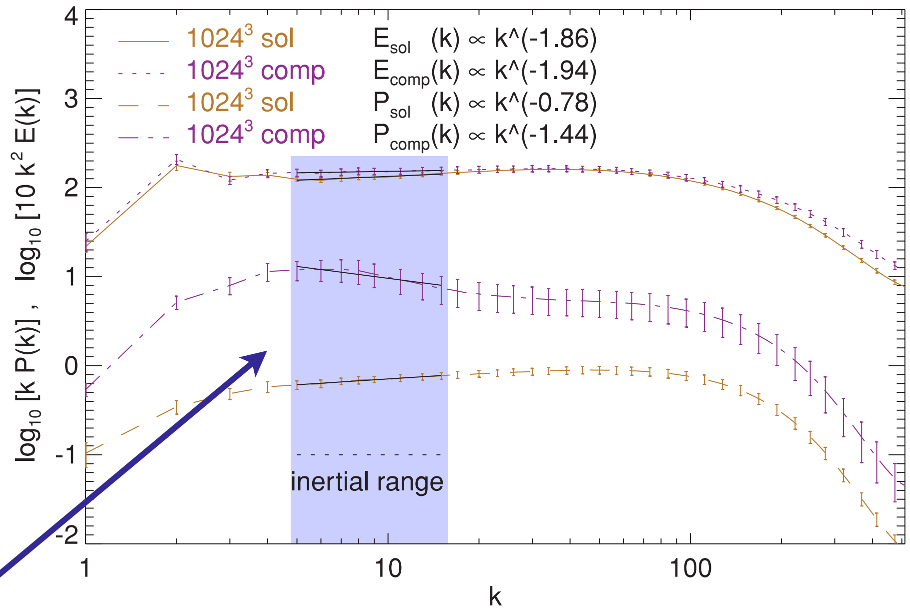

compensated power spectrum $\mathcal{E}(k)$

NOTE: SMALL INERTIAL RANGE!

top: compensated power spectrum kinetic energy density $\mathcal{E}(k)$
bottom: compensated power spectrum of density $P(k)$

Kritsuk et al. (2007, ApJ, 665, 416)

Federrath et al. (2009, ApJ, 692, 364)

Δ variance

- wavelet technique that works entirely in real space (no Fourier transform needed)
- good for maps with inhomogeneous structure (in terms of spatial coverage and resolution)

$$\sigma_\Delta^2(L) = \frac{1}{2\pi} \langle (s * \odot_L)^2 \rangle_{x,y},$$

where

$$\odot_L(r) = \begin{cases} \frac{1}{\pi(L/2)^2} & (r \leq \frac{L}{2}) \\ \frac{-1}{8\pi(L/2)^2} & (\frac{L}{2} < r \leq \frac{3L}{2}) \\ 0 & (r > \frac{3L}{2}) \end{cases}$$

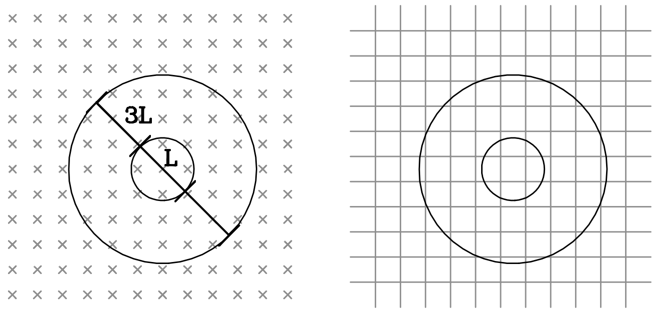

Bensch et al. (2001, A&A, 366, 636)

$$\sigma_\Delta^2(L) = \frac{1}{2\pi} \iint P_\mathrm{s} \, |\tilde{\odot}_L|^2 \, \mathrm{d}k_x \mathrm{d}k_y.$$

relation to wave number space

typically “Mexican hat” filter functions are used:

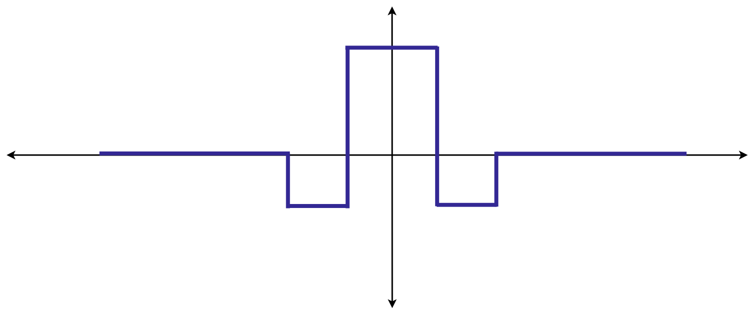

Δ variance

- high-density tracers (e.g.) reveal that density structure is dominated by small-scales modes in star forming regions:
- you pick up dense protostellar cores!

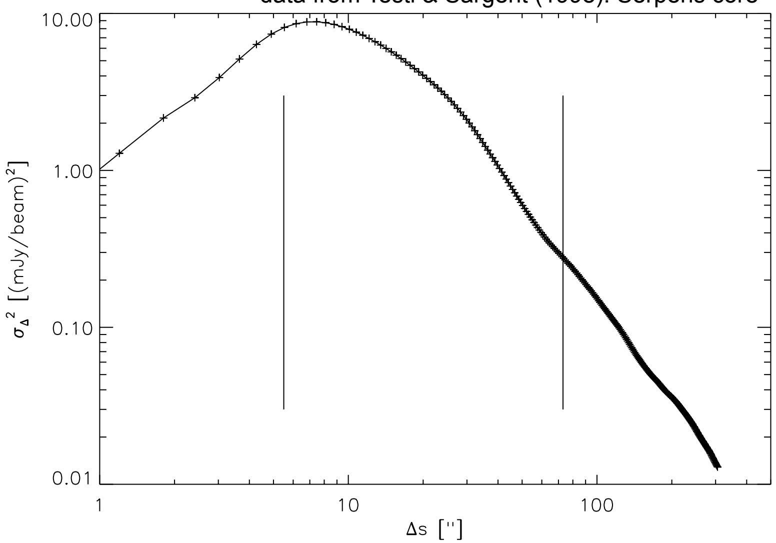

- this is reproduced in star-cluster forming simulations:

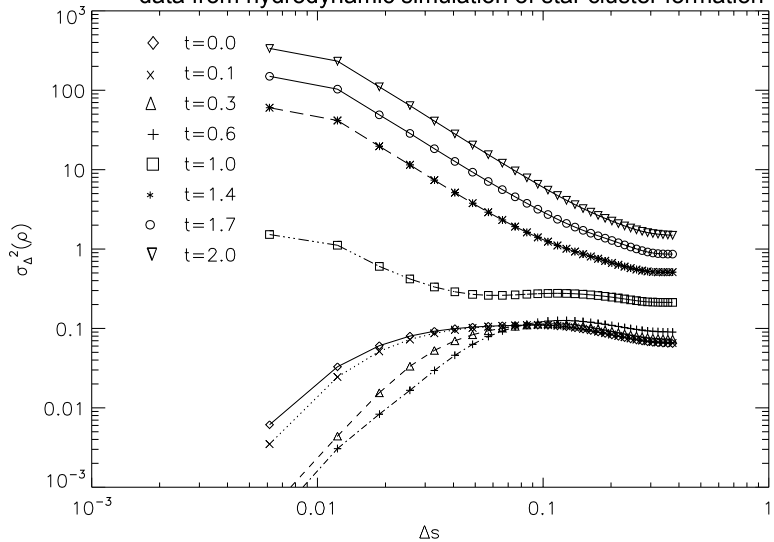

Ossenkopf et al. (2001, A&A, 379, 1005)

Δ variance

- NOTE: this is NOT seen in low-density tracers (e.g. in CO)

- you see only the tenuous gas *between* the dense cores in a limited density range
- at *low* densities, molecule is not efficiently excited by collisions
- at *high* densities, emission becomes optically thick, OR: the gas tracer is depleted on grains (ice mantles)

- again chemistry and radiation transfer matter!

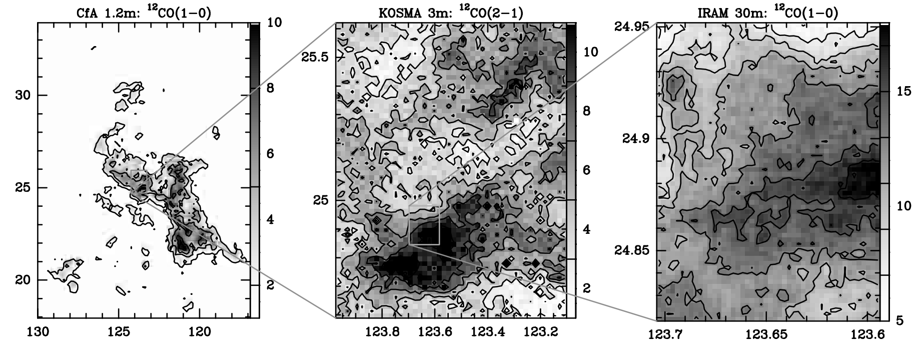

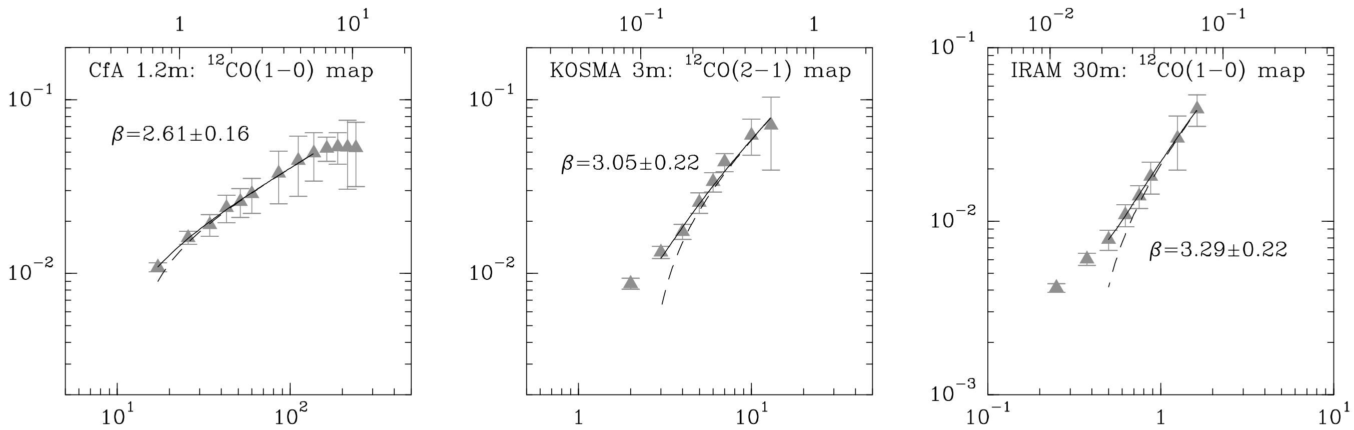

Bensch et al. (2001, A&A 366, 636)

centroid velocity increments

- centroid velocity increments: compare the velocity of the LOS line centroid at different positions in a PPV cube:

$$\delta C_\ell(\boldsymbol{r}) = \langle C(\boldsymbol{r}) - C(\boldsymbol{r} + \boldsymbol{\ell}) \rangle,$$

with the centroid velocity defined as

$$C(\boldsymbol{r}) = \frac{\int \rho(\boldsymbol{r}, z)\, v_z(\boldsymbol{r}, z)\, \mathrm{d}z}{\int \rho(\boldsymbol{r}, z)\, \mathrm{d}z}$$

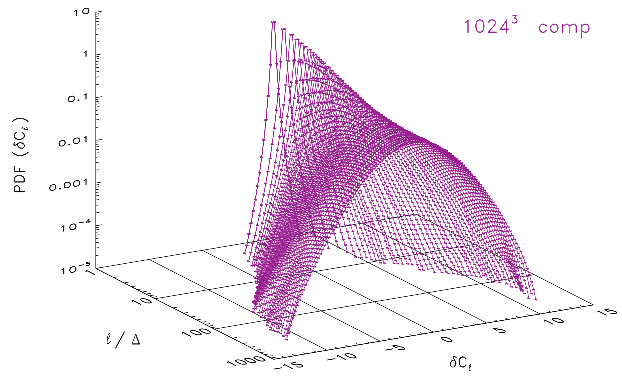

Federrath et al. (2010, A&A 512, A81)

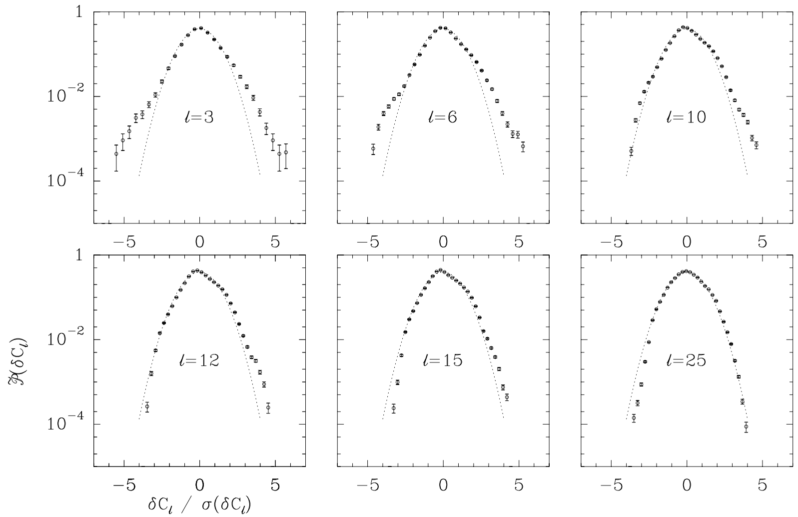

Hily-Blant et al. (2008, A&A, 481, 367)

exponential for small lags
Gaußian for large spatial lags

structure functions 1

- how are the velocities at two different points in time or two different locations related?

- Lagrangian structure function: compare the velocity of the same fluid element at two different times

$$\delta v_i^m(t,\tau) = v_i^m(t+\tau) - v_i^m(t).$$

where $v_i^m(t)$ is the velocity in the $i \in \{x,y,z\}$ direction of fluid element m, and where τ is the time lag
(works well for particle-based hydro codes, in grid codes tracer particles are needed)

- Eulerian structure function: compare the velocity at different locations at the same time

$$\delta v_i^{mn}(\boldsymbol{r},\boldsymbol{\ell}) = v_i^m(\boldsymbol{r}+\boldsymbol{\ell}) - v_i^n(\boldsymbol{r})$$
$$\delta v_\parallel^{mn}(\boldsymbol{r},\boldsymbol{\ell}) = v_\parallel^m(\boldsymbol{r}+\boldsymbol{\ell}) - v_\parallel^n(\boldsymbol{r}),$$

where $\boldsymbol{r}$ is the location and $\boldsymbol{\ell}$ the spatial lag between two cells (m=n) or between two differen SPH or tracer particles (m, n), we can do that for each velocity component i or for the parallel or perpendicular projects ($v_\parallel = \boldsymbol{v}\cdot\hat{\boldsymbol{\ell}}$.) with $\hat{\boldsymbol{\ell}} = \boldsymbol{\ell}/\ell$

from Konstandin et al. (2012, JFM, 692, 183)

structure functions 2

- note: these δv are related to the velocity increments discussed before . . .
  (BUT here we do it in 6D+1 phase space, and not in the reduced 3D PPV space)

- as before, we see that the δv turn from (super)exponential to Gaußian for increasing lag

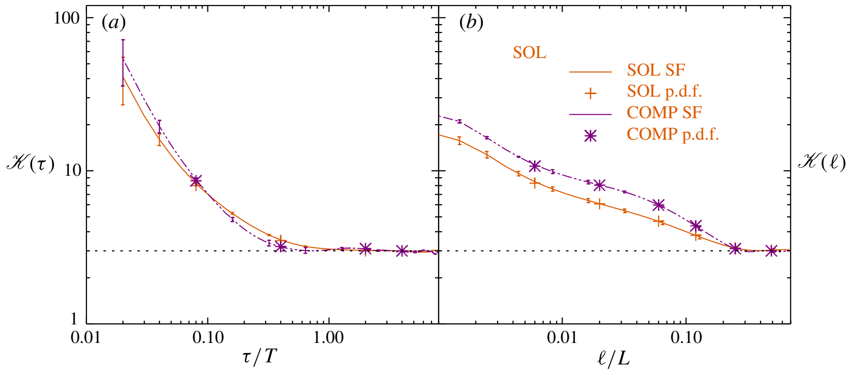

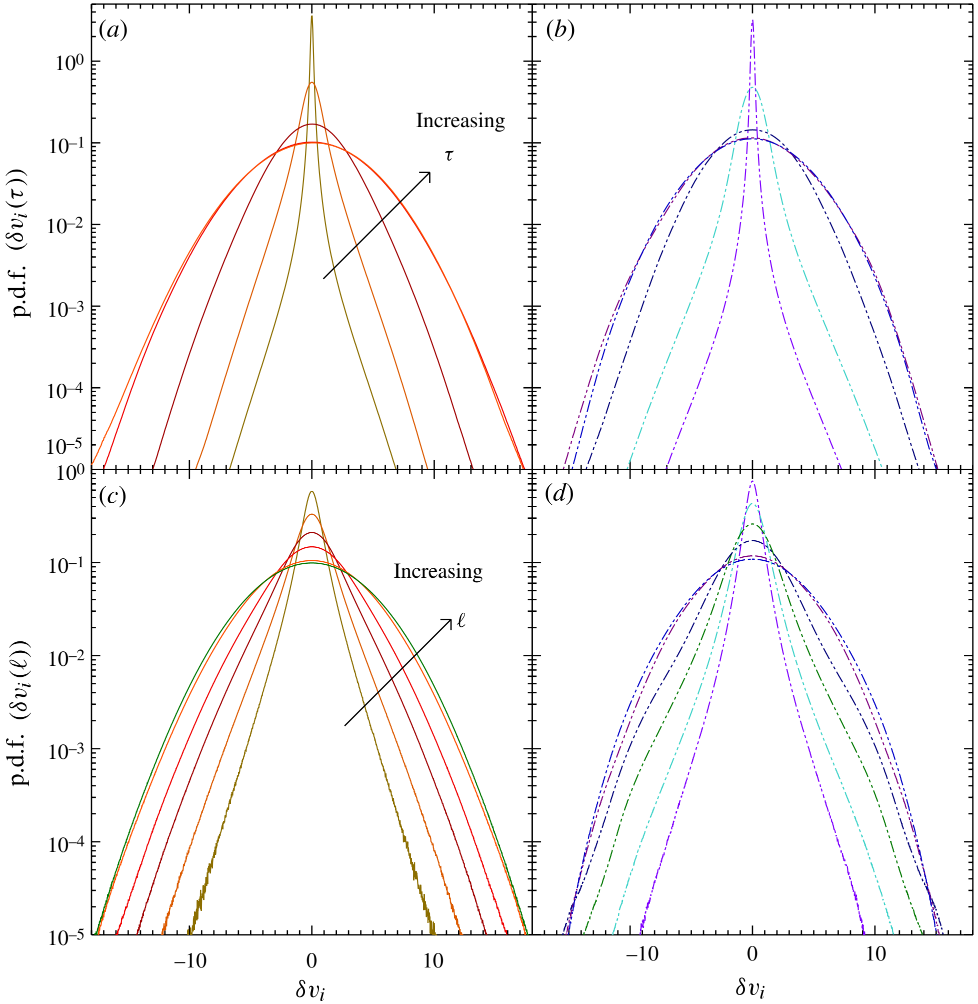

- kurtosis goes from κ > 6 (exp.) to κ = 3 (Gaußian)

from Konstandin et al. (2012, JFM, 692, 183)

structure functions 3

- the structure functions are then
- Lagrangian SF:

$$LS^p(\tau) = \langle \langle |\delta v_x^m(t,\tau)\,|^p \rangle_m + \langle |\delta v_y^m(t,\tau)\,|^p \rangle_m + \langle |\delta v_z^m(t,\tau)\,|^p \rangle_m \rangle_t /3$$

where we take the average over all three spatial directions

- Eulerian SF:

$$ES^p(\ell) \equiv \langle \langle |\delta v_x^{mn}(\boldsymbol{r},\ell)|^p \rangle_{mn} + \langle |\delta v_y^{mn}(\boldsymbol{r},\ell)|^p \rangle_{mn} + \langle |\delta v_z^{mn}(\boldsymbol{r},\ell)|^p \rangle_{mn} \rangle_t /3$$

$$ES_\parallel^p(\ell) \equiv \langle |\delta v_\parallel^{mn}(\boldsymbol{r},\ell)|^p \rangle_{mn,t},$$

- the exponent p gives the order of the structure function
- note: in an “ideal world” both approaches should have similar statistical characteristics (ergodic theorem)

from Konstandin et al. (2012, JFM, 692, 183)

structure functions 4

- results from numerical simulations

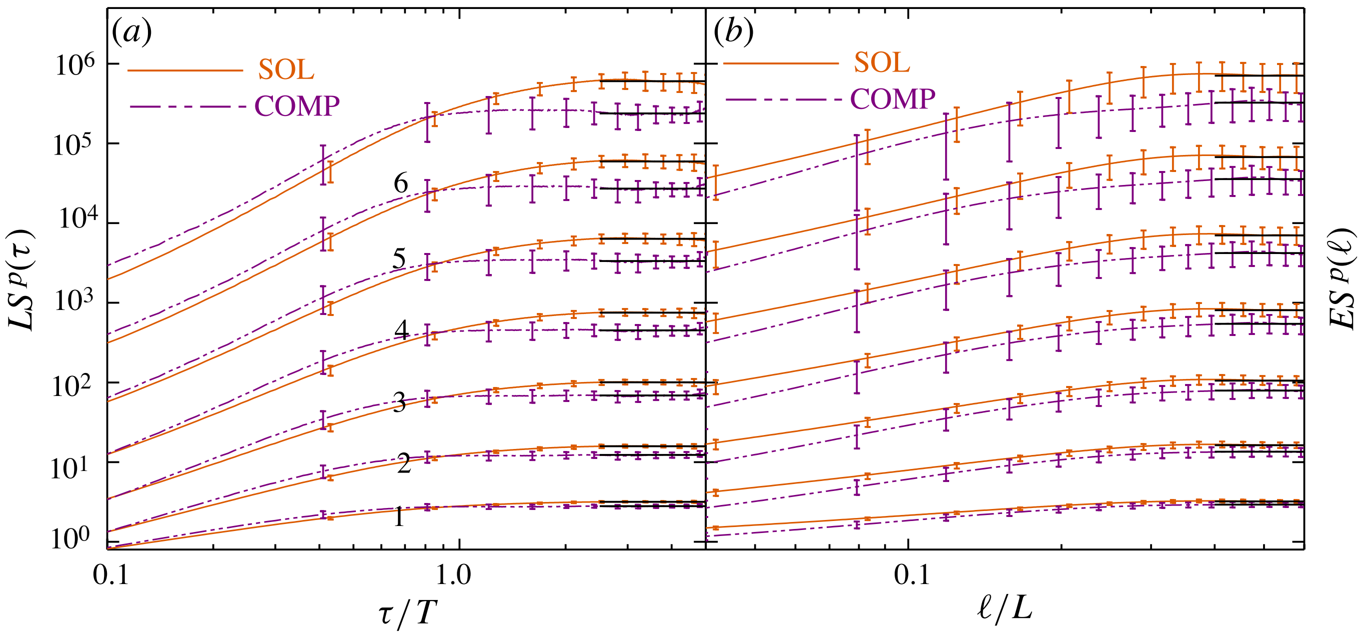

- turbulence theory makes predictions of the slope of the SF in the inertial range

$$LS(p) \propto \tau^{\xi(p)}, \quad ES(p) \propto \ell^{\zeta(p)}.$$

- BUT: where is the inertial range? (these are already state-of-the-art 1024^3 simulations!)

from Konstandin et al. (2012, JFM, 692, 183)

structure functions 5

- to get around this problems, turbulence theorists look at the “extended self similarity”
- this is a “trick” where the structure functions are divided by the 2nd or 3rd order SF:

$$Z_L(p) = \frac{\xi(p)}{\xi(2)}, \quad Z_E(p) = \frac{\zeta(p)}{\zeta(3)}$$

- this makes it easier to measure the scaling exponent

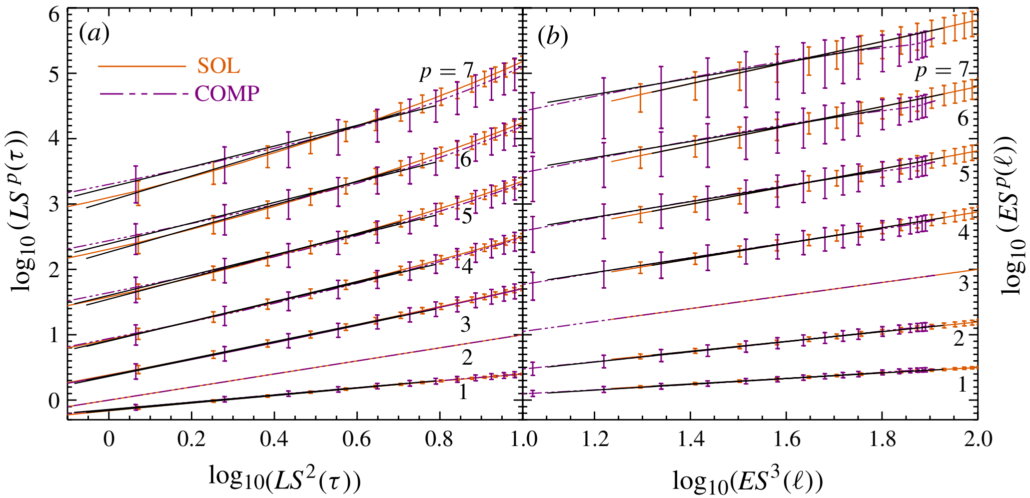

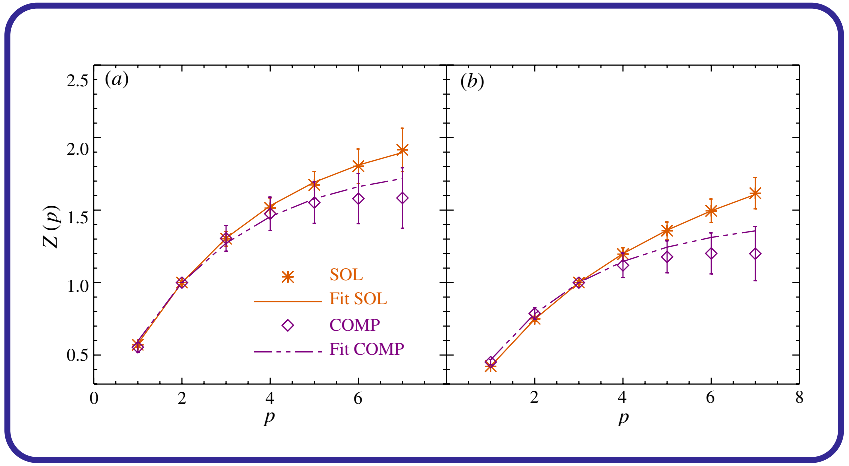

from Konstandin et al. (2012, JFM, 692, 183)

structure functions 6

- simple statistical model for large lags:
- structure function can be expressed as statistical moments PDF of velocity increments

$$S^p(\alpha) = \int |\delta v|^p P(\delta v, \alpha)\, \mathrm{d}(\delta v)$$

where $P(\delta v, \alpha)$ is the distribution function of the δv with lag α

- we can integrate that for a Gaußian distribution ($\alpha \to \infty$

$$S^p(\alpha \to \infty) = \frac{2}{\sigma\sqrt{2\pi}} \int_0^\infty (\delta v)^p \, \mathrm{e}^{-(\delta v)^2/(2\sigma^2)} \mathrm{d}(\delta v)$$
$$= \frac{\Gamma\left(\dfrac{p+1}{2}\right)}{\sqrt{\pi}} (\sqrt{2}\sigma)^p,$$

- with $\langle(\delta v(\ell \to \infty))^2\rangle = 2\mathscr{M}_M^2 c_s^2$ we get

$$S^p(\alpha \to \infty) = \frac{\Gamma\left(\frac{p+1}{2}\right)}{\sqrt{\pi}} \left(\frac{2}{\sqrt{3}}\mathscr{M}_M\right)^p.$$

from Konstandin et al. (2012, JFM, 692, 183)

structure functions 7

- with $\langle(\delta v(\ell \to \infty))^2\rangle = 2\mathscr{M}_M^2 c_s^2$ we get

$$S^p(\alpha \to \infty) = \frac{\Gamma\left(\frac{p+1}{2}\right)}{\sqrt{\pi}}\left(\frac{2}{\sqrt{3}}\mathscr{M}_M\right)^p$$

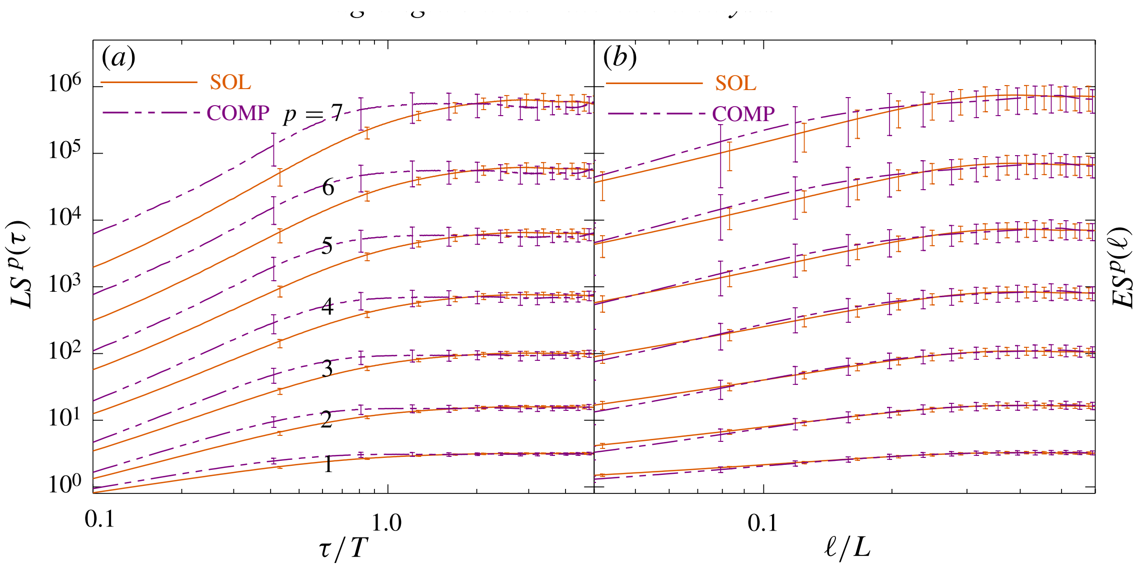

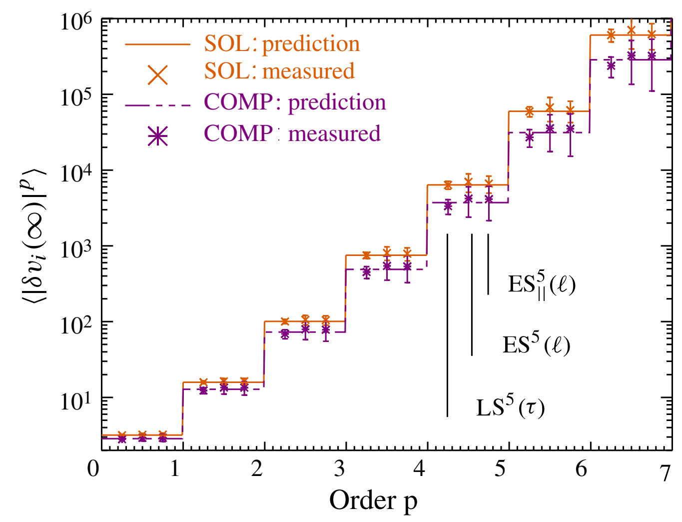

from Konstandin et al. (2012, JFM, 692, 183)

Linewidth size relation (example)

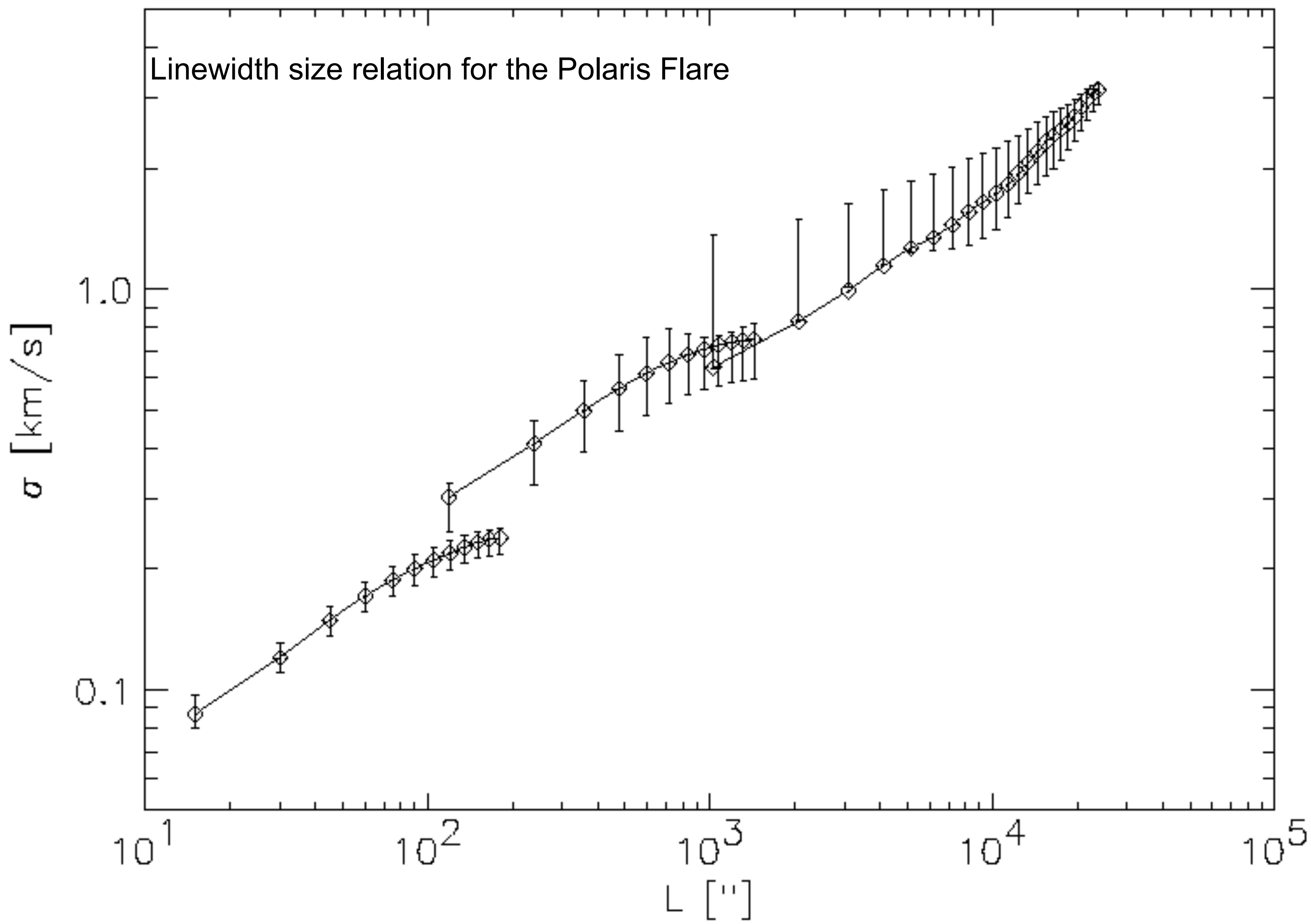

Ossenkopf & Mac Low (2002)

Larson Relations

- Larson (1981) found the following relations between linewidth and size and mean density and size:

$\rho \propto R^{\alpha}$	$\alpha \approx -1$	*density size relation*	(1)
$\sigma \propto R^{\beta}$	$\beta \approx 1/2$	*linewidth size relation*	(2)

- In virial equilibrium: $\alpha \approx -1$, $\beta \approx \frac{1}{2}$
- Molecular clouds appear gravitationally bound. (3)
- Values:
  - $\sigma = (0.72 \pm 0.07)$ km/s $(R/pc)^{0.5 \pm 0.05}$ (Solomon et al.)
  - $\sigma = 0.55$ km/s $(R/pc)^{0.51}$ (Caselli & Myers)
  - $\langle N_H \rangle = (1.5 \pm 0.3) \times 10^{22}$ cm^{-2} $(R/pc)^{0.0 \pm 0.1}$ (Solomon et al.)
- Only two of the three statements (1,2,3) are independent.

Larson Relations

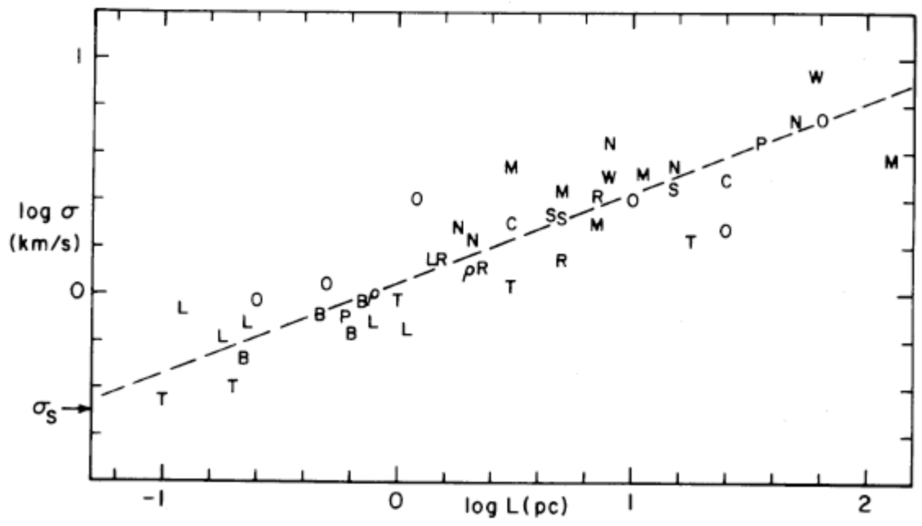

Richard Larson (1981, MNRAS, 184, 809)

linewidth-size relation:

$$\delta v \propto \ell^{-\beta} \quad \text{with} \quad \beta \approx \frac{1}{2}$$

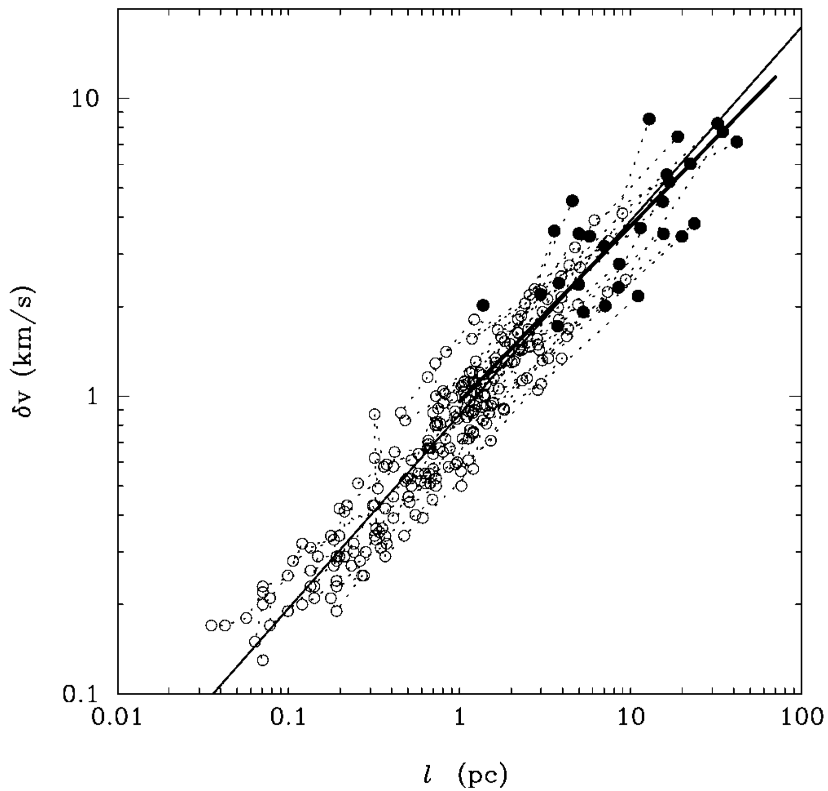

Heyer & Brunt (2004, ApJ, 615, L45)

Larson Relations

linewidth-size relation: $\delta v \propto \ell^{-\beta}$

- Larson compared different clouds (and parts of different clouds)
- modern determinations use more sophisticated statistics: e.g. PCA (principle component analysis)

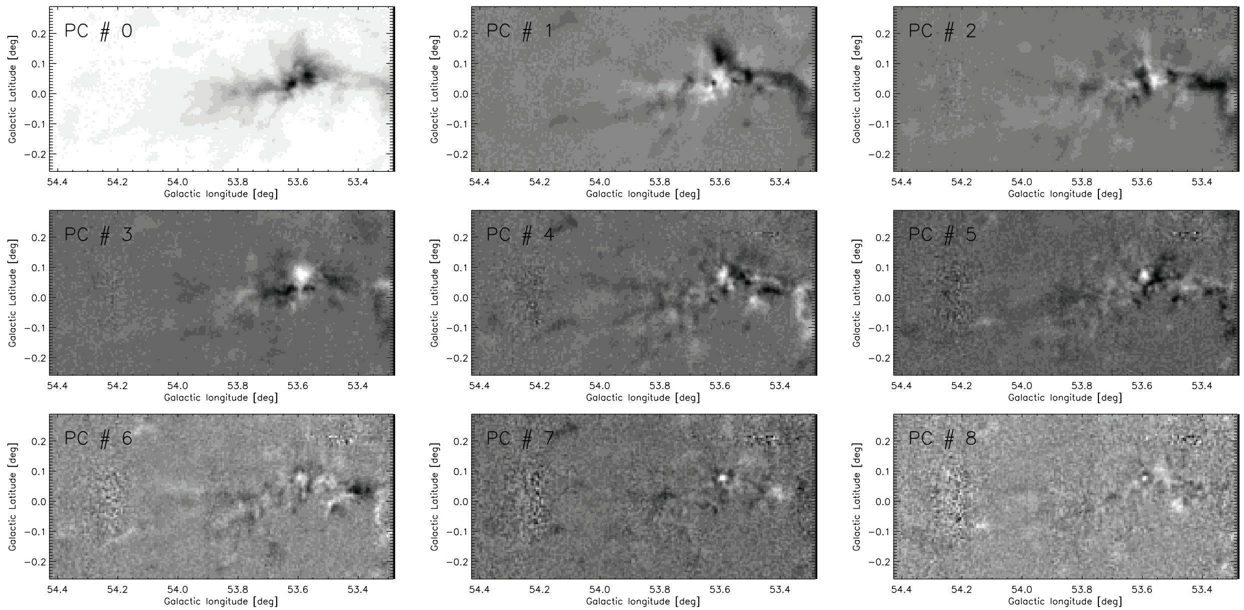

Figure 8. Nine first principal components for molecular cloud GRSMC G053.59+00.04, randomly selected from our sample of 367 molecular clouds from the Galactic Ring Survey.

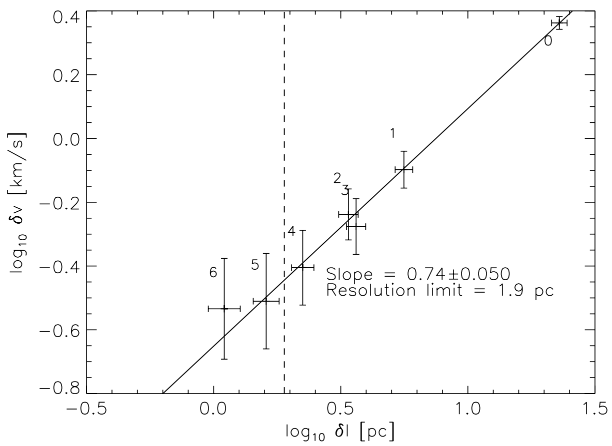

Figure 9. PCA pseudo-structure function for molecular cloud GRSMC G053.59+00.04. The order of the principal component for each pair of spatial and spectral scales is indicated next to each data point. The vertical dashed line shows the resolution limit. Scales detected in the 5th and 6th are smaller than the resolution limit after scale correction, but above it before the correction and thus need to be included in the fit. The solid line represents a power-law fit, the slope of which is indicated in the figure.

Roman-Duval et al. (2011, ApJ, 740, 120)

Larson Relations

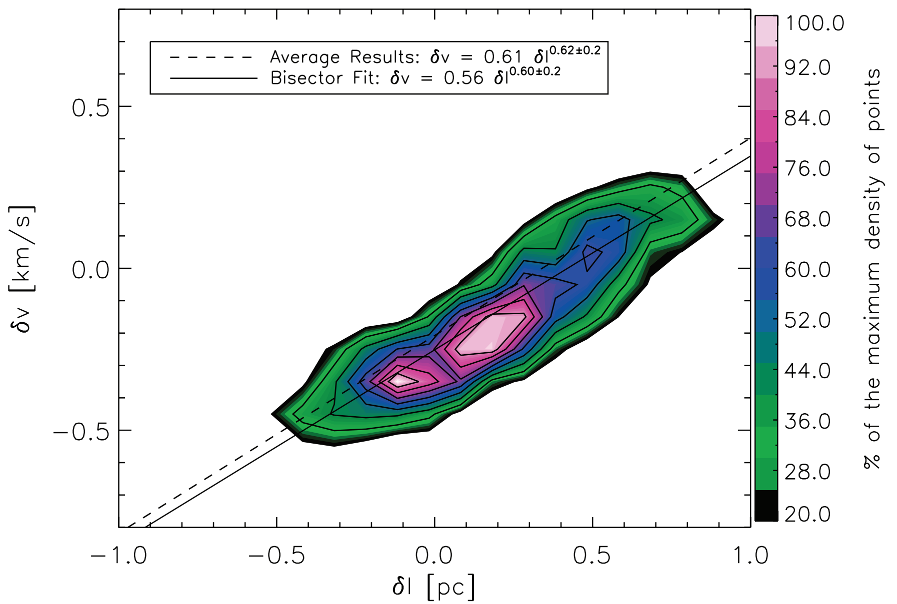

Figure 11. Composite PCA pseudo-structure function (composed of all the spatial and velocity scales detected in all 367 GRS molecular clouds) shown as a density of points. The dashed line indicates a power law of slope 0.62, the average slope of the PCA pseudo-structure function in the GRS sample, and the solid line shows a bisector fit with slope $\alpha_{\mathrm{PCA}} = 0.6$.

$$\delta v \propto \ell^{-\beta}$$

we can use this information to learn more about the statistical properties of molecular cloud turbulence

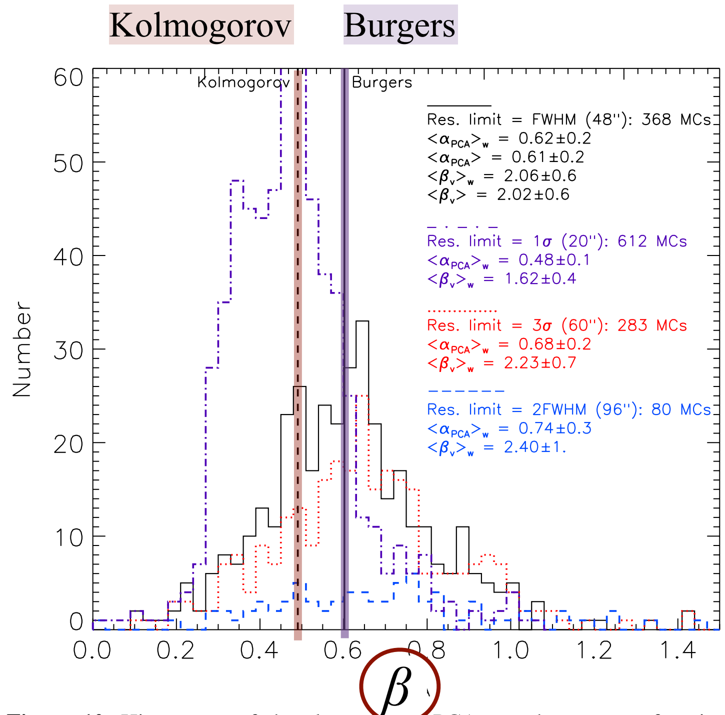

Figure 10. Histograms of the slope of the PCA pseudo-structure function obtained from GRS clouds, and the exponent β_v of the turbulent spectrum obtained from the calibration derived from fBms with purely lognormal PDFs. The errors in the legend correspond to the standard deviation of the distributions. The black histogram was derived using the FWHM of the beam as the resolution limit (fiducial case). The purple, red, and blue histograms show the histogram of α_{PCA} derived with resolution limits defined as the 1σ, 3σ and $2 \times$ FWHM widths of the beam, respectively. The corresponding mean PCA slopes and β_v are also indicated for each case.

Roman-Duval et al. (2011, ApJ, 740, 120)

Larson Relations

normalization of linewidth-size relation seems to depend on column density

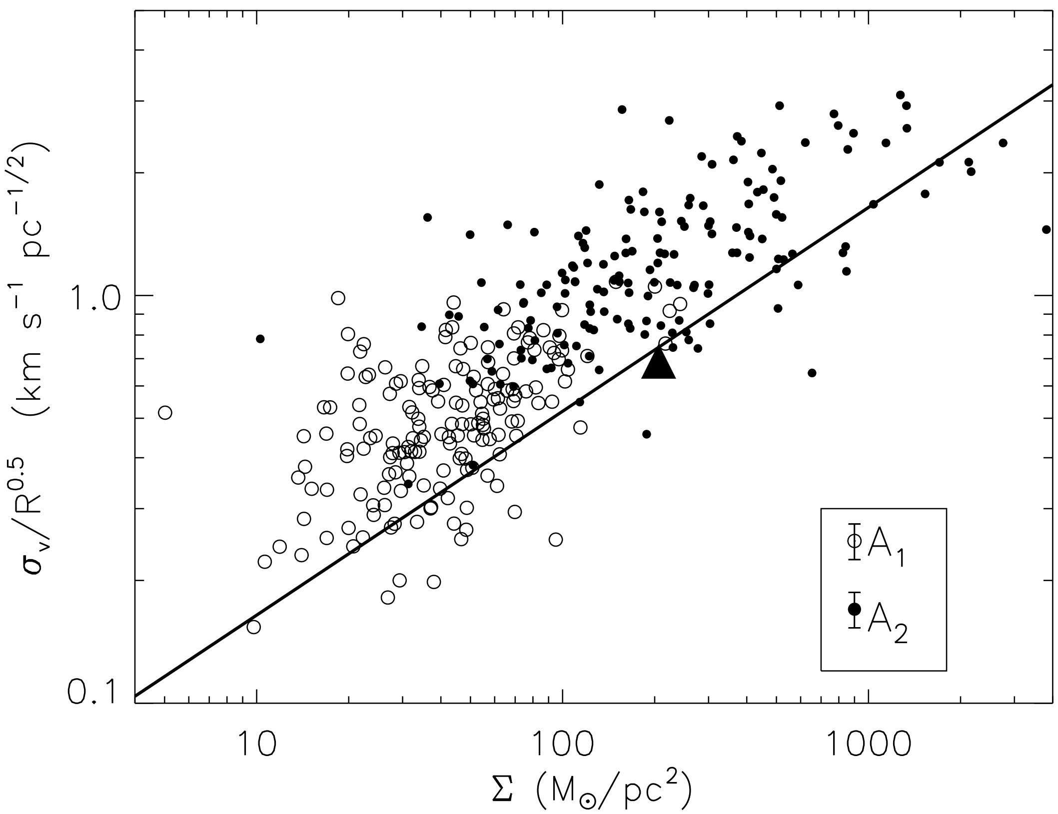

Figure 7. Variation of the scaling coefficient, $v_\circ = \sigma_v / R^{1/2}$, with mass surface density derived within the SRBY cloud boundaries (open circles) and the 1/2 maximum isophote of H_2 column density (filled circles). The filled triangle denotes the value derived by SRBY. The solid line shows the loci of points corresponding to gravitationally bound clouds. There is a dependence of the coefficient with mass surface density in contrast to Larson's velocity scaling relationship. The error bars in the legend reflect a 20% uncertainty of the distance to each cloud.

Heyer et al. (2009, ApJ, 699, 1092)

Larson Relations

normalization of linewidth-size relation also depends on environment

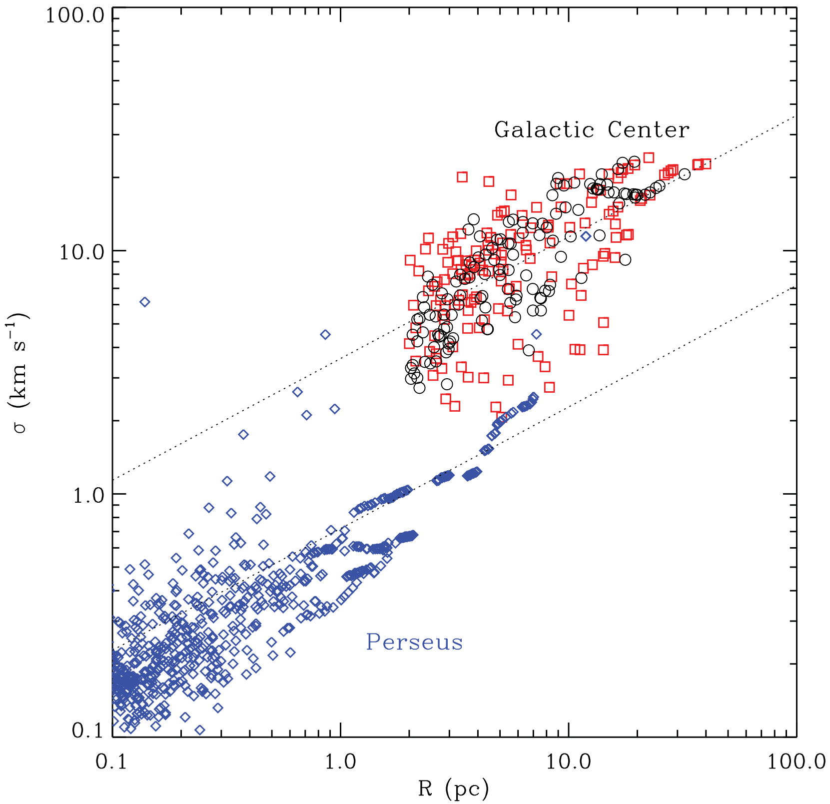

Figure 8. Comparison of the linewidth and size of structures traced by N_2H^+ (black circles) and HCN (red squares) in the GC with ^{13}CO features from the Milky Way MC Perseus. The lower dashed line is the best-fitting relationship from Solomon et al. (1987), $\sigma = 0.7R^{0.5}$. The upper dashed line is the same relationship, but where the coefficient is 3.6.

Shetty et al. (2012, MNRAS, 425, 720)

Larson Relations

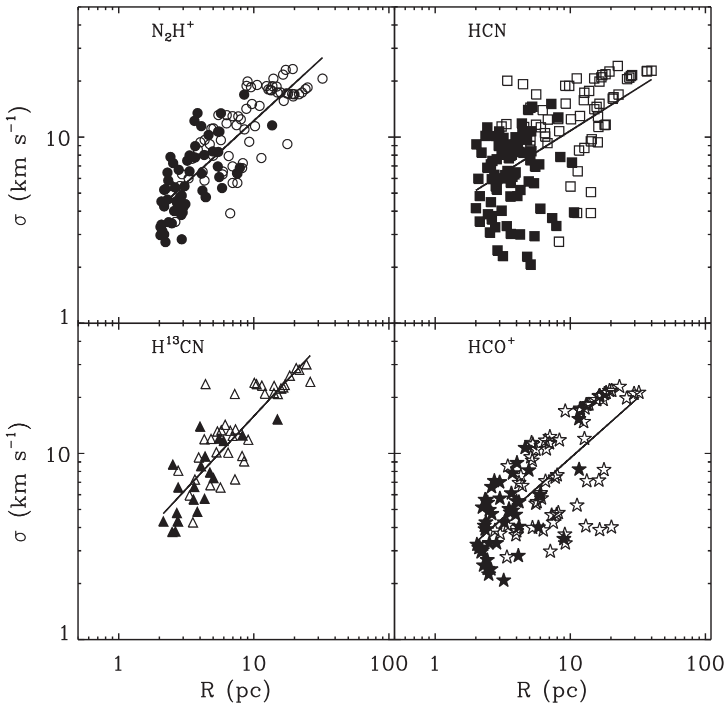

Figure 2. Linewidth–size relationship in the CMZ, as measured within dendrogram-identified structures in N_2H^+, HCN, $H^{13}CN$ and HCO^+. Filled symbols correspond to 'leaves' that do not enclose additional higher level structures. Open symbols are structures that do contain higher level structures. Lines show the best (χ^2) power-law fits.

different tracers give different linewidth-size relations

Shetty et al. (2012, MNRAS, 425, 720)

Larson Relations

- Only *ONE* of the two Larson relation appears real (in the sense that it exists for the real 3D clumps)
- *Density size relation* is likely not to exist in 3D data, but is only observed in projected data due to limited dynamic range of tracer molecules (corresponding to a roughly constant column density)
- Velocity size relation may exist in real 3D data (but may only be marginal).

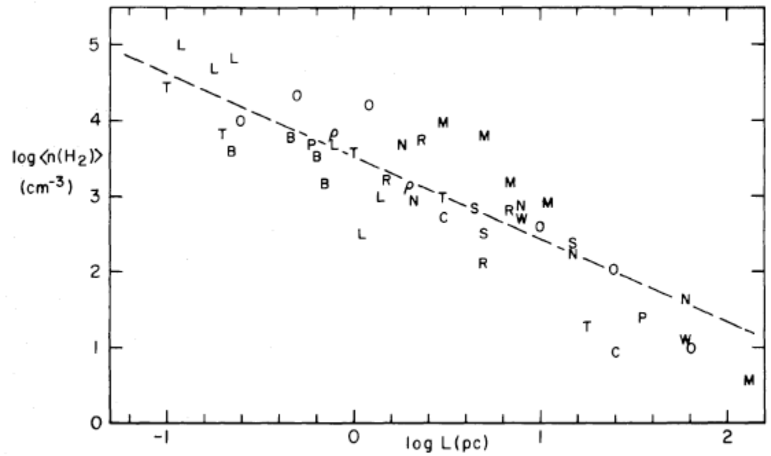

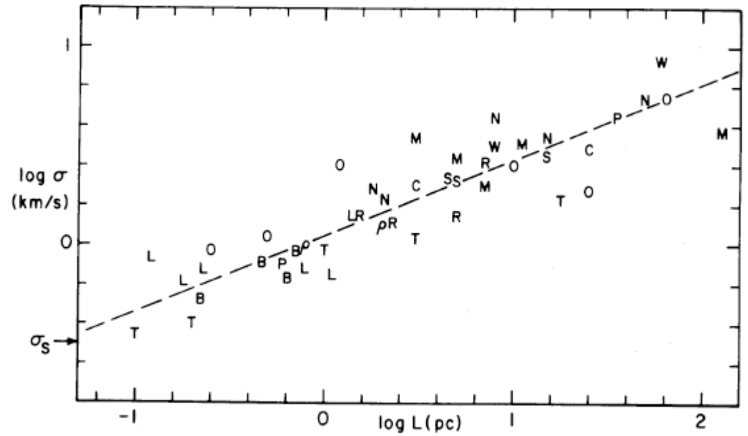

Richard Larson (1981, MNRAS, 184, 809)

ρ-PDF - Mach number relation

- turbulence in compressible fluids and gases induces density variations

- there is a close relation between the width of the density PDF and the rms Mach number

$$\sigma_\rho / \langle \rho \rangle_V = b\,\mathcal{M},$$

- it is more natural to look at $s = \ln(\rho / \langle \rho \rangle_V)$ the PDF is roughly log-normal around the peak of the distribution

$$p(s) = \frac{1}{\sqrt{2\pi\sigma_s}} \exp\left(\frac{-(s - \langle s \rangle)^2}{2\sigma_s^2}\right).$$

- note, one can convert between volume and mass weighted distributions via

$$\langle s \rangle_V = -\langle s \rangle_M = -\frac{{\sigma_s}^2}{2}$$

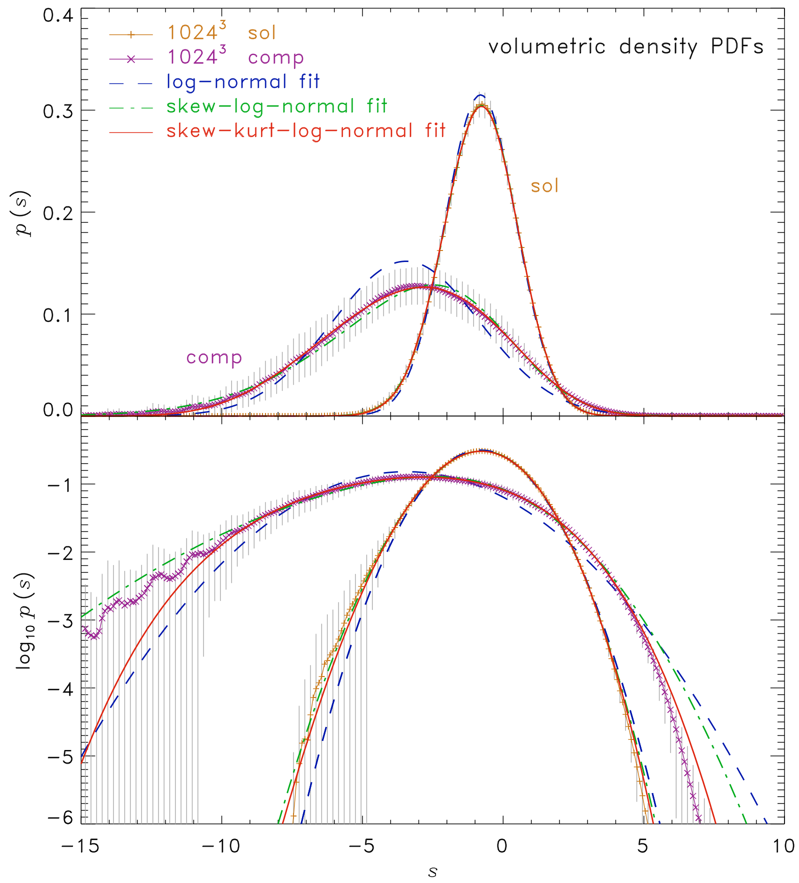

Federrath et al. (2010, A&A 512, A81)

ρ-PDF - Mach number relation

- the relation between the width of the ρ and s distributions is

$$\sigma_s^2 = \ln\left(1 + \sigma_\rho^2\right)$$

this holds for log-normal PDFs and for mass weighting

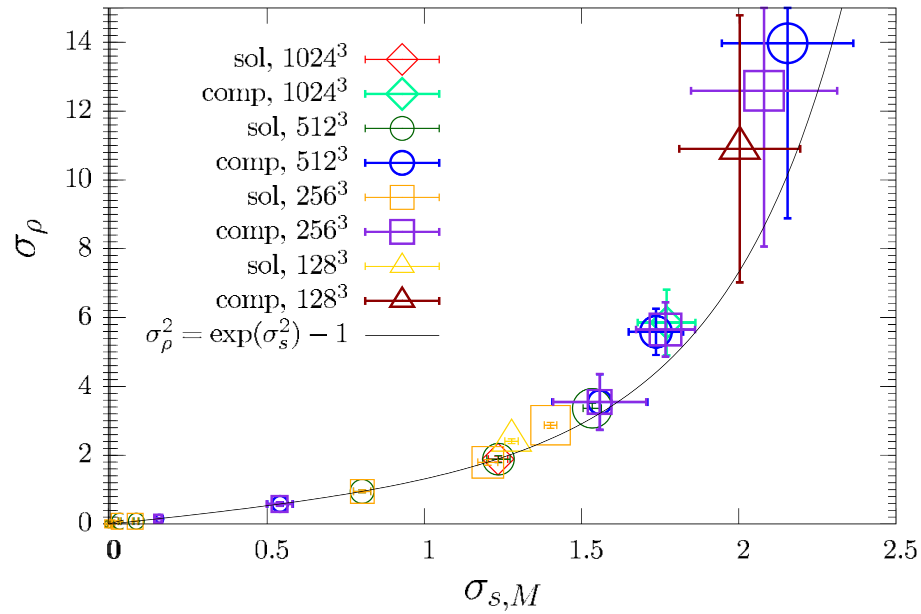

Konstantin et al. (2012, ApJ, 761, 149)

ρ-PDF - Mach number relation

- the relation between the width of the ρ and s distributions is

$$\sigma_s^2 = \ln\left(1 + \sigma_\rho^2\right)$$

this holds for log-normal PDFs and for mass weighting

- the width of the PDF depends on the Mach number of the *compressive* modes!

$$\sigma_\rho = \alpha\sqrt{3}\mathcal{M}_{\mathrm{comp}}^{\beta},$$

with $\alpha = 1.0 \pm 0.1$
and $\beta = 0.85 \pm 0.04.$

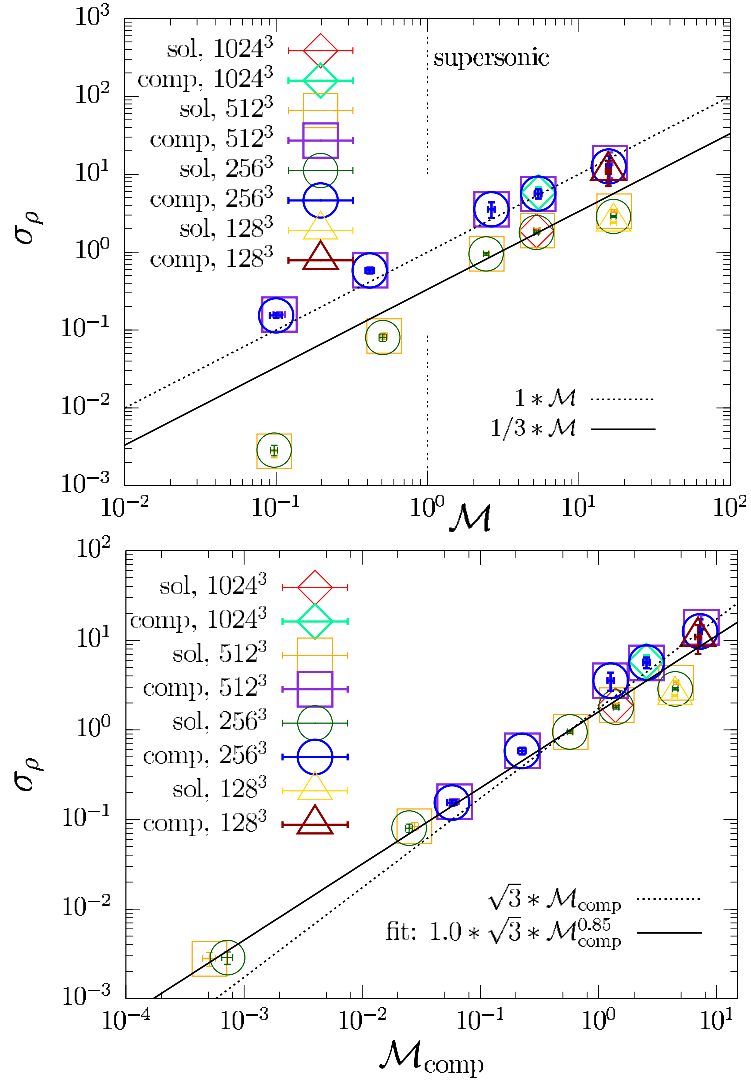

Konstantin et al. (2012, ApJ, 761, 149)

ρ-PDF - Mach number relation

- turbulence in compressible fluids and gases induces density variations

- there is a close relation between the width of the density PDF and the rms Mach number

$$\sigma_\rho / \langle\rho\rangle_V = b\,\mathcal{M},$$

- it is more natural to look at $s = \ln(\rho / \langle\rho\rangle_V)$ the PDF is roughly log-normal around the peak of the distribution

$$p(s) = \frac{1}{\sqrt{2\pi}\,\sigma_s} \exp\left(\frac{-(s - \langle s \rangle)^2}{2\sigma_s^2} \right).$$

- note, one can convert between volume and mass weighted distributions via

$$\langle s \rangle_V = -\langle s \rangle_M = -\frac{\sigma_s{}^2}{2}$$

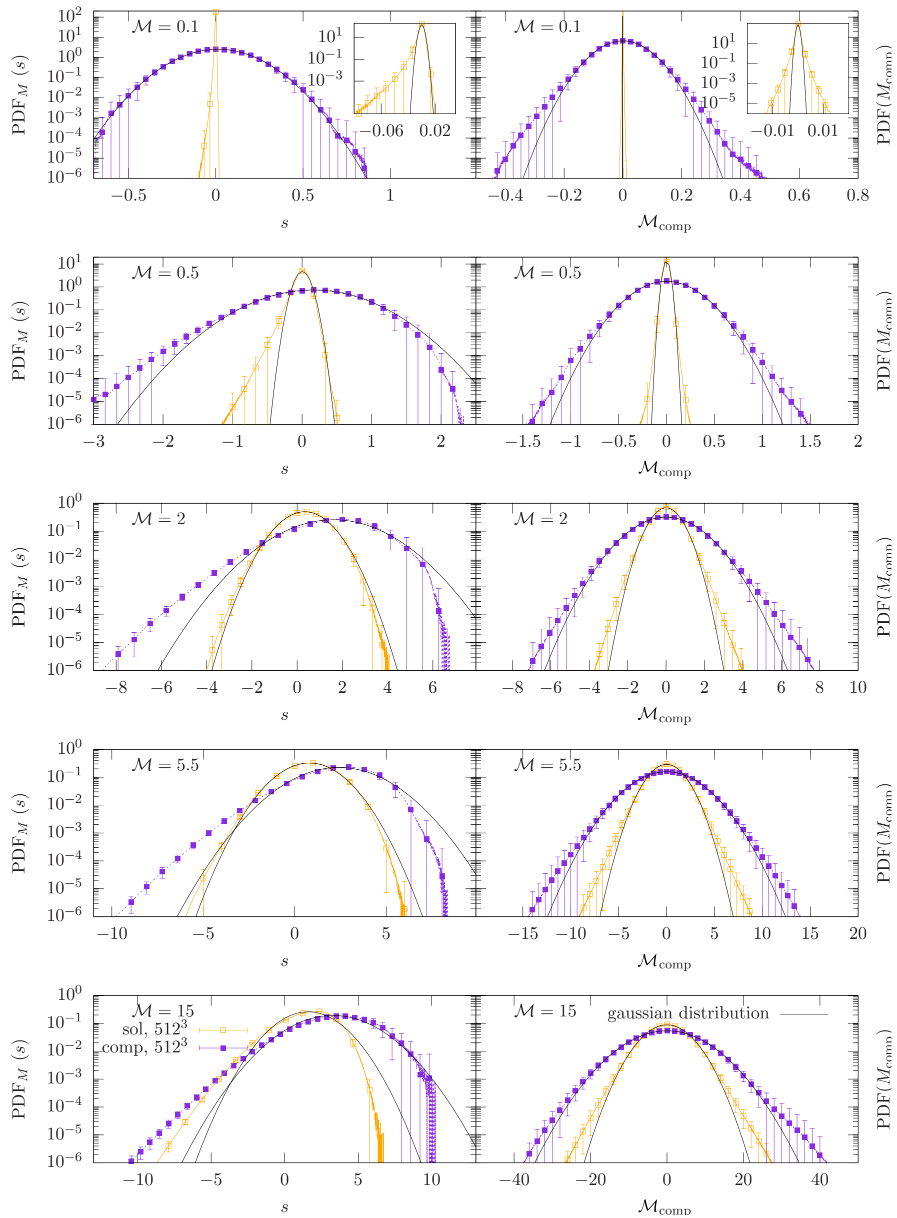

ρ-PDF - Mach number relation

- this relation also depends on the magnetic field strength

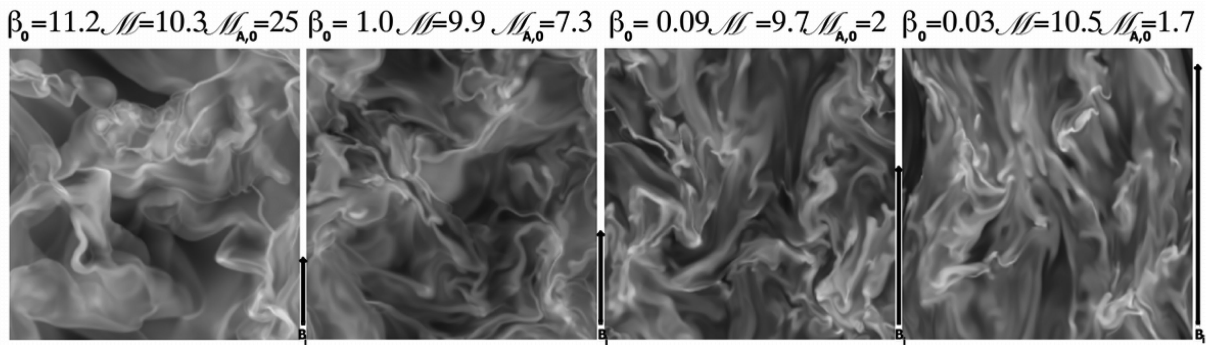

slices through MHD turbulence with increasing field strength

- the width of the density PDF now depends on the rms Alfvenic Mach number

$$\sigma_{s,1/2}^2 = \ln\left[1 + b^2\mathcal{M}^2\left(\frac{\beta_0}{\beta_0+1}\right)\right]$$

where $\boldsymbol{B} \propto \boldsymbol{\rho}^{1/2}$ is assumed

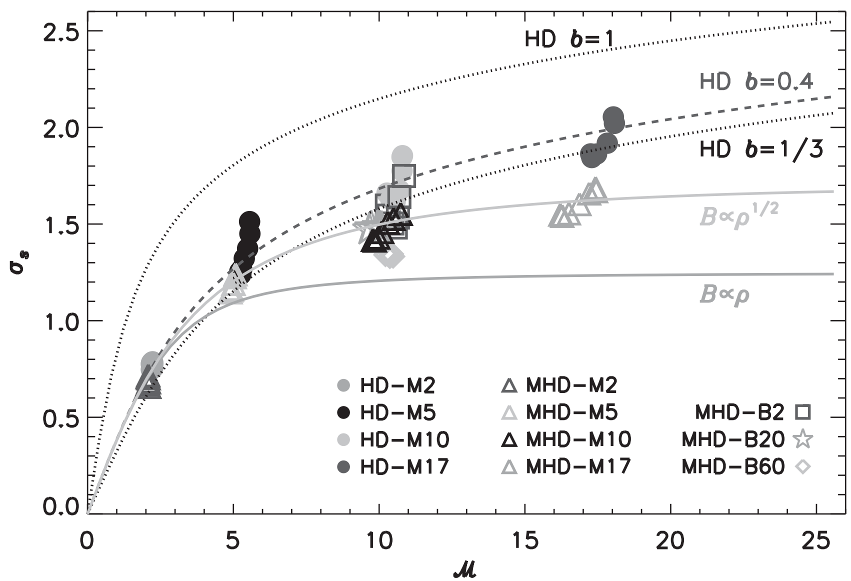

end

Hokusai: In the wake of the great wave of Tanakawa